NASA CONTRACTOR REPORT

NASA CR-155
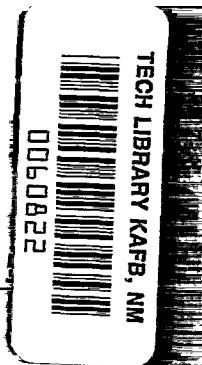
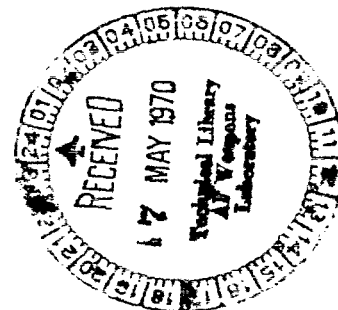C. 1

NASA CR-1551

INTERACTING EFFECTS OF GRAVITY AND SIZE UPON THE PEAK AND MINIMUM POOL BOILING HEAT FLUXES

by John H. Lienhard

Prepared by
UNIVERSITY OF KENTUCKY
Lexington, Ky.
for Lewis Research Center

NATIONAL AERONAUTICS AND SPACE ADMINISTRATION • WASHINGTON, D. C. • MAY 1970

0060822

1. Report No. NASA CR-1551	2. Government Accession No.	3. Recipient's Catalog No.
4. Title and Subtitle INTERACTING EFFECTS OF GRAVITY AND SIZE UPON THE PEAK AND MINIMUM POOL BOILING HEAT FLUXES		5. Report Date May 1970
		6. Performing Organization Code
7. Author(s) by John H. Lienhard		8. Performing Organization Report No. None
9. Performing Organization Name and Address University of Kentucky, Lexington, Kentucky		10. Work Unit No.
		11. Contract or Grant No. NGR 18-001-035
		13. Type of Report and Period Covered Contractor Report
12. Sponsoring Agency Name and Address National Aeronautics and Space Administration Washington, D.C. 20546		
		14. Sponsoring Agency Code

15. Supplementary Notes

16. Abstract

Interacting effects of gravity and the size of heaters on the peak and minimum pool boiling heat fluxes are studied with the aid of a centrifuge facility. Several geometries are studied. A scheme of correlation is developed and proven over very large ranges of gravity, size, boiled liquid, pressure, and configuration. Accurate analytical expressions are obtained for the peak and minimum heat fluxes, and the Taylor unstable wavelength on horizontal cylinders. An induced convection effect during boiling is identified and correlated. A drastic change in the boiling mechanism is identified for small heaters and for low gravities.

17. Key Words (Suggested by Author(s)) Film Boiling High gravity Peak heat flux	18. Distribution Statement Unclassified - unlimited		
19. Security Classif. (of this report) Unclassified	20. Security Classif. (of this page) Unclassified	21. No. of Pages 87	22. Price* $3.00

FOREWORD

The work described in this report was done in the Boiling and Phase-Change Laboratory of the Mechanical Engineering Department at the University of Kentucky. It was supported by NASA Grant NGR 18-001-035 under the cognizance of Mr. Thomas H. Cochran, Spacecraft Technology Division, NASA-Lewis Research Center, as Project Manager.

CONTENTS

SUMMARY

This report describes the first two years of work on
a project aimed at learning how the peak and minimum pool
boiling heat fluxes are influenced by gravity, size, and con-
figuration, as well as other variables.

The first months of this endeavor were devoted to the
design and fabrication of a centrifuge facility which allowed
a 100-fold variation of gravity. This apparatus is described
briefly and the following experiments are reported:

1.) The Taylor unstable wavelengths are measured
during film boiling on horizontal cylinders and their range
is shown to be describable by adaptations of existing theory
over a wide range of conditions, but a low gravity (or small
size) limitation is imposed. The minimum heat flux based
upon this wavelength is also discussed. These microstudies
of the transition from film to nucleate boiling provide the
basis for acceptance of the hydrodynamic theory and put some
limitations on the range of acceptance.

2.) The peak heat flux on horizontal cylinders is pre-
dicted on the basis of the hydrodynamic theory and verified
with almost a thousand data points over a very wide variety
of conditions. The low gravity (small size) limitation is
corroborated in the peak heat flux case.

3.) About 900 observations of the peak heat flux on
horizontal ribbons verify that induced convection can serious-
ly influence the peak heat flux. A method is developed for
correlating this effect.

Throughout these individual studies a general function-
al expression is developed for correlating the peak and min-
imum heat fluxes. This relation gives the ratio of the ex-
treme heat flux in a particular configuration, to the corres-
ponding value on a flat plate, as function of two scale para-
meters. Contact angle and the liquid-vapor density ratio are
additional weak influences that can appear in the function.
A number of observations as to the characteristic behavior
and limitations of this expression are advanced.

I. INTRODUCTION

This report summarizes a two-year study of the peak and minimum pool boiling heat fluxes, q_{max} and q_{min}, under a wide variety of conditions. The study was motivated by the fact that gravity, g, and size exert inter-related effects upon the extreme heat fluxes. This notion was suggested in 1963 by Costello and Adams [1][1] and later developed more quantitatively in references [2] and [3].

Actually, the intrinsic complexity of the effect of gravity began to come to light about the turn of this decade when the first experimental investigations of the extreme heat fluxes were made. Many investigators, notably Costello and Adams [4], Siegel and Howell [5] and Merte et al. [6], [7] have since measured q_{max} and q_{min} under conditions of both elevated and reduced gravity. Their data indicate that the "one-quarter power" dependence of q_{max} and q_{min} upon g, that is suggested by Zuber's [8],[9] equations, is only approximate in some cases and inaccurate in others.

Zuber's equations were developed upon consideration of the hydrodynamic stability of vapor removal during the boiling of an inviscid liquid on an infinite horizontal flat plate. Designating the flat plate configuration with the subscript, F, we can write Zuber's equations in the form[2]:

$$q_{max_F} = \frac{\pi}{24} \rho_g^{1/2} h_{fg} [\sigma g (\rho_f - \rho_g)]^{1/4} \left\{ \left(1 + \frac{\rho_g}{\rho_f}\right)^{1/2} \left(1 + \frac{\pi}{16-\pi} \frac{\rho_g}{\rho_f}\right)^{-1} \right\} \quad (1)$$

and

$$q_{min_F} = \frac{\pi^2}{60} \left(\frac{4}{3}\right)^{1/4} \rho_g h_{fg} \left[\frac{\sigma g (\rho_f - \rho_g)}{(\rho_f + \rho_g)^2}\right]^{1/4} \quad (2)$$

The factor in braces in equation (1) characterizes the inflow of makeup liquid to compensate vapor removal. It varies from very near unity over most of the range of pressure, up to 1.14 at the critical point. Thus we can write with very good accuracy:

$$q_{max_F} \simeq \frac{\pi}{24} \rho_g^{1/2} h_{fg} [\sigma g (\rho_f - \rho_g)]^{1/4} \quad (3)$$

Unless noted otherwise, q_{max_F} will be used to designate the estimate of the peak heat flux on a flat plate given by equation (3).

---

[1]Numbers in square brackets denote entries in the References section.

[2]Symbols not defined in context are explained in the Nomenclature section.

In 1963 Lienhard and Wong [10] provided some explanation for the failure of the relation,

$$q_{max_F} \text{ or } q_{min_F} \sim g^{1/4} , \tag{4}$$

suggested by equations (1) and (2) or (3). They presented a hydrodynamic derivation of q_{min} for a configuration with a characteristic length, namely infinite horizontal cylinders of radius, R. They obtained the relation

$$q_{min} = .057 \frac{\rho_g h_{fg}}{R} \left[2g \frac{(\rho_f - \rho_g)}{(\rho_f + \rho_g)} + \frac{\sigma}{(\rho_f + \rho_g)R^2} \right]^{1/2} \left[\frac{g(\rho_f - \rho_g)}{\sigma} + \frac{1}{2R^2} \right]^{-3/4} \tag{5}$$

which differs greatly from equation (2), especially as q_{min} depends on g.

Two years later Lienhard and Watanabe [2] noted that equation (5) could be put in a dimensionless form which can be cast as follows:

$$q_{min} = q_{min_F} \left[\frac{1}{3.8} \right] \left[\frac{18}{R'^2 (2R'^2 + 1)} \right]^{1/4} \tag{6}$$

where R' is a dimensionless radius defined as

$$R' \equiv R[g(\rho_f - \rho_g)/\sigma]^{1/2} \tag{7}$$

They then provided experimental data to show that, at least for horizontal cylinders, both

$$\frac{q_{max}}{q_{max_F}} \text{ and } \frac{q_{min}}{q_{min_F}} = f(R') \tag{8}$$

were true. Reference [3] went on to validate this suggestion using variable gravity data from a variety of sources, and in additional geometric configurations. In non-cylindrical geometries, the function, f(R') was replaced by f(L') where L' was

$$L' \equiv L[g(\rho_f - \rho_g)/\sigma]^{1/2} \tag{7a}$$

and L was the characteristic length appropriate to the geometry under consideration.

It was clear at this point that equation (4) could only be true for the very restrictive case in which f(L') = constant. The influence of gravity appeared both as a $g^{1/4}$ factor in q_{max_F} and in the function, f(L'), of the scale parameter, L', as well.

The present work was initiated in the Fall of 1967 with the

2

following objectives in mind:

1.) The applicability and limitations of equation (8) were to be fully explored.

2.) q_{max}/q_{max_F} and q_{min}/q_{min_F} versus L' surfaces were to be developed for a variety of configurations, so that they would be available for design use.

3.) The dynamics of vapor removal were to be studied in an effort to create additional explicit predictions of q_{max} and/or q_{min} comparable with equations (1),(2), and (5).

Chapters IV, V, and VI discuss three experiments and analyses, each of which will bear upon all three objectives. Chapter II will briefly describe the variable gravity apparatus that was developed here for this work, and will introduce the experiments. Chapter III explains in greater detail our á priori thoughts about the first objective, above.

II. EXPERIMENT

The basic experimental requirement in this work was an apparatus that would permit variation of the independent variable, R' or L', in equation (8) and observation of the resulting dependent variable, q_{max}/q_{max_F}. Three factors influence L': the size, L; the gravity, g; and the liquid being boiled. Thus, provision had to be made for mounting heaters of various sizes in each configuration of interest, for varying the gravity over a wide range, and for accomodating diverse saturated liquids. Provision for supplying electric power to the heater, and for reading this power at burnout, was needed for the dependent variable.

The answer to this requirement was a general purpose centrifuge apparatus which is described in detail in [11]. Figure 1 is a general view of this facility and Fig. 2 provides a schematic view showing the various slip rings and other access on the underside.

The centrifuge provides a capability for varying gravity between about 5 and 100 times earth normal gravity. Slip rings provide 2 - 50 amp power circuits, 3 - 20 amp power circuits, and 6 low current instrumentation circuits. A main rotating seal permits evacuation of a test capsule to any desired reduced pressure, and a secondary rotating seal facilitates measurement of this pressure.

Users of the centrifuge are protected by a 0.32 cm (1/8 in.) thick steel cylinder from the danger of any mishap that might occur during operation. The foreground of Fig. 1 is designated the "service side" and all handling of the test section is done through an access door on this side. The opposite side is covered with plexiglas to protect the experimenter during visual observation of the tests. This side is designated the "observation side" of the facility.

Three kinds of visual studies are made. Figures 1 and 2 show the centrifuge rigged for one of these, namely high speed motion picture photography which is accomplished through two removable mirrors. Still photography can also be done with a camera located directly above the path of the centrifuge arm on the observation side, after removing the motion picture mirrors and light. The still photos are illuminated with a photoelectrically triggered strobe light directly below the camera. Visual observations were made by looking directly through the test section into the diffused strobe light. By triggering the light on each revolution of the arm it was possible to create the illusion of a static boiling process under high gravity, and to observe the transitions as though they were standing still.
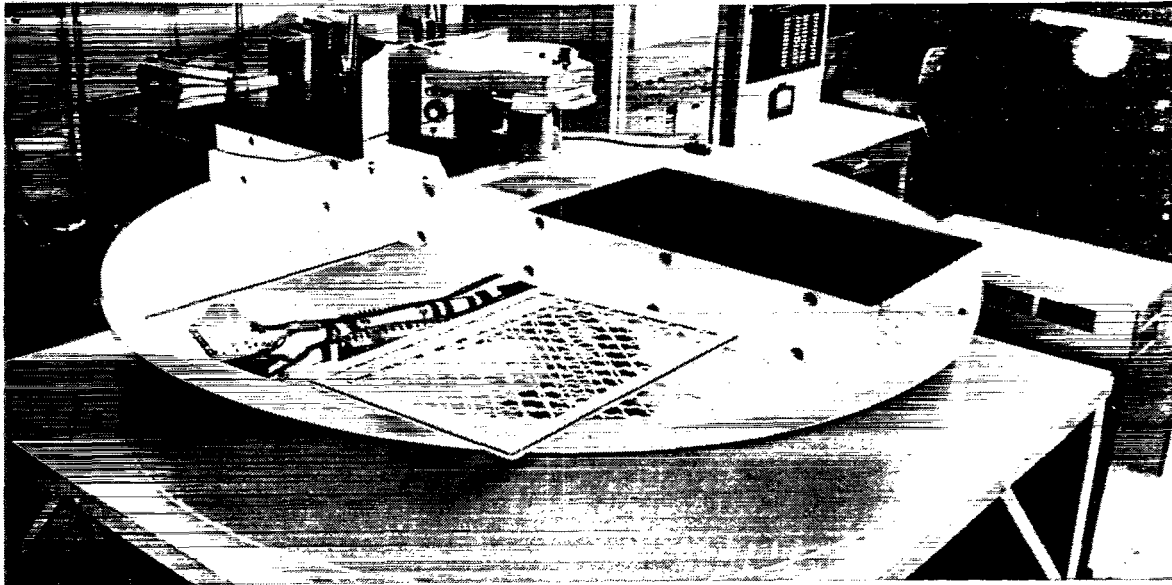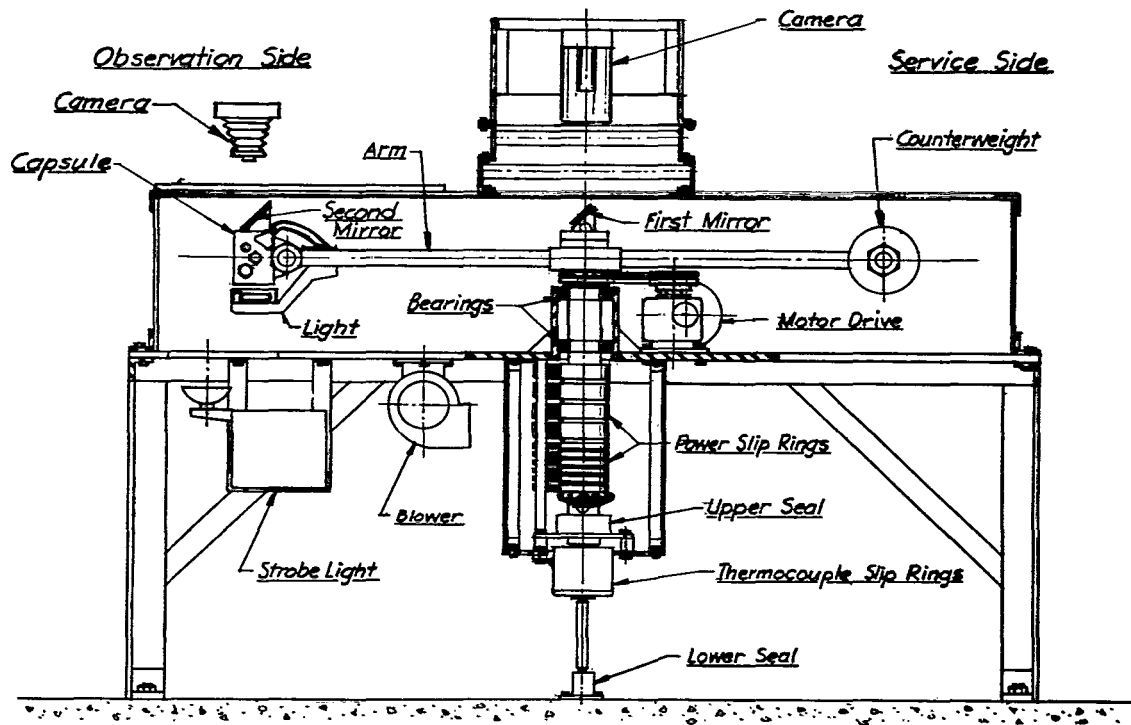
4

Fig. 1 General view of centrifuge facility

Fig. 2 Schematic view of centrifuge facility

The test capsule used in all of the present experiments is shown in Fig. 3. The inside of the capsule is 17.8 cm (7 in.) long, by 7.6 cm (3 in.) high, by 9.5 cm (3.75 in.) wide. The tab shown in the center is cut to exactly 2.540 ± .003 cm (1.000 ± .001 in.) across the outer edges to provide a scale in photographic observations.
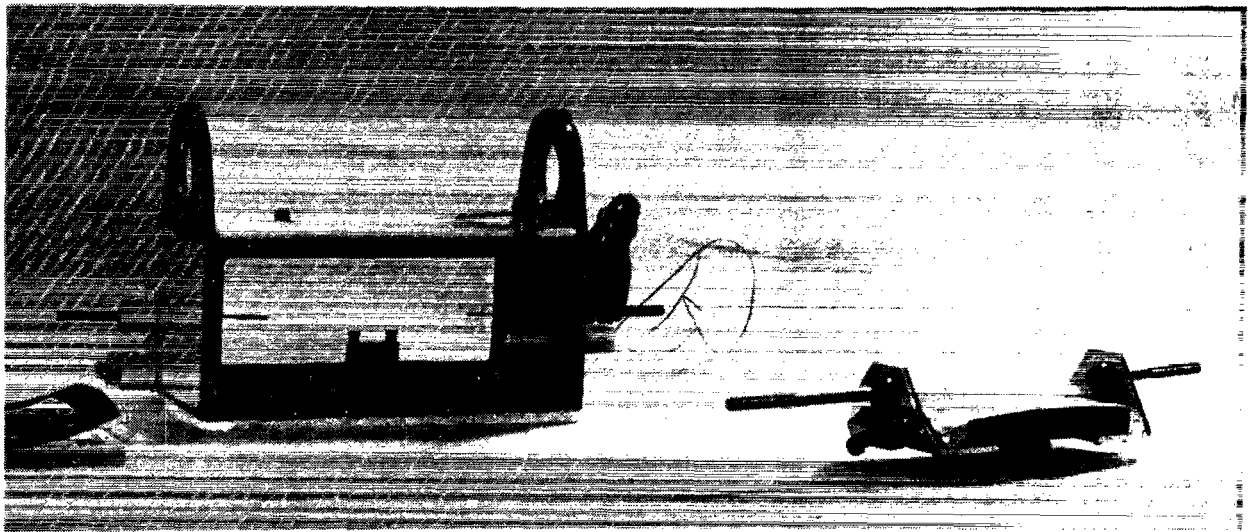

Fig. 3   The test capsule mounted with a horizontal wire heater, and an alternate ribbon heater

The capsule is shown loaded with a horizontal wire heater, 10.16 cm (4.00 in.) in length--the standard length that we used for all of our wire heaters. The mounting schemes that we used for these heaters is shown in Fig. 4. These configurations were devised to minimize possible vapor pockets, heat loss, and electrical resistance.

An alternate test heater configuration is also shown in Fig. 3. This is a long horizontal ribbon of limited width. It is 10.16 cm (4.00 in.) in length and mounted on a wide insulating plate.

All tests reported here were made on either of these heaters. The wires used in the horizontal cylinder configuration ranged from 36 to 12 gage in size. The flat ribbons ranged from .117 to 2.54 cm in width.

The results of three basic experiments made on these heaters will be included in this report in support of our predictions

electrode — Solder — Heater wire
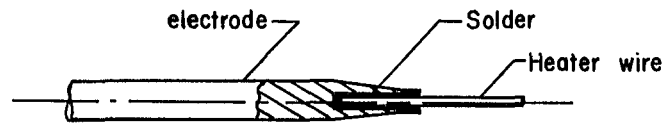
Alternate mounting for heavy gage wires

Brass electrode — Capsule wall — Copper lead — O-ring — Spring — Nut — Set screw — Heater wire — Tied with thin copper wire and soldered — Nylon fitting — Nylon fitting — Washer
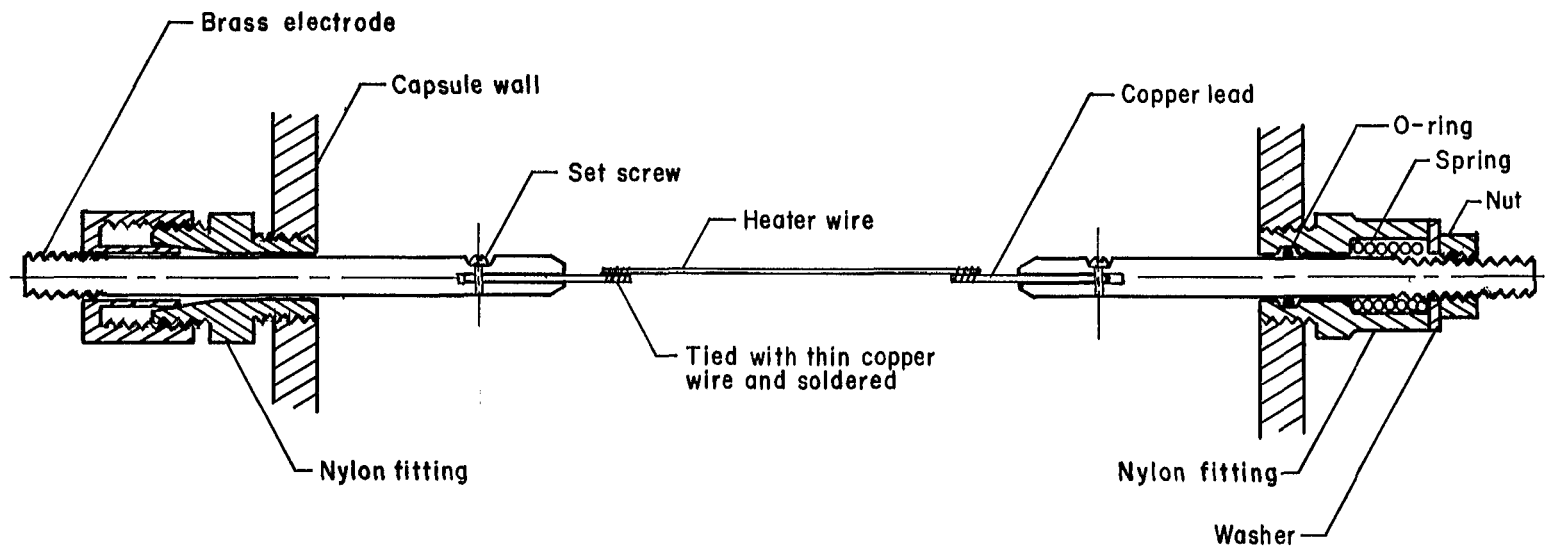
FIG. 4   CONFIGURATION OF CYLINDRICAL HEATER WIRE ATTACHMENT

and methods of correlation. They are:

1.) <u>Measurements of the wavelengths during film boiling on horizontal cylinders</u>. These experiments are described in full detail in [11] and the results are reported in [12].

2.) <u>Measurements of q_{max} on horizontal cylinders</u>. These experiments and the results are described in full detail in [13].

3.) <u>Measurements of q_{max} on ribbons</u>. These experiments are described in full detail in [14] and the results are reported in [15].

In general, these tests were made in five liquids: water, methanol, isopropanol, acetone, and benzene. Before each observation or small set of observations, the heater was carefully washed in soap and very hot water, and then rinsed in acetone. It was then installed in the capsule; the capsule was charged with liquid; and the liquid was brought to saturation and boiled for at least 10 minutes prior to making measurements.

III. SCALING LAWS

The Relevant Variables

Equation (8) is suggested by a theory which ignores viscosity and incorporates other simplifications that are not true in general. To obtain a broader scaling law we might first consider the relationship

$$q_{max} \text{ or } q_{min} = f(h_{fg}, \ \rho_f - \rho_g, \ \rho_g, \ g, \ \sigma, \ L, \ \mu, \ \theta_c) \qquad (9)$$

In this expression, we adopt the point of view that the density difference $(\rho_f - \rho_g)$ is a more fundamental variable than the liquid density alone. This is because it is basic to the buoyant force $g(\rho_f - \rho_g)$ which is important in most boiling processes. Certain other variables have been omitted since there is a good deal of experience that indicates they do not influence q_{max} and q_{min} appreciably. These include thermal conductivities and heat capacities, viscosity of the vapor phase, and surface roughness which we shall discuss below.

Equation (8) was based on the implicit assumptions that the last two independent variables, μ and θ_c, were also unimportant, and that $\rho_g/\rho_f \ll 1$. Let us see how these three assumptions come about and what they imply.

1.) The liquid viscosity, μ, is generally ignored in hydrodynamic theories of boiling since it does not impose serious damping in interfacial waves. However, heaters of finite size can induce flows around themselves through the viscous drag exerted by the rising bubbles. These flows can, in turn, disrupt the vapor removal pattern above a heater and seriously influence q_{max} or q_{min}.

We shall look only for this kind of "induced convection" effect of viscosity and ignore its influence on the stability of interfacial waves. It is a secondary effect in that the viscous action itself is not important in the hydrodynamic "crisis" of transition. Instead, viscous action acts far away from the immediate heater surface and it serves to create a flow field which in turn exerts the actual influence on the transitions.

9

Borishanski [16] suggested the dimensionless group[3]

$$N \equiv \frac{\rho_f \sigma}{\mu^2} [\sigma/g(\rho_f - \rho_g)]^{1/2} \qquad (10)$$

to correlate viscous effects. A few years before Zuber predicted q_{max_F}, Borishanski established the following experimental expression for q_{max} on fairly large horizontal disc heaters:

$$q_{max} = [1 + 30.5/N^{2/5}] \, q_{max_F} \qquad (11)$$

In most cases, N is sufficiently large that $30.5/N^{2/5} << 1$, so the term in brackets proved to be a very minor correction factor. We shall also find that the influence of N is negligible in the horizontal cylindrical geometry. Chapter VI, however, will describe a situation in which N exerts great importance.

2.) The contact angle, θ_c, is probably the correct variable to characterize those surface effects that do not arise from mechanical roughness. It has been established by Berenson [17] and Lyon [18] that surface roughness is an unimportant variable, but that chemical effects can cause variations in q_{max} that reach the order of 10 percent on fairly large heaters under extreme circumstances of surface preparation. Costello and Frea [19] present data that indicate these effects upon q_{max} can be even more pronounced, but only in smaller scale geometries. The very early q_{max} data of Cichelli and Bonilla [19] indicated that very serious chemical deterioration of large flat plates resulted in as much as a 15 percent increase in q_{max}.

Berenson's observations of q_{min} on flat plates showed that surface energy effects could cause very serious upward deviations of q_{min} from the limiting hydrodynamic minimum.

In our work we shall deal only with data obtained on carefully cleaned surfaces. It appears to be true that θ_c is very nearly the same (about zero) for most materials in most fluids. Thus cleaning will minimize (but not eliminate) the influence of θ_c--at least for q_{max} on comparatively large heaters.

3.) The density of vapor, ρ_g, apparently exerts an independent influence on q_{max} when the inflow of liquid, required to balance vapor outflow, has to be considered. The velocity of inflow, which can alter the point of Helmholtz instability of escaping vapor jets, will be appreciable only when ρ_g begins to approach the order of magnitude of $\rho_f - \rho_g$. At almost all saturation temperature: of practical interest, $\rho_f - \rho_g$ is much larger than ρ_g as we note in

---

[3]Perhaps the factor ρ_f in this expression would better be written as $(\rho_f - \rho_g) + \rho_g$ in keeping with our emphasis upon $(\rho_f - \rho_g)$ as a more significant quantity than ρ_f.

Fig. 5. It is this influence that was reflected in the factor in braces in equation (1), and (at least in that instance) the resulting effect on q_{max} was only a 14 percent increase near the critical point. It is entirely possible that the ratio, $\rho_g/(\rho_f-\rho_g)$, is generally of little consequence.
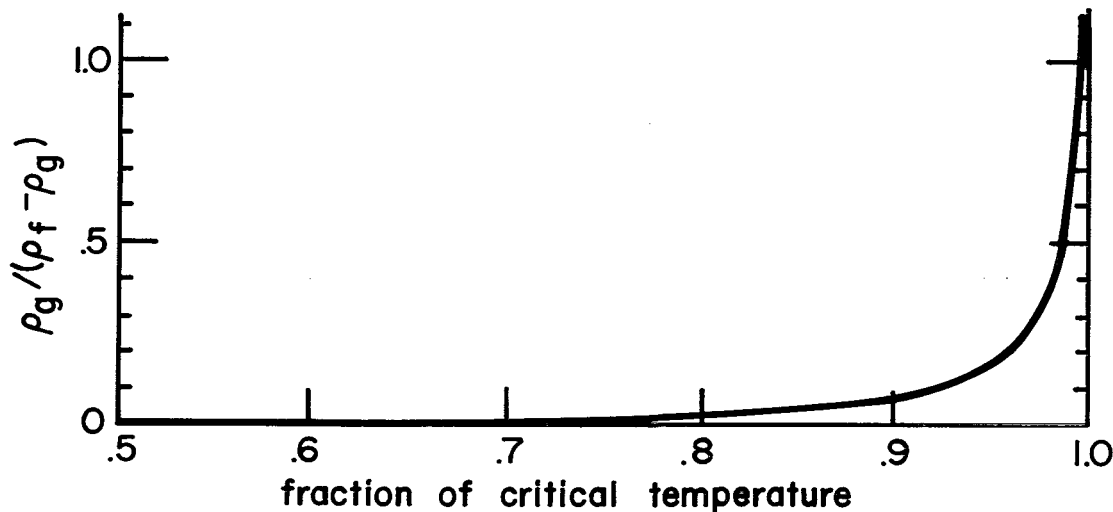

Fig. 5   Temperature dependence of $\rho_g/(\rho_f-\rho_g)$ for water

The Form of Correlation Equations and Predictions

Before we proceed to develop the more general dimensionless form of equation (9), let us consider the form it takes when the influences of viscous drag and surface energy are neglected. Without μ and θ_c equation (9) becomes:

$$q_{max} \text{ or } q_{min} = f(h_{fg}, \rho_f-\rho_g, \rho_g, g, \sigma, L) \tag{12}$$

Equation (12) relates seven variables in the four dimensions: thermal energy, length, time, and force or mass. The Buckingham Pi theorem shows that equation (12) must be reducible to a relation among any 7 minus 4 or three independent dimensionless groups of these variables.

The three groups that we shall construct are: the independent variable, L', the parameter, $\rho_g(\rho_f-\rho_g)$, and the dependent variable,

$$q_{max}/\rho_g^{1/2}h_{fg}[\sigma g(\rho_f-\rho_g)]^{1/4}$$

for q_{min} it is advantageous to multiply this group by a function of $\rho_g/(\rho_f-\rho_g)$ equal to $[(\rho_f-\rho_g)\rho_g]^{1/2}[1+2\,\rho_g/(\rho_f-\rho_g)]^{1/2}$, to get:

$$q_{min} / \rho_g h_{fg} [\sigma g (\rho_f - \rho_g) / (\rho_f + \rho_q)^2]^{1/4}$$

Finally, if the appropriate constants are incorporated in these dependent variables, the correlating equations become:

$$\frac{q_{max}}{q_{max_F}} \text{ or } \frac{q_{min}}{q_{min_F}} = f[L', \rho_g / (\rho_f - \rho_g)] \tag{13}$$

We should like to have q_{max_F} and q_{min_F} represent as closely as possible the actual extreme heat fluxes on infinite flat plates. The dependent variable will then provide a physically meaningful comparison of observed values with an apt reference. There are few data available with which to check Zuber's equations in the geometry for which they were intended. However, those data available for heaters which approach flat plates, strongly suggest that equation (1) or (3) for q_{max} is the best estimate we can presently make.

Berenson showed that this is not the case for q_{min}, though. His analysis revealed that the constant, $(\pi^2/60)(4/3)^{1/4}$, was incorrectly derived and had to be replaced with an experimental number. For this he obtained .09, so we shall henceforth use

$$q_{min_F} = .09 \rho_g h_{fg} \left[\frac{\sigma g (\rho_f - \rho_g)}{(\rho_f + \rho_g)^2} \right]^{1/4} \tag{14}$$

in equation (13).

A word about the scale parameter, L', is in order at this point. In the form that we have given it, it has been named after both Rayleigh who used it and Laplace who probably originated it. In this form it compares the size of the heater, L, with a fraction of either a capillary wavelength or a bubble departure diameter. In squared form it is exactly the Bond number.

$$L'^2 \equiv \text{Bond number}, \quad \frac{g(\rho_f - \rho_g)L^3}{\sigma L} = \frac{\text{buoyant force}}{\text{surface tension force}} \tag{15}$$

By using L' instead of L'^2 in our studies we are laying heavier stress on its geometrical interpretation, than on its dynamical interpretation.

If the influences of μ and θ_c are not to be ignored then one more dimensionless group is required by the Pi theorem for each. θ_c is already dimensionless and N (recall equation (10)) is an appropriate group containing μ. Thus we have

$$\frac{q_{max}}{q_{max_F}} \text{ or } \frac{q_{min}}{q_{min_F}} = f[L', N, \rho_g / (\rho_f - \rho_g), \theta_c] \tag{16}$$

12

We shall name, N, the induced convection buoyancy parameter since it compares gravity (or buoyancy) forces with the other forces in the following rather complex way:

$$N = \frac{(\text{inertia force})(\text{surface tension force})^{3/2}}{(\text{viscous force})^2 (\text{buoyant force})^{1/2}} \qquad (17)$$

The word "convection" in this context alludes to the flow induced by the viscous drag which is exerted by bubbles buoying upward from the heater.

From a practical viewpoint we shall see shortly that it is advantageous to replace N in equation (15) with a scale parameter, i.e., with a parameter that increases with L. It will also prove useful to replace it with a parameter that does not depend upon gravity. Accordingly we shall define an induced convection scale parameter, I, as

$$I \equiv \sqrt{NL'} = \sqrt{\rho_f L \sigma / \mu^2} \qquad (18)$$

which characterizes the relevant forces in the following way:

$$I = \frac{[(\text{inertia force})(\text{surface tension force})]^{1/2}}{\text{viscous force}} \qquad (19)$$

Thus we have as an alternative to equation (16) the following correlating equation:

$$\frac{q_{max}}{q_{max_F}} \text{ or } \frac{q_{min}}{q_{min_F}} = f[L', \ I, \ \rho_g/(\rho_f - \rho_g), \ \theta_c] \qquad (20)$$

Some of the limiting behavior of this expression can be anticipated. We have already indicated that we do not expect to see $\rho_g/(\rho_f - \rho_g)$ exert a great influence, especially when it is small (or when the saturation temperature is much below the critical temperature). Likewise θ_c should normally have little importance with heaters that are not very small.

Since L' and I are scale parameters, we anticipate that they will exert decreasing influence as heaters become large. The reason is that very large L' and I imply that buoyancy and inertia completely over-balance surface tension and viscosity. Once these forces have been over-balanced, further increases of L' and I do not correspond with any changes in the situation and we expect that

$$\underset{L', I \to \infty}{\text{Limit}} \ \frac{q_{max}}{q_{max_F}} \text{ or } \frac{q_{min}}{q_{min_F}} = \text{constant} \qquad (21)$$

13

The low L' and I limits are harder to anticipate, and we shall defer a discussion of them to the last section.

Equations (20) and (16) represent our basic correlation methods and we shall repeatedly apply them in the subsequent sections.

IV. FILM BOILING FROM HORIZONTAL CYLINDERS

Theory

The theoretical expression for the minimum film boiling heat flux on horizontal cylinders, equation (5), was developed in [10] on the basis of an assumed interface configuration shown in Fig. 6a. It was shown that the frequency of bubble departure was the following real number $(i\omega)$:

$$(i\omega) = \left[kg \frac{\rho_f - \rho_g}{\rho_f + \rho_g} - \frac{\sigma k^3}{\rho_f + \rho_g} + \frac{\sigma k}{2(\rho_f + \rho_g)R^2} \right]^{1/2} \tag{22}$$

where k is the wave number of the collapsing waves that feed the bubbles. It was also shown that the dominant wavelength, λ_d, during film boiling could be obtained by maximizing this frequency. The result was:

$$\lambda_d = \frac{2\sqrt{3}\ \pi}{\sqrt{\dfrac{g(\rho_f - \rho_g)}{\sigma} + \dfrac{1}{2R^2}}} \tag{23}$$

Finally, it was shown that by paraphrasing Zuber's [8] and Berenson's [17] arguments, equation (23) could be used as the basis for the prediction of q_{min}, equation (5). Equation (23) was verified with a limited number of data for isopropanol and benzene in a fairly low range of R'. However, no attempt has yet been made to verify it under conditions of variable gravity. Equation (5) has been subjected to even less experimental verification.

The use of several transformations will put equations (22), (23),(5) into convenient dimensionless form. We first introduce a dimensionless wavelength:
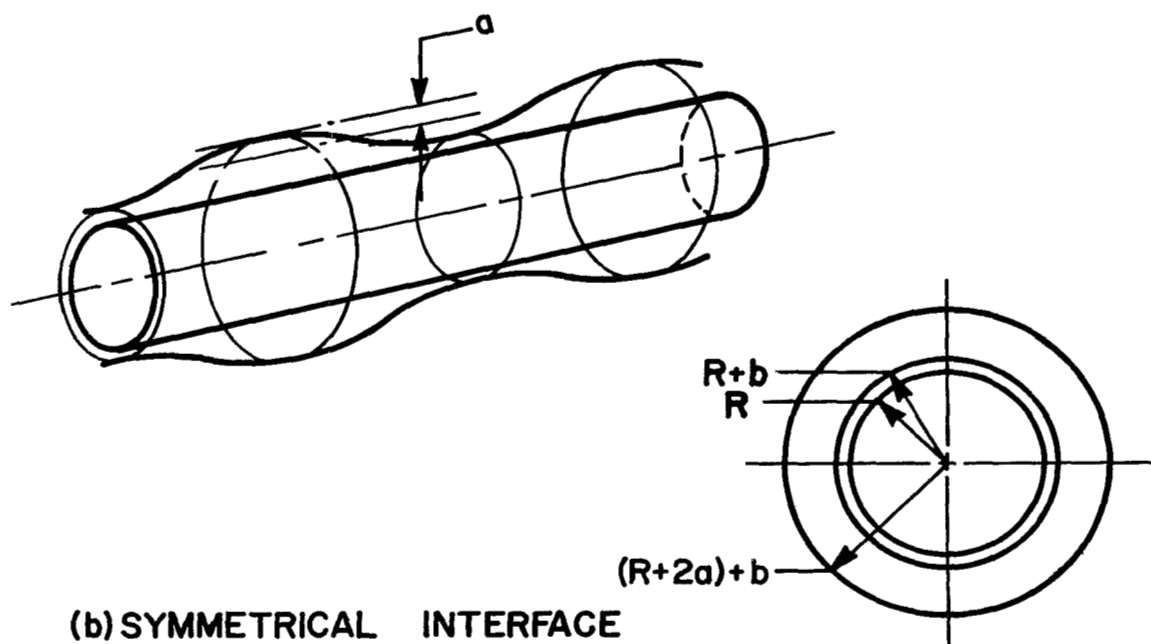
$$\Lambda \equiv \lambda_d / \lambda_{d_F} \tag{24}$$

where λ_{d_F} is Bellman's and Pennington's [21] wavelength for capillary gravity waves in a plane, horizontal, liquid-vapor interface as might exist during film boiling above a flat plate,

$$\lambda_{d_F} = \frac{2\sqrt{3}\ \pi}{\sqrt{\dfrac{g(\rho_f - \rho_g)}{\sigma}}} \tag{25}$$

15
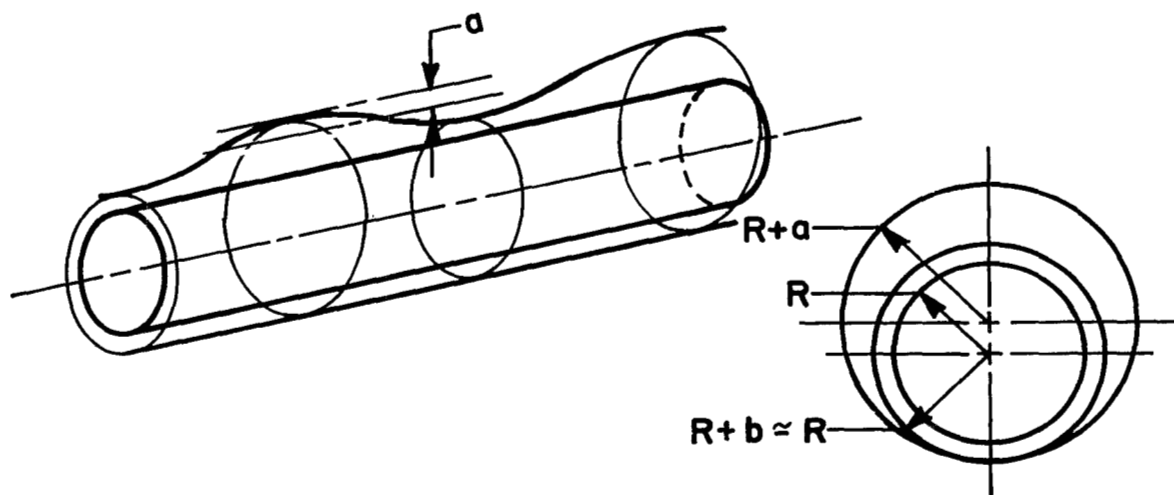
(a) ASYMMETRICAL INTERFACE WITHOUT WAVES ON THE BOTTOM

(b) SYMMETRICAL INTERFACE

Fig. 6 Possible configurations of the liquid−vapor interface around horizontal cylindrical heaters during film boiling

We next introduce a dimensionless frequency,

$$\Omega \equiv i\omega[\sigma/g^3(\rho_f-\rho_g)]^{1/4} \qquad (26)$$

and we finally introduce the dimensionless radius, R'. Then equation (22) becomes

$$\Omega^2 = \frac{1}{\sqrt{3}\,\Lambda_{LW}}\left[1 + \frac{1}{2R'^2} - \frac{1}{3\Lambda_{LW}^2}\right]\left[\frac{\rho_f-\rho_g}{\rho_f+\rho_g}\right] \qquad (22a)$$

where in the present applications, $(\rho_f-\rho_g)/(\rho_f+\rho_g) \simeq 1$ in all cases. Equation (23) becomes

$$\Lambda_{LW} = \sqrt{\frac{R'^2}{R'^2 + 1/2}} \qquad (23a)$$

where the subscript LW has been introduced to distinguish the Lienhard-Wong results from those of other authors we wish to consider. Equation (5) becomes, not equation (6), but

$$q_{min}/q_{min_F} = 0.515\ f(R') \qquad (27)$$

where the constant .515 arises because q_{min_F} is Berenson's result, equation (14), instead of Zuber's equation (2), and where

$$f(R') = \left[\frac{18}{R'^2(2R'^2 + 1)}\right]^{1/4} \qquad (28)$$

Data [10] in the range of dimensionless radius, R', from .017 to 0.25 showed that equation (23a) predicted wavelengths about 25 percent too low. In the discussion of [10], the authors pointed out that this could probably be improved by including the minimum vapor blanket thickness, b, in the calculation. Two subsequent attempts were accordingly made to improve the accuracy of equation (23a). The first was by Siegel and Keshock [22] who assumed that the interface was shaped as shown in Fig. 6b[4] instead of Fig. 6a and who retained b in their analysis. They obtained:

$$\Lambda_{SK} = \sqrt{\frac{R'^2}{R'^2 + (1 + b/R)^{-2}}} \qquad (29)$$

---

[4]This point might not be entirely clear in reference [22] which includes both the left-hand sketch in Fig. 6a along with the right-hand sketch in Fig. 6b. The analysis in [22] is based on Fig. 6b, however.

We can also modify equation (23a) so that it takes account of a finite vapor blanket. This is done replacing R with the radius (R+b) of the minimum interface radius in equation (23) and carrying out the nondimensionalization. The result is:

$$\Lambda_{LW} \text{ with } (1 + \frac{b}{R}) = \sqrt{\frac{R'^2}{R'^2 + 1/[2(1 + b/R)^2]}} \tag{30}$$

While Siegel and Keshock did not evaluate b or make experimental comparisons, Baumeister and Hamill [23] succeeded in deriving an expression for b, two years later. They used an assumption that the heat transfer must be maximum, subject to appropriate constraints, and their vapor "escapement" assumption differed from those proposed in Fig. 6. Instead of taking the top of the interface to be wavelike they imagined spherical domes connected by annular passages. They obtained:

$$\Lambda_{BH} = \frac{2}{\sqrt{3}\,\pi} \left\{ \frac{\sqrt{1 + 6R'^2(1 + b/R)^2} - 1}{\sqrt{R'^2(1 + b/R)^2}} \right\} \tag{31}$$

Their analysis also permitted them to predict $(1 + b/R)$;

$$(1 + b/R) = \exp\{3.65[k\mu\Delta T/R\rho_g\sigma h_{fg}^+]^{1/4}\} \tag{32}$$

where h_{fg}^+ is a latent heat that includes a sensible heat correction

$$h_{fg}^+ = \left[1 + \frac{0.34c_v\Delta T}{h_{fg}}\right]^2 h_{fg} \tag{33}$$

Comparison of Wavelength Results with Theory

In an attempt to assess equations (23a),(29),(30), and (31) for Λ, we made 233 still photographs during film boiling at over 50 different conditions of gravity and radius [11]. Although we can scale lengths with an accuracy of about 3 percent, the wavelengths exhibited wide variability. Most of them were obtained in acetone, but several observations in methanol and isopropanol were included to insure that other fluids obeyed the same relationships.

The heat flux was arbitrarily regulated to some value well below the peak and hopefully not far above the minimum. We found that, although Lienhard and Wong observed no effect of heat flux upon λ in the range $q/q_{min} \leq 4$, it was possible to distort the wave action and increase the merging of adjacent bubbles at higher heat fluxes. This is consistent with the studies Nishikawa et al. [24] who observed, not λ, but the spacing of bubbles leaving wires in water over an eightfold variation of q up to the order

of magnitude of the peak heat flux, at R' = 0.14. They found that bubble spacing increased about twofold in this range.

Figure 7 shows six typical photographs of film boiling under a variety of conditions, arranged in order in increasing R'. Let us consider each of these:

7a. Careful scrutiny of motion picture records in the R' range typified by this picture shows that the Taylor unstable wavelength briefly appears in the interface in the wake of departing bubbles. It is much shorter than the spacing between the bubbles on the wire and it very quickly merges into these bubbles. Since the bubbles must grow quite large by successive mergers before they have enough buoyancy to overcome the capillary forces that hold them to the wire, the bubble spacing is much larger than λ_d. We shall refer to this vapor removal process, which can be made out in Fig. 7a, as the "bubble-merger" mechanism. Gravity exerts little influence on the interface, and Fig. 6b might possibly provide a more apt description of the interface than Fig. 6a.

7b. The Lienhard-Wong description fits almost perfectly here. Transverse surface tension, axial surface tension, and gravity are all in good balance. Vapor removal is accomplished by the orderly growth of Taylor unstable waves and their subsequent collapse into departing bubbles. We shall subsequently refer to this as the "wave-collapse" mechanism of vapor removal.

7c. The radius is smaller than in 7b but g is larger and the resultant R' is somewhat higher than in 7b. The heat flux is much higher than q_{min} and, while a wave pattern is clear, the wavelength varies along the length of the wire.

7d. The next value of R' is obtained by subjecting a small wire to a high g. The wave pattern is again clear and faithful to Fig. 6a, but it exhibits almost 2 to 1 variability.

7e. For a value of R' almost equal to unity, the relative diminution of transverse surface tension results in a deterioration of the form of the wave pattern

7f. The shaping effect of transverse surface tension is almost wholly lost in this case and estimates of wavelength were made mainly from the spacing of departing bubbles.

The wavelength data are presented graphically in dimensionless forms in Figs. 8 and 9. Figure 8 also includes the low R' results from Lienhard's and Wong's stationary tests. The reader should remember as he scans Figs. 7, 8, and 9, that while Λ increases monatonically with R', λ does not. Fig. 7d, for example,
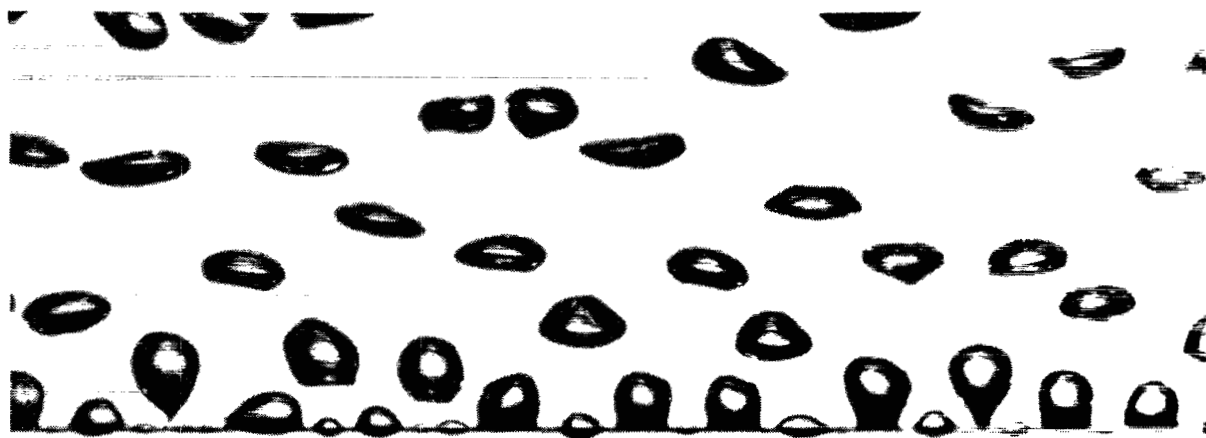
a) $g=1g_e$, R=.0102 cm., acetone, q=3.90 cal/cm^{2}sec,   R'=.0642
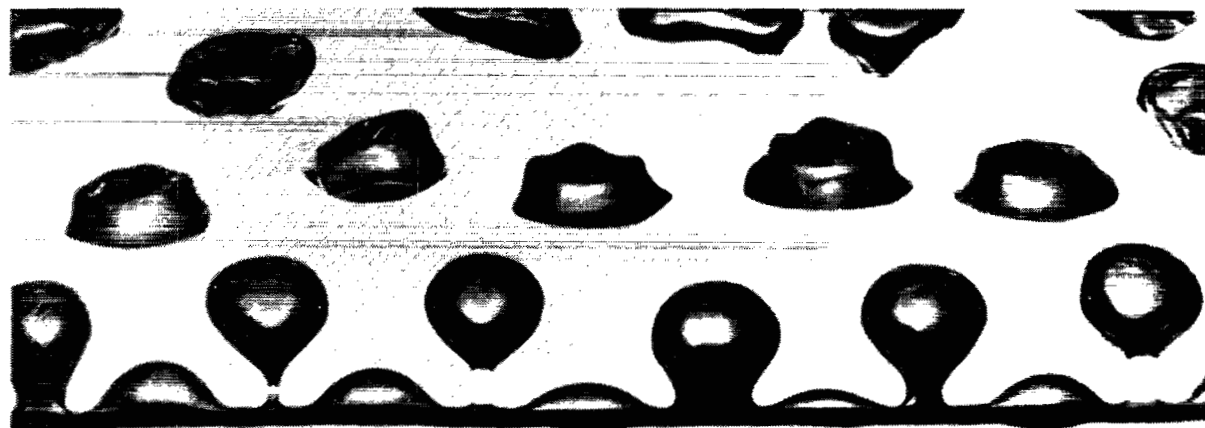
b) $g=1g_e$, R=.0322 cm., acetone, q=3.10 cal/cm^{2}sec,   R'=.203

Fig. 7   Vapor removal configuration for six typical cases of film
         boiling, in order of increasing R'.

20

c) $g=10g_e$, R=.0160 cm., methanol, q=9.93 cal/cm^{2}sec,   R'=.322
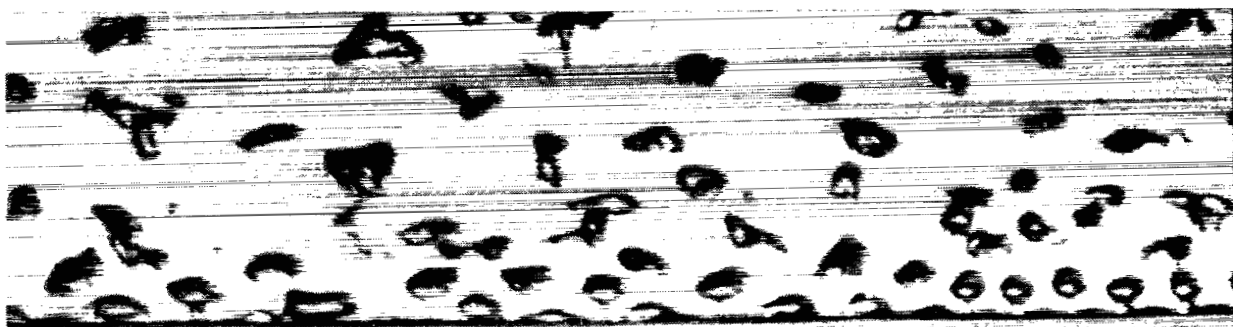
d) $g=38g_e$, R=.0127 cm, acetone, q=7.45 cal/cm^{2}sec,   R'=.497

Fig. 7 Continued

21

e) g=8g$_e$, R=.0508 cm., acetone, q=3.06 cal/cm^{2}sec, R'=.905

f) g=26g$_e$, R=.0508 cm., acetone, q=4.52 cal/cm^{2}sec, R'=1.64

Fig. 7 Continued
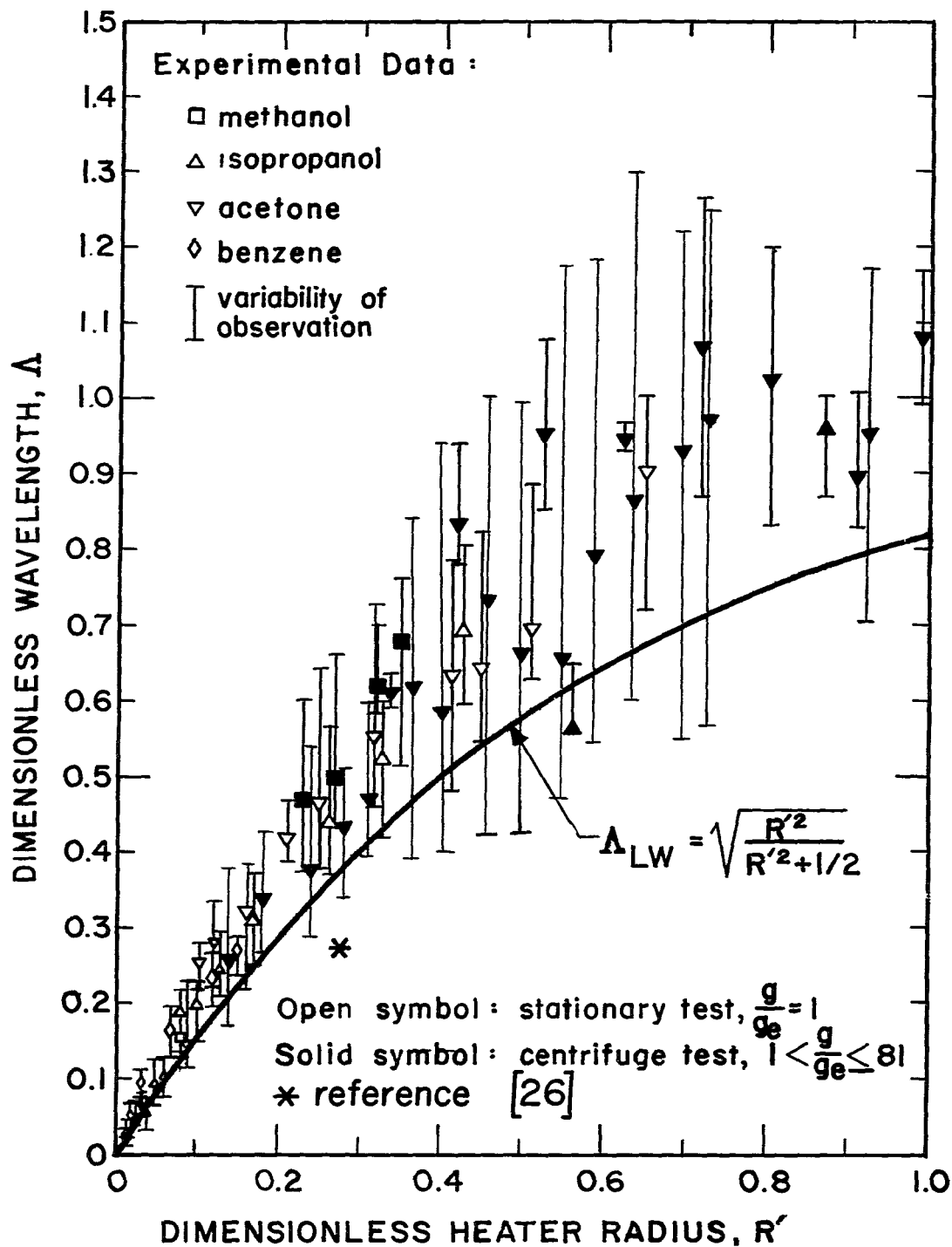
Fig. 8 Experimental wavelength on horizontal cylinders -- low R' range
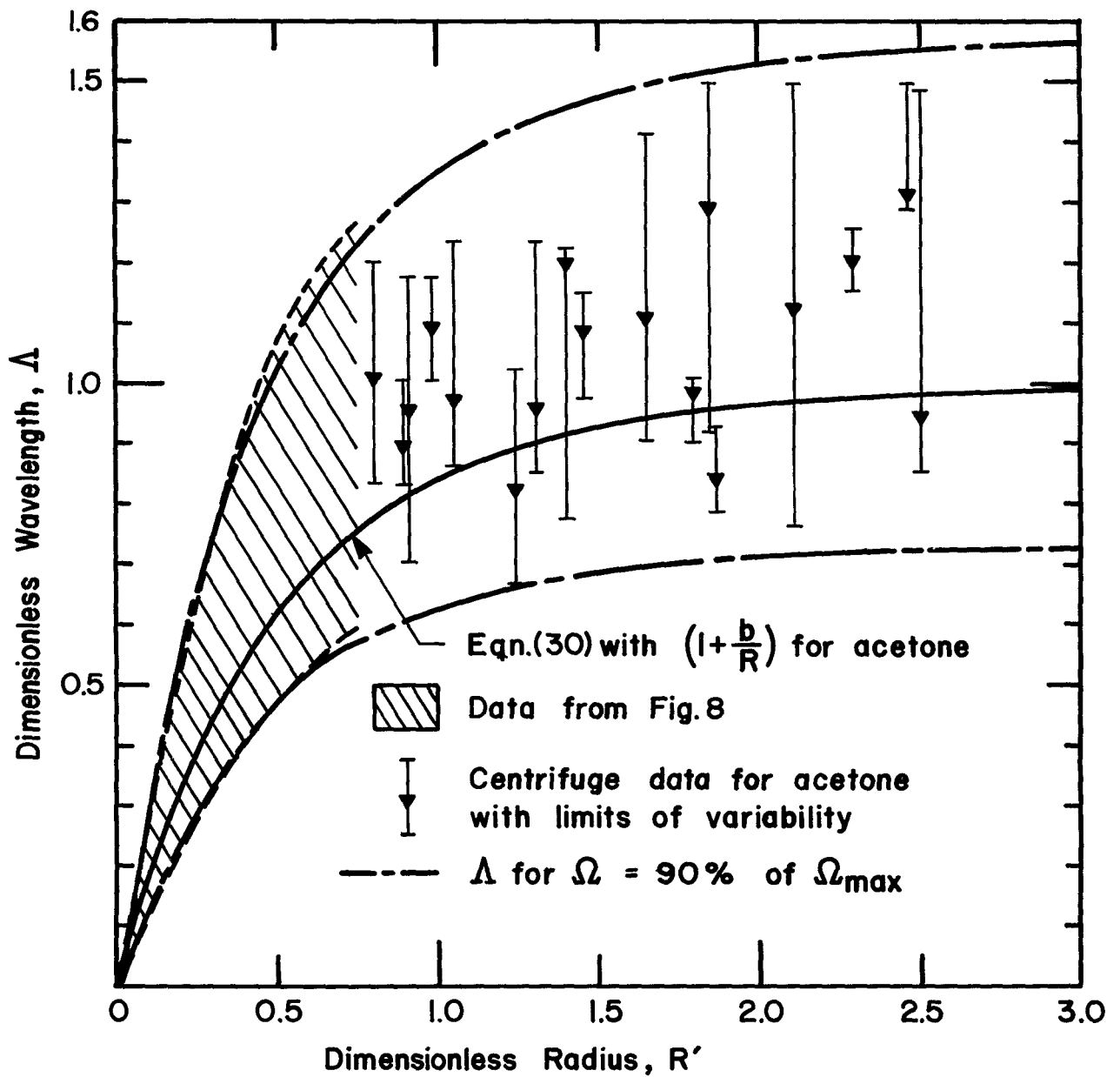
Fig. 9 Experimental wavelength on horizontal cylinders — — high R' range

Legend within figure:

Eqn.(30) with $\left(1+\dfrac{b}{R}\right)$ for acetone

Data from Fig. 8

Centrifuge data for acetone with limits of variability

Λ for $\Omega = 90\%$ of Ω_{max}

Axis labels:
Dimensionless Wavelength, Λ
Dimensionless Radius, R'

24

corresponds with a large Λ, even though λ is low at this high gravity.

On the basis of the photographic results, we find that the Lienhard-Wong description is quite valid in the range $0.12 \le R'< 0.9$, but that it deteriorates in the range $0.07 < R' < 0.12$. For $R' \le 0.07$, the bubble-merger mechanism is completely in control of vapor dynamics.

For $R' \ge 0.9$, the orderliness of the analytical model no longer exists in reality. Secondary wave motions and misalignment tend to disrupt the pattern. Fig. 6a appears to give only a reasonable first-order description of what is becoming an increasingly complicated phenomenon at larger R'. However, we were able to discern ragged waves up to $R' > 2.5$ and the Taylor theory still appears to account for the magnitude of these waves.

We now wish to reconsider the three predictions of Λ: equation (23a) or (30), equation (29), and equation (31). We have evaluated $(1+b/R)$ on the computer for acetone, using equation (32). Fortunately this expression is only very weakly dependent upon ΔT in the ranges of interest. It was safe to assume $\Delta T \simeq 333°C$ since an error of 2 or 3 hundred degrees would not seriously change the predicted value of $(1+b/R)$. This computation is probably not very precise, and it should only be viewed as indicative of the influence of b.

Figure 10 shows Λ_{LW}, Λ_{SK}, and Λ_{BH} together for comparison. The contribution of the vapor blanket thickness is slight in this case, as illustrated by the slight difference between the Λ_{LW} curves including and neglecting b. The Λ_{SK} and Λ_{BH} curves both fall beneath the Λ_{LW} curves and, as we can see in Fig. 9, the data fall on and above Λ_{LW}.

Thus, Λ_{SK} is probably based upon an erroneous description of the interface--at least in the range $R' \ge 0.07$. (A more detailed discussion of λ in the range $R' < 0.07$ will be deferred until later in this Chapter.) The fact that the Baumeister-Hamill result is so low probably reflects the comparative crudity of their model for the configuration. They solved a much more complete overall heat transfer problem and had to make stronger simplifying assumptions.

The broad variability of the wavelength data in Figs. 8 and 9 is explainable if we keep sight of the basic assumption underlying the prediction of both Λ_{LW} and Λ_{SK}. This is the supposition that λ is equal to λ_d, the wavelength for which the frequency, Ω, of oscillation is a maximum. Figure 11 shows a plot of Ω against Λ, based upon equation (22a). This plot shows that the relationship is almost neutrally stable over a broad range
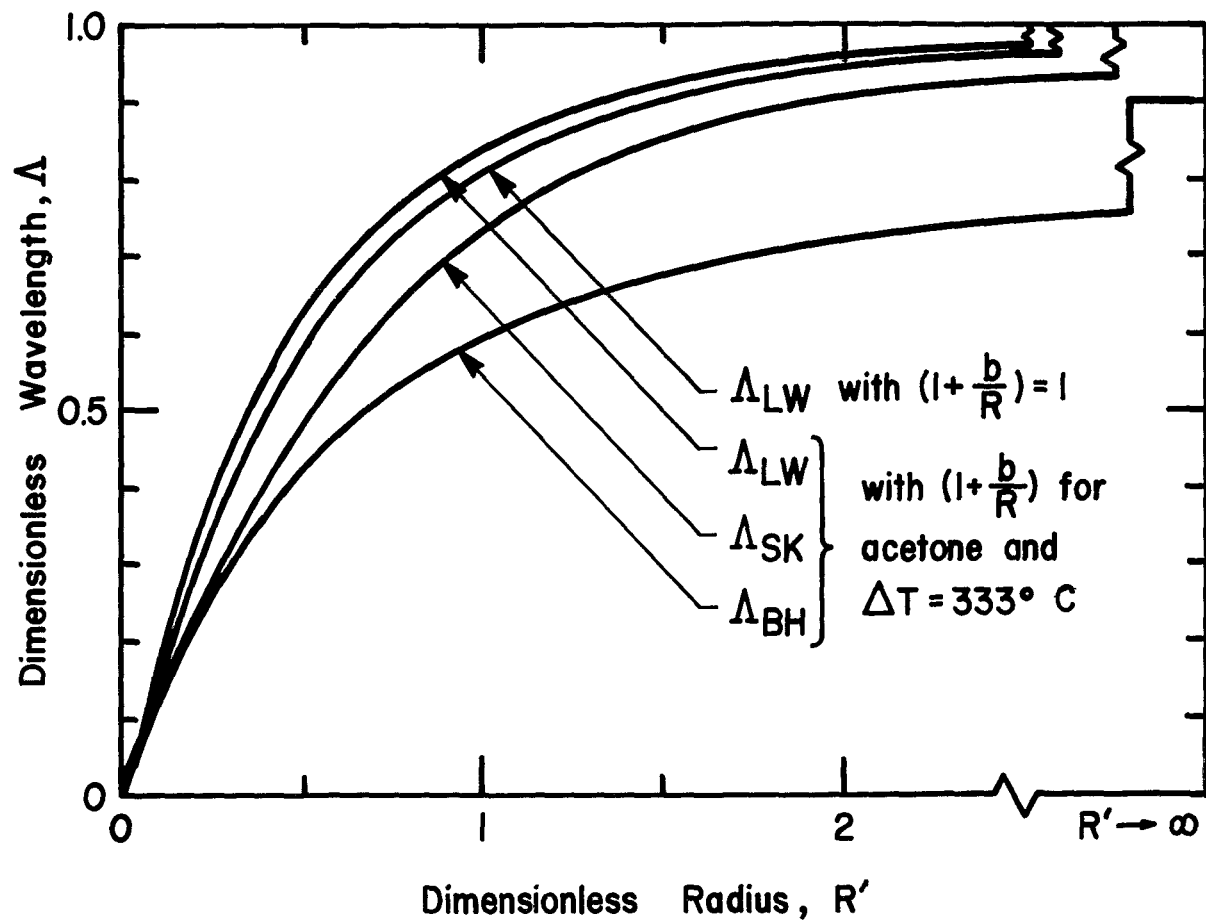
Fig. 10 Comparison of predictions of Λ
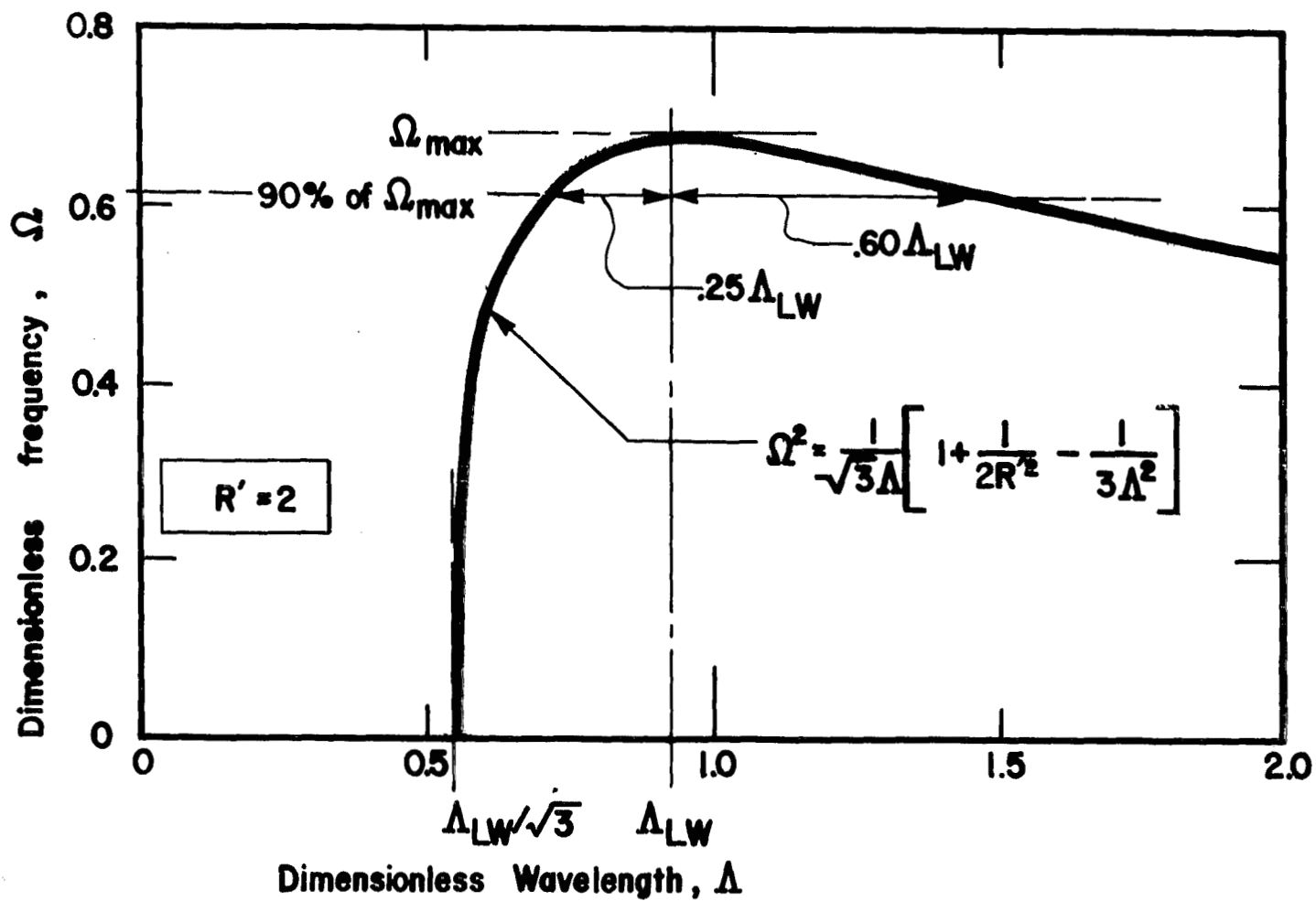
Fig. II Illustration of the variation of Λ in the vicinity of Ω_{max}

Ω_{max}

90% of Ω_{max}

$.60\,\Lambda_{LW}$

$.25\,\Lambda_{LW}$

$R' = 2$

$$\Omega^2 = \frac{1}{\sqrt{3}\Lambda}\left[1 + \frac{1}{2R'^{\frac{1}{2}}} - \frac{1}{3\Lambda^2}\right]$$

Dimensionless frequency, Ω

$\Lambda_{LW}/\sqrt{3}$ Λ_{LW}

Dimensionless Wavelength, Λ

27

of Λ. The narrow range of frequency, $\Omega \geq 0.9\Omega_{max}$, subtends a wavelength range of $0.75\Lambda_{LW} \leq \Lambda \leq 1.60\Lambda_{LW}$.

The implication is that there is a broad band of frequencies favored almost equally with Ω_{max}. We should therefore expect to measure wavelengths in the range of, say, $0.75\Lambda_{LW}$ to $1.6\Lambda_{LW}$. The choice of a 10 percent deviation of Ω below Ω_{max} is of course arbitrary, but the use of this band in Fig. 9 appears to match the observed variability of data quite well.

The Minimum Heat Flux

The fact that we can predict λ_d with reasonable accuracy under variable g conditions gives us added confidence in equation (6) for q_{min}, which was developed in [10] on the basis of the λ_d prediction. We also know that we must distrust equation (6) below R'=0.07 because the mechanism upon which it is based is no longer valid in this range.

In the present case we anticipate no influence of viscosity, there is no liquid-surface contact, and we expect that the major effects of elevated pressure have been accounted in the derivation of q_{min_F}. Thus equation (20) reduces to equation (8) for this case. Equation (6) is of this form, but Berenson's equation (14) should be used to express q_{min_F} instead of Zuber's equation (2). Thus equation (6) will change by a multiplying constant of $[\pi^2 \sqrt[4]{4/3}/60]/0.09$, and we obtain

$$\frac{q_{min}}{q_{min_F}} = \left[\frac{1.289}{R'^2(2R'^2+1)} \right] \tag{34}$$

Equation (34) can also be redeveloped to incorporate the vapor blanket thickness introduced through λ_d. To do this we must redo the analysis in reference [10]. This is straight forward and the result is not surprising. It is (cf. equation (29))

$$\frac{q_{min}}{q_{min_F}} = \left[\frac{1.289}{R'^2[2R'^2+(1+\frac{b}{R})^{-2}]} \right]^{1/4} \tag{34a}$$

On the basis of computations of (1+b/R) for typical situations, using equation (32), we can conclude that the blanket thickness will not alter q_{min}/q_{min_F} by more than a few percent in the worst cases. Therefore, we shall only consider predictions in the form of equation (34) and hereafter ignore equation (34a).

Before attempting to compare equation (34) with data, it is well to consider a serious experimental difficulty in obtaining q_{min} for horizontal cylinders. References [10], [2], and [11] refer to the difficulties of eliminating end effects which cause

28

the film-to-nucleate boiling transition to occur at heat fluxes above the true q_{min}. Very recently Kovalev [25] devised an experimental trick for determining the true q_{min}. He bent the ends of his horizontal cylindrical heater 90° into the vertical position and led them out of the bath. In doing so he removed the end effect problem and obtained q_{min} data that are probably reliable. His results are lower than other q_{min} data that have been reported at comparable conditions.

Another recent study by Grigull and Abadzic [26] gives q_{min} data for CO_2 and Freon-13 at extremely high reduced pressures, which we shall wish to consider. However, there is generally a paucity of reliable q_{min} data for cylinders, owing to the problems of end effects and surface impurities that affect so many sets of data. In particular, there is a lack of usable data in the range $R' > 1.0$.

Data from [10],[25], and [26] are compared with equation (34) in Fig. 12. The recent data of Kovalev and Grigull-Abadzic are lower than those from [10]--probably owing to even greater care taken to avoid end effects. The highest R' points in both the CO_2 and Freon-13 series were measured so near the critical temperature as to reflect some of the anomalous behavior associated with the critical point. Therefore we have entered these points with dashed lines. The Grigull-Abadzic paper also included one photo made at low R' and at 96 percent of the critical pressure, from which we extracted an approximate data point for inclusion in Fig. 8.

Since the multiplying constant in equation (34) is empirical, it should probably be chosen lower than it was in [10] to give a better representation of the ultimate hydrodynamic minimum film boiling heat flux. Accordingly we recommend

$$\frac{q_{min}}{q_{min_F}} = \left[\frac{0.0217}{R'^2(2R'^2+1)}\right]^{1/4} \tag{35}$$

for the real minimum as suggested by the data in Fig. 12. Equation (35) is included in Fig. 12.

From a practical viewpoint, however, equation (35) will almost always predict lower q_{min}'s than will be observed, since every normal experimental difficulty will tend to give values greater than the ultimate hydrodynamic minimum. For this reason Berenson [17] spoke of a minimum, minimum heat flux. Indeed, Kovalev's experiments cast the same kind of ugly light on q_{min} measurements that the early surface roughness measurements of Corty and Faust [27] cast upon nucleate boiling. In either case the variable of interest appears to become swamped by capricious system variables.
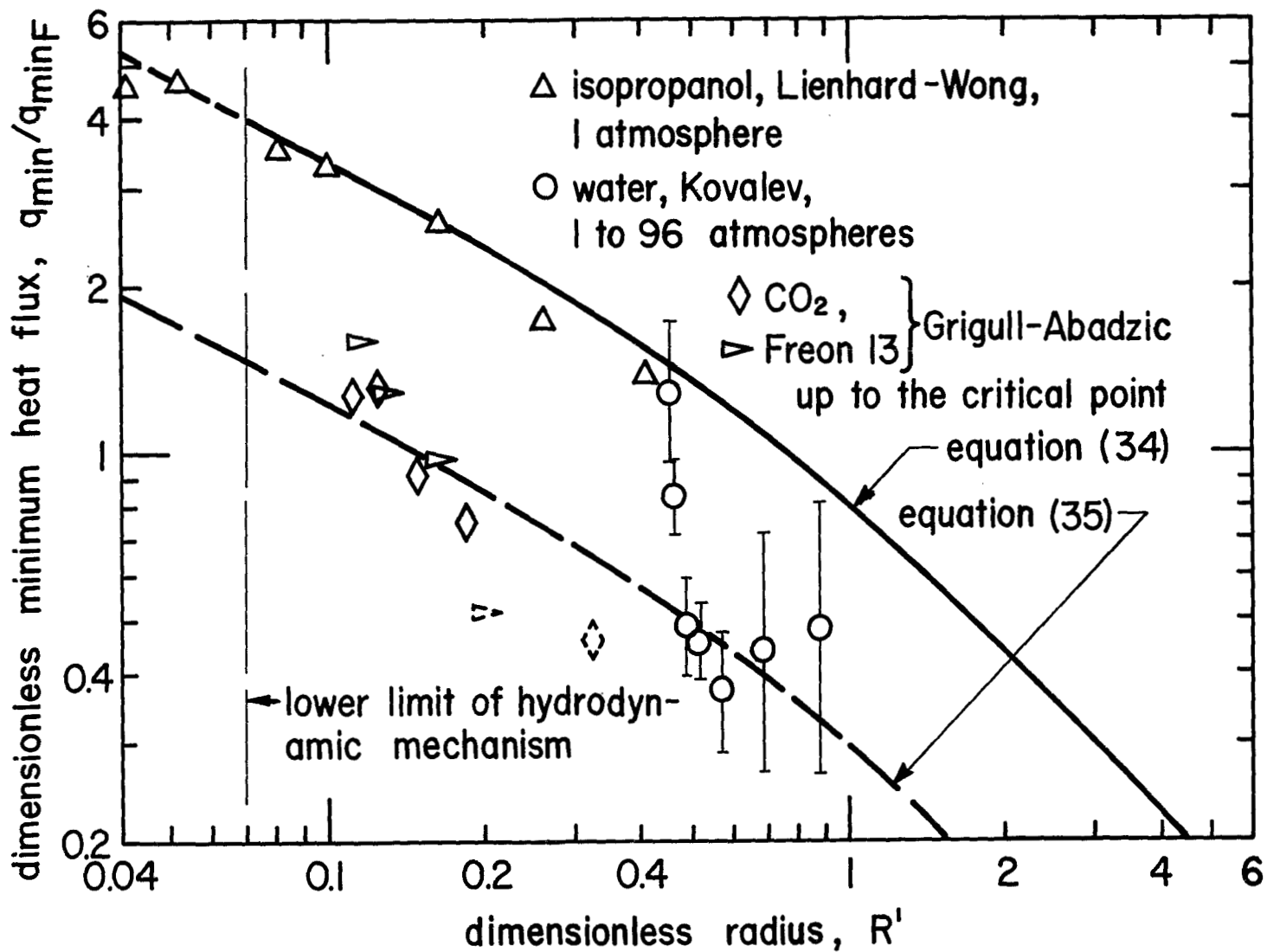
Fig. 12   Predicted and observed minimum heat fluxes on horizontal cylinders

The Limits of Large and Small R'

Large R'. The clean wave-collapse mechanism described in [10] and displayed in Figs. 7b through 7d or 7e loses its coherence as R' exceeds 0.9. Nevertheless, the observed "wavelengths" still obeyed equation (23) up to the limit of our experiments at R'=2.52--at least in-so-far as wavelengths could be identified. In this range, the measured values and equation (23) both approach λ_{d_F} as a limit.

There is some evidence that λ_{d_F} is approximately the correct limit for even larger R'. Pomerantz [28] measured heat transfer coefficients during the film boiling of Freon-113 on 3/16 in. diameter tubes, under variable gravity. He also gave three ranges of bubble spacings (which probably approximate Taylor wavelengths at his large R''s and relatively low heat fluxes). They reduce to

$$\Lambda(R' = 2.27) = 0.5 \text{ to } 2.32$$
$$\Lambda(R' = 4.55) = 0.59 \text{ to } 1.0$$
$$\Lambda(R' = 5.9) = 0.65 \text{ to } 1.18$$

All three of these values scatter widely about $\Lambda = 1$, or $\lambda_d = \lambda_{d_F}$. He also claimed an average value of $\Lambda = 1.1$ for his bubble spacings, which is consistent with the trend of our wavelength data. The early photographic study of Westwater and Santangelo [29] provides one very clear photograph of methanol in film boiling on a horizontal tube from which we obtain

$$\Lambda(R' = 3.03) = 0.80 \text{ to } 1.1$$

This also corroborates the trend at large R'.

These observed wavelengths at large values of R' are all probably low by a small but unknown amount owing to foreshortening, since the waves no longer align in the axial plane. Unfortunately, no one has yet documented the way in which three-dimensionality develops at large R'.

The minimum heat flux prediction--equation (35)--will be valid until these three-dimensional effects start to be significant. This will probably occur above R' = 2. Once the wave pattern ceases to align on the axis, more bubble releases can be accomodated on top of the wire, and the minimum heat flux should exceed the prediction. We have already noted that q_{min}/q_{min_F} should level out to a constant value (recall equation (21)). In the subsequent sections of this report we shall show that this is clearly the case for q_{max}/q_{max_F} in several configurations and for q_{min}/q_{min_F} in at least one other case.

But there are no reliable q_{min} data available for large radius horizontal cylinders, and the limiting behavior is simply not known at this time. A recent and very extensive survey of film and transition boiling by Jordan [30], for example, provides only one additional q_{min} data point that we might have used. This was quoted from [29] and was far too high to have represented a true minimum.

Small R'. The transition in the range $0.07 \leq R' \leq 0.12$, between the "bubble-merger" and the "wave-collapse" mechanisms is much more severe and far more distinct than the gradual deterioration of the wave-collapse mechanism at large R'. The following mechanism can be established for this transition:

A study of many photographs shows that bubble departure takes place roughly as shown in Fig. 13. The radius, $\lambda_d/16$, shown in the sketch appears to be characteristic of this configuration.

This sharp corner can exist as long as it is not opposed by an equally strong counter-curvature of the interface around the cylinder. But for small wires the counter-curvature will prevent the corner from indenting inward and nipping off the bubble. At this point the departing bubble will have to spread out before it can depart, and merge with its neighbors, if R is sufficiently small.

It is now possible to compare $\lambda_d/16$ with the radius of the wire at the observed transition from the wave-collapse mechanism to the bubble-merger mechanism. We have the condition:

$$R' \geq 0.07 \text{ for wave-collapse mechanism} \tag{36}$$

which becomes

$$\frac{R}{\lambda_{d_F}} \geq \frac{0.07}{2\sqrt{3}\pi} = 0.00644$$

But from equation (23a)

$$\left.\frac{\lambda_d}{\lambda_{d_F}}\right|_{R'=0.07} = \sqrt{\frac{0.07^2}{0.07^2 + 1/2}} = 0.0986$$

Therefore condition (36) takes the form

$$\frac{R}{\lambda_d} \geq \frac{0.00644}{0.0986} = \frac{1}{15.3}$$

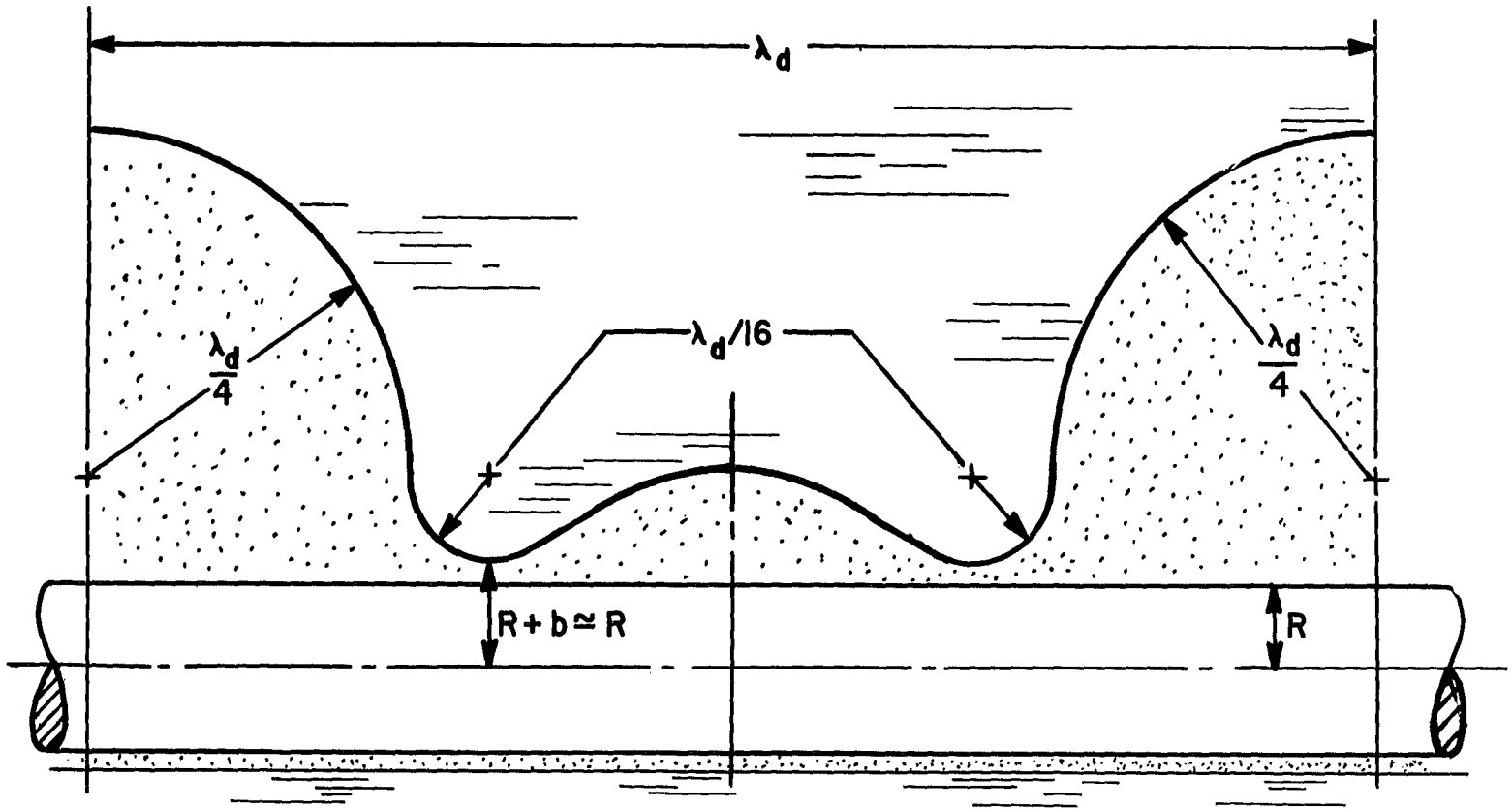which corresponds very well with photographic observations.

32

Fig. 13 Schematic representation of observed bubbled departure configuration during film boiling

The problem of developing a description of vapor removal from small cylindrical heaters in film boiling at low gravity remains to be done. So too does the prediction of q_{min}. When they are accomplished such analyses will focus upon a force balance between surface tension and buoyancy. They will not be based upon considerations of Zuber's capillary waves.

Conclusions

1. The best prediction of Λ that we presently can make is:

$$\Lambda = \sqrt{\frac{R'^2}{R'^2 + 1/[2(1+b/R)^2]}} \tag{30}$$

   where $(1+b/R)$ can best be estimated at present using equation (32). The variability of actual data will be slightly less than +60 percent and -25 percent because the wave motion approaches neutral stability over this range.

2. It is not relevant whether Λ is changed by varying, R, g, or the liquid being boiled. The single parameter, R', correctly accounts for all of these effects upon Λ.

3. Our best prediction of the absolute minimum q_{min} for horizontal cylinders is:

$$q_{min}/q_{max} = \left[\frac{0.0217}{R'^2(2R'^2 + 1)}\right]^{1/4} \tag{35}$$

4. For $R' < 0.07$ no mechanism has yet been formulated to describe the vapor removal process or q_{min}.

5. For $R' > 2$ the hydrodynamic mechanism for the vapor removal process is unclear and q_{min} is not known. Reliable q_{min} data and extensive photographs are needed in this range.

34

V. q_{max} ON HORIZONTAL CYLINDERS

Prefatory Remarks

Without doubt the most thoroughly studied pool boiling configuration todate has been the horizontal cylinder, and rightly so, since so many cylindrical heaters are used in practice. The quest for the influence of gravity on q_{max} has more often than not focused on this geometry (see, e.g., the review by Siegel [31]), and a great deal of data exist for cylinders under a variety of conditions.

To some 4 or 5 hundred existing q_{max} data we have added about 440 of our own. These data provide an extremely complete verification of our method of correlation and of the prediction that we shall offer. We shall first develop the prediction and then consider the available data.

The prediction will be based on the three assumptions suggested after equation (9). Of these, the second two assumptions—that θ_c and $\rho_g/(\rho_f-\rho_g)$ are unimportant—have been adequately discussed. The assumption that μ can be neglected will be largely justified ex post facto. It is not unreasonable because the flows induced by bubbles rising above a cylinder will not be drawn into the bubble departure pattern. The next Chapter will treat a different situation where this is not the case and μ is most important.

Under these assumptions we can anticipate that the general functional expression for q_{max}, equation (20), will reduce to the simple form

$$\frac{q_{max}}{q_{max_F}} = f(R')$$ (8)

This is the form that our predictions will have to take.

The previous Chapter showed that we should be alert for three regimes of hydrodynamic behavior. In the first $R' \ll 1$ and capillary forces completely overwhelm buoyant forces. For the moment this regime will be considered to lie outside of our range of interest since it cannot be treated by any adaptation of the hydrodynamic theory.

The middle regime is one in which capillary and buoyancy forces exert comparable influence and their ratio $(R')^2$ should be on the order of unity. This is the range in which we are presently interested, and any theory we reach should reflect a distinct interaction of these forces.

In the third regime--R' >> 1--the influence of capillary should cease to have any role in shaping and scaling the process. It is in this regime that theory should yield a result in the form of equation (21).

The primary assumption that must be made in formulating the problem is the idealization of the vapor removal configuration. Our vapor removal hypothesis is sketched in Fig. 14. We shall consider a horizontal cylindrical heater submerged in saturated liquid. Vapor is generated around the cylinder and rises in the direction of acceleration of the system. We imagine that there is a plane above the cylinder, where the bubbles from the upper half and lower half of the cylinder merge and form vapor columns. On this plane, the liquid is supported by the vapor in a Taylor-instable interface. The jets will be spaced on the Taylor-instable wavelength, λ_{dF}. This wavelength is chosen in preference to the wavelength for a cylindrical interface since the configurations shown in Fig. 6 were not replicated in our observations of boiling at the peak heat flux transition.

Figure 15 includes five typical photographs of boiling just below the peak heat flux transition, over the range $0.0695 \leq R' \leq 2.68$. These are typical of some 640 such pictures that we made to serve as a basis for the several suppositions made thus far about the character of the process, and for those that will be made subsequently.

q_{max} for R' on the Order of Unity

We shall base the analysis upon consideration of a "unit cell" of one wavelength, λ_{dF}. If A_H is the area of the heater surface within a cell and A_g is the cross-sectional area of a vapor jet, then

$$\frac{A_g}{A_H} = \frac{\pi (R+\delta)^2}{2\pi R \lambda_d} = \frac{(R+\delta)^2}{2R\lambda_d} \tag{36}$$

The heat flux, q, from the heater during saturated boiling is balanced by the latent heat carried away in the vapor bubbles. Since all the bubbles merge and form vapor jets with area, A_g, we can write an energy balance in the form

$$q = \rho_g \, h_{fg} \, U_g \, \frac{A_g}{A_H} = \rho_g \, h_{fg} \, U_g \, \frac{(R+\delta)^2}{2R\lambda_d} \tag{37}$$

where U_g is the velocity of the vapor in the jet. The heat flux reaches q_{max} when the velocity of the vapor jets reaches the critical value, U_{gc}, at which they become Helmholtz-instable.

36

(a) Vapor jets from the heater surface.
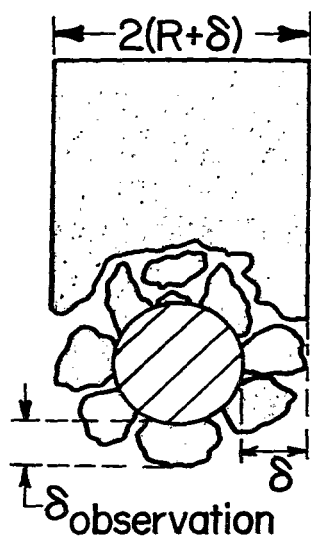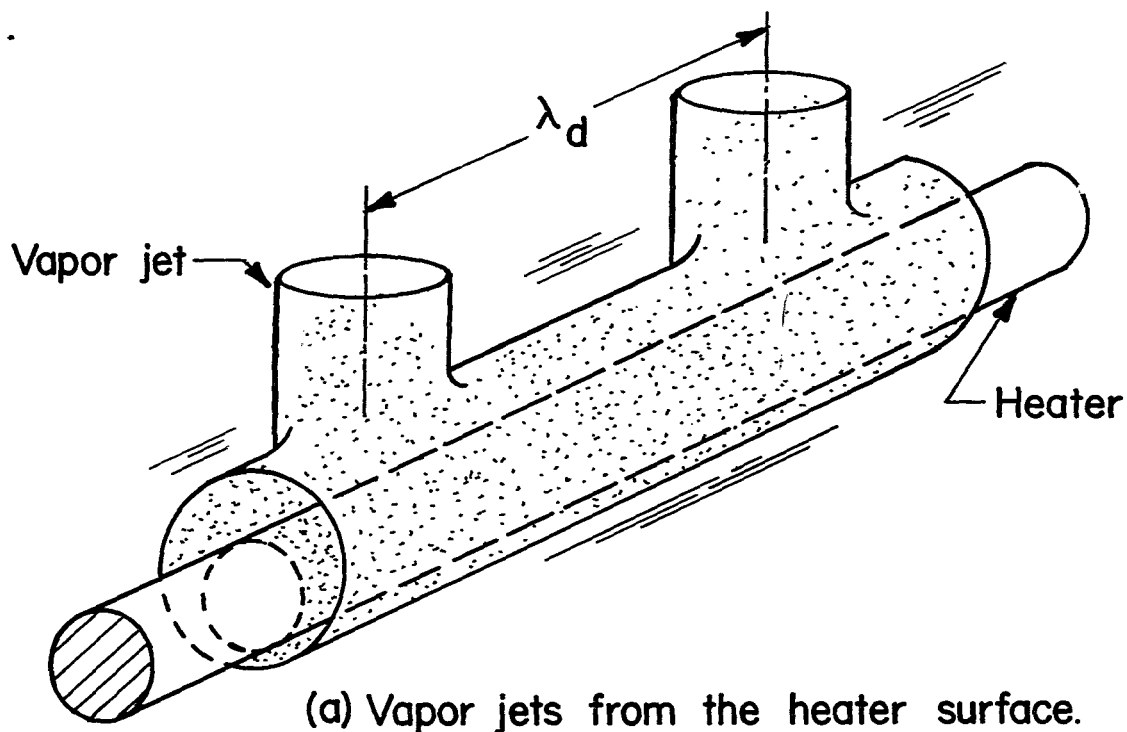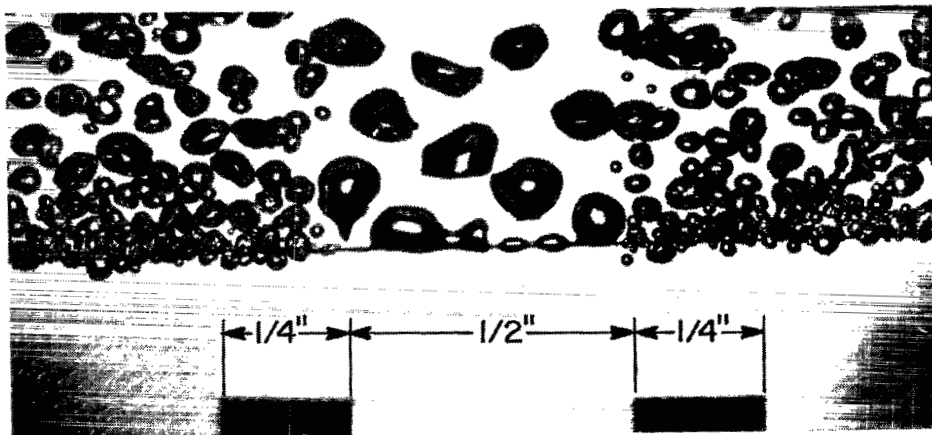

(b) Cross-sectional view of a vapor jet.

Fig. 14 Model for the peak pool boiling heat flux on horizontal cylindrical heater, (R' on the order of unity).

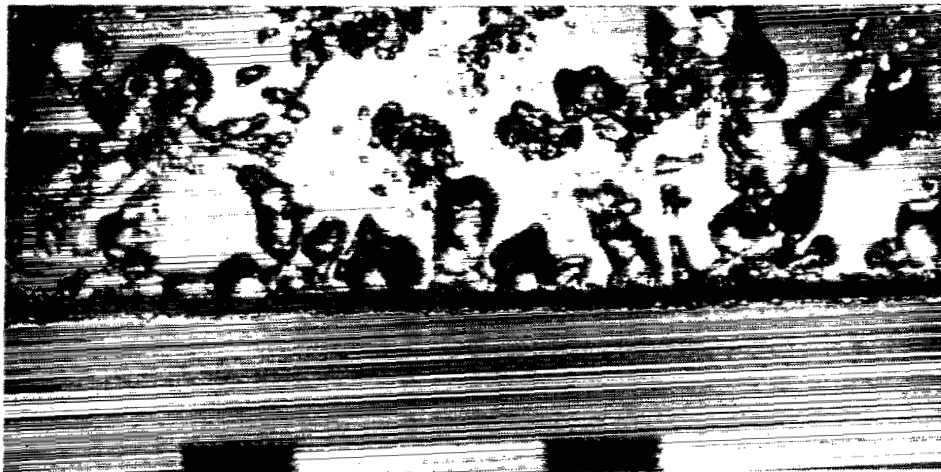a) $g/g_e=1$, R=.0102 cm, methanol, q=11.9 cal/cm^{2}sec, R'=.0645

b) $g/g_e=1$, R=.0647 cm, benzene, q=8.35 cal/cm^{2}sec, R'=.388

c) $g/g_e=9.9$, R=.0322 cm, methanol, q=24.85 cal/cm^{2}sec, R'=.642

Fig. 15   Photographs of nucleate boiling at q just below q_{max}

38

d) g/g_e=14.7, R=.0508 cm, isopropanol, q=17.7 cal/cm^{2}sec, R'=1.281

e) g/g_e=26.8, R=.0811 cm, methanol, q=23.4 cal/cm^{2}sec, R'=2.68

Fig. 15   Continued

Therefore,

$$q_{max} = \rho_g \; h_{fg} \; U_{gc} \; \frac{(R+\delta)^2}{2R\lambda_d} \tag{37a}$$

Next, we must determine U_{gc}. We shall assume, as Zuber did, that the Helmholtz-instable collapse of the jet occurs as a result of a major disturbance arising from Rayleigh's capillary instability. According to Rayleigh [32, p.473], the minimum wavelength that will be capillary-instable is one circumference, or $2\pi(R+\delta)$, in length. This will be the major disturbance in the jet and it will be Helmholtz-instable when U_g reaches a value U_{gc} such that [32, p.462]

$$2\pi(R+\delta) \;=\; 2\pi \; \frac{\rho_f + \rho_g}{\rho_f \; \rho_g} \left[\frac{\sigma}{(U_f + U_{gc})^2} \right] \tag{38}$$

Thus, if we neglect the velocity, U_f, of liquid in-flow, and employ the equivalent assumption, $\rho_g << \rho_f$,

$$U_{gc} = \sqrt{\frac{\sigma}{\rho_g (R+\delta)}} \tag{39}$$

Substituting equation (39) into equation (37) gives the equation for the peak heat flux on a horizontal cylinder

$$q_{max} = \frac{(R+\delta)^2}{2R\lambda_{d_F}} \; \rho_g \; h_{fg} \sqrt{\frac{\sigma}{\rho_g (R+\delta)}} \tag{40}$$

While the radius of the cylinder and the physical properties are known, the vapor blanket thickness, δ, remains to be determined. If we define a dimensionless vapor blanket thickness

$$\Delta \equiv \delta [g(\rho_f - \rho_g)/\sigma]^{1/2} \tag{41}$$

and combine equations (25) and (41) with equation (40), we get

$$q_{max} = \left\{ \frac{\pi}{24} \; \sqrt{\rho_g} \; h_{fg} \; [\sigma g(\rho_f - \rho_g)]^{1/4} \right\} \left\{ \frac{6}{\pi^2 \sqrt{3}} \; \frac{(R'+\Delta)^{3/2}}{R'} \right\} \tag{42}$$

The first group on the right hand side of equation (42) contains a constant which has been balanced against the second term so that it matches Zuber's flat plate prediction, q_{max_F}. Thus

$$\frac{q_{max}}{q_{max_F}} = \frac{6}{\pi^2 \sqrt{3}} \; \frac{(R'+\Delta)^{3/2}}{R'} \tag{43}$$

where Δ remains to be determined as a function of R', with the help of experiments.

Prediction of q_{max} for $R' \gg 1$

We have assumed that vapor jets with a radius of $(R+\delta)$ are spaced on the wavelength, λ_{d_F}. But λ_{d_F} decreases with increasing gravity, g, so the spacing between jets will decrease as R' increases. According to the previous analytical model, the jets will touch one another when $(R'+\Delta)$ reaches $2\pi\sqrt{3}/2$. However, we did not see this happen in the present investigation of pool boiling.[5] Therefore, the preceding model should fail at some $(R'+\Delta)$ smaller than $\pi\sqrt{3}$. An illustrative sequence of sketches showing the supposed variation of the jets with increasing R' is given in Fig. 16.

When R' is small, the unstable wavelength, λ_d, is greater than twice the jet diameter, $4(R+\delta)$, as shown in Fig. 16a. As R' increases, the difference between λ_d and $4(R+\delta)$ becomes smaller. We believe that, when R' is very large, the open space between two jets will be equal to $2(R+\delta)$ and the jet configuration will remain unchanged. The jets will stay as shown in Fig. 16c instead of moving any closer as indicated in Fig. 16b. This is analogous to Zuber's assumption that the jet diameter on a flat plate is equal to the open space between two jets, and our photographic studies verified that it is a realistic assumption.

When R' becomes very large, disturbances with the wavelength, λ_d, will exist in the horizontal vapor-liquid interface, but they will be much smaller than the jet diameter. The vapor jets will pick up these disturbances from the intervening liquid-vapor interface. It is probably this disturbance that triggers Helmholtz-instability instead of the longer wavelength of the Rayleigh-instability. Thus we shall assume that the jet diameter is $2(R+\delta)$, but that the distance between centerlines of jets is $4(R+\delta)$ instead of λ_{d_F}. Finally, we use λ_{d_F} instead of $2\pi(R+\delta)$ for the left-hand side of equation (38) and obtain
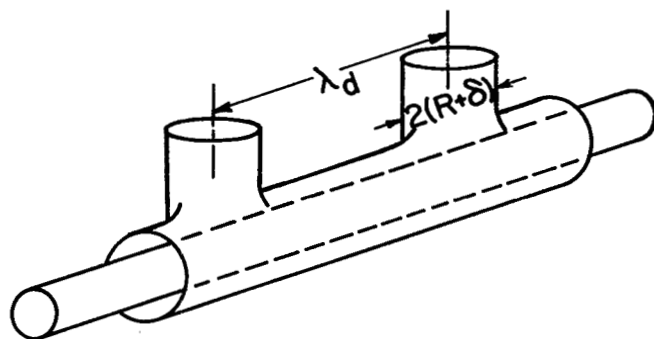
$$U_{gc} = \sqrt{\frac{2\pi\sigma}{\rho_g \lambda_{d_F}}} \tag{44}$$
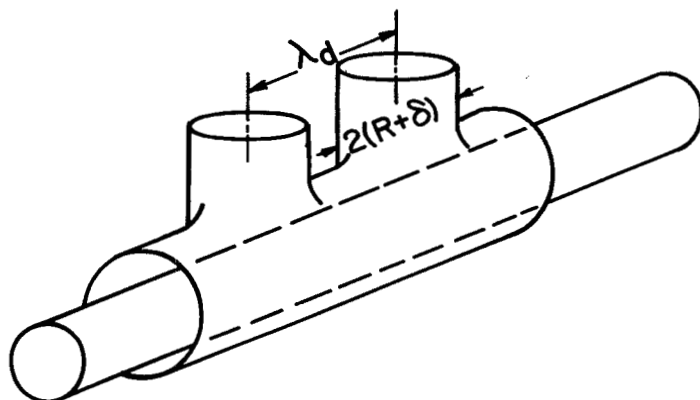
in the place of equation (39).

Combining equations (25) and (44) with equation (37) gives

$$q_{max} = \left[\frac{\pi}{24} \rho_g \, h_{fg} \sqrt[4]{\frac{\sigma g (\rho_f - \rho_g)}{\rho_g^2}}\right] \left[\frac{3^{3/4}}{\pi} \frac{(R'+\Delta)}{R'}\right] \tag{45}$$
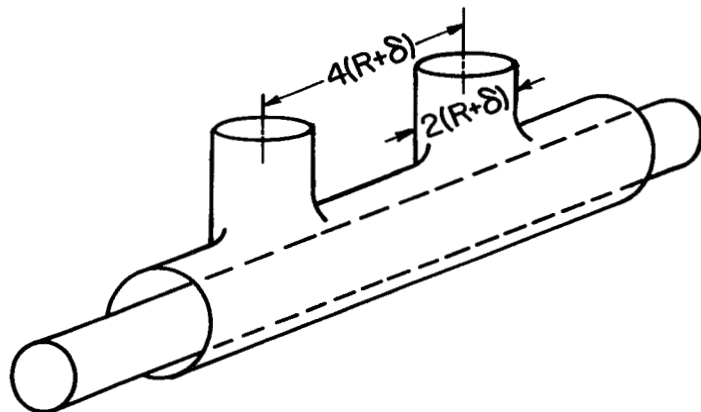
---

[5] It was observed by Vliet and Leppert [33] that, in a strong forced convection boiling system, no jetting occurred. The vapor appeared instead to cover the whole wake region of the cylinder.

(a) small R', $\lambda_d > 4(R+\delta)$

(b) $\left[\lambda_d - 2(R+\delta)\right]$ cannot be much less than $2(R+\delta)$

(c) $R' + \triangle \geq 4.28$, suggested model for $R' \rightarrow \infty$

Fig. 16   Variation of jet spacing as R' changes

or

$$\frac{q_{max}}{q_{max_F}} = \frac{3^{3/4}}{\pi} \frac{(R'+\Delta)}{R'} \tag{46}$$

Equations (43) and (46) should each give the same peak heat flux at the point where one configuration shifts to another. Thus, we can write, for this particular value of R',

$$\frac{3^{3/4}}{\pi} \frac{(R'+\Delta)}{R'} = \frac{6}{\pi^2\sqrt{3}} \frac{(R'+\Delta)^{2/3}}{R'} \tag{47}$$

This gives, for the transition between the two analytical models,

$$R' + \Delta = 4.28 \tag{48}$$

Finally, the expression for q_{max} at very large R' should become

$$\frac{q_{max}}{q_{max_F}} = \frac{3^{3/4}}{\pi} \frac{R'+\Delta}{R'} = \text{constant}, \quad R' + \Delta \geq 4.28 \tag{46a}$$

where the dimensionless vapor blanket thickness still must be determined. Once Δ is known at (R'+Δ)=4.28, the constant in equation (46a) can be fixed.

The jet diameter reaches $\lambda_d/2$ at (R'+Δ)=$\pi\sqrt{3}/2$ according to the model for R' on the order of unity. Beyond this size the open space between the two jets must become less than the jet diameter (or, conversely, the jet spacing might start to increase beyond λ_d) until (R'+Δ) reaches 4.28. Thus (R'+Δ)=4.28 is actually the upper bound for a transition which might occur gradually over the range $\pi\sqrt{3}/2 <$ (R'+Δ) < 4.28.

The two predictions--equations (43) and (46)--require measurements of δ before they can be completed, and they require considerable q_{max} data for verification. But we shall first consider the correlation of q_{max} data in accordance with equation (8).

Correlation of q_{max} Data

A total of about 900 q_{max} data were collected, both from the present experiments and from other sources. These observed q_{max} were divided by Zuber's q_{max_F}, which was computed with some care in [13] and is plotted for typical fluids in Fig. 17.

Figure 18 displays the present data, as well as data of Cumo, Farello and Pinchera [34] and Lienhard and Watanabe [2],
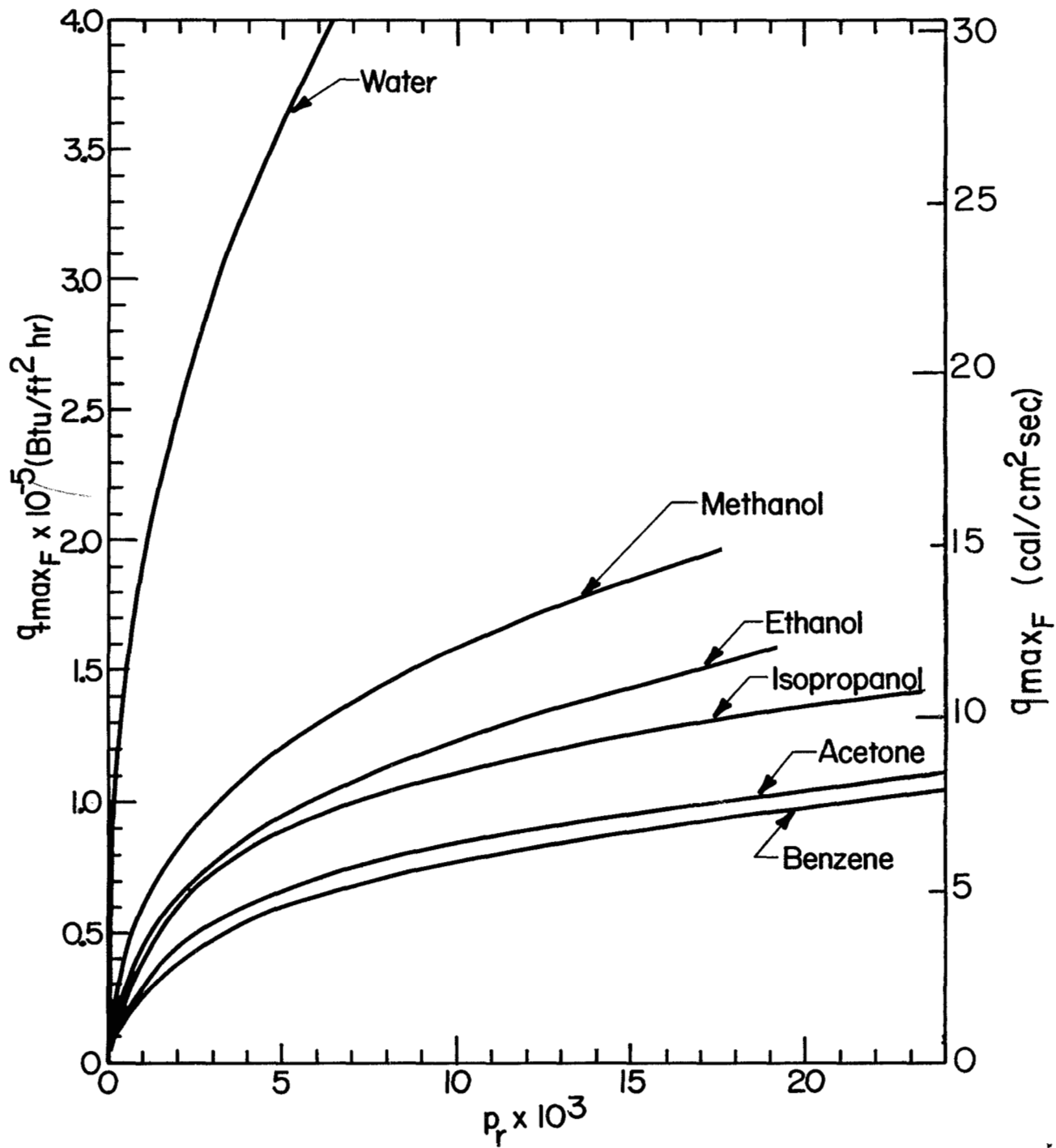
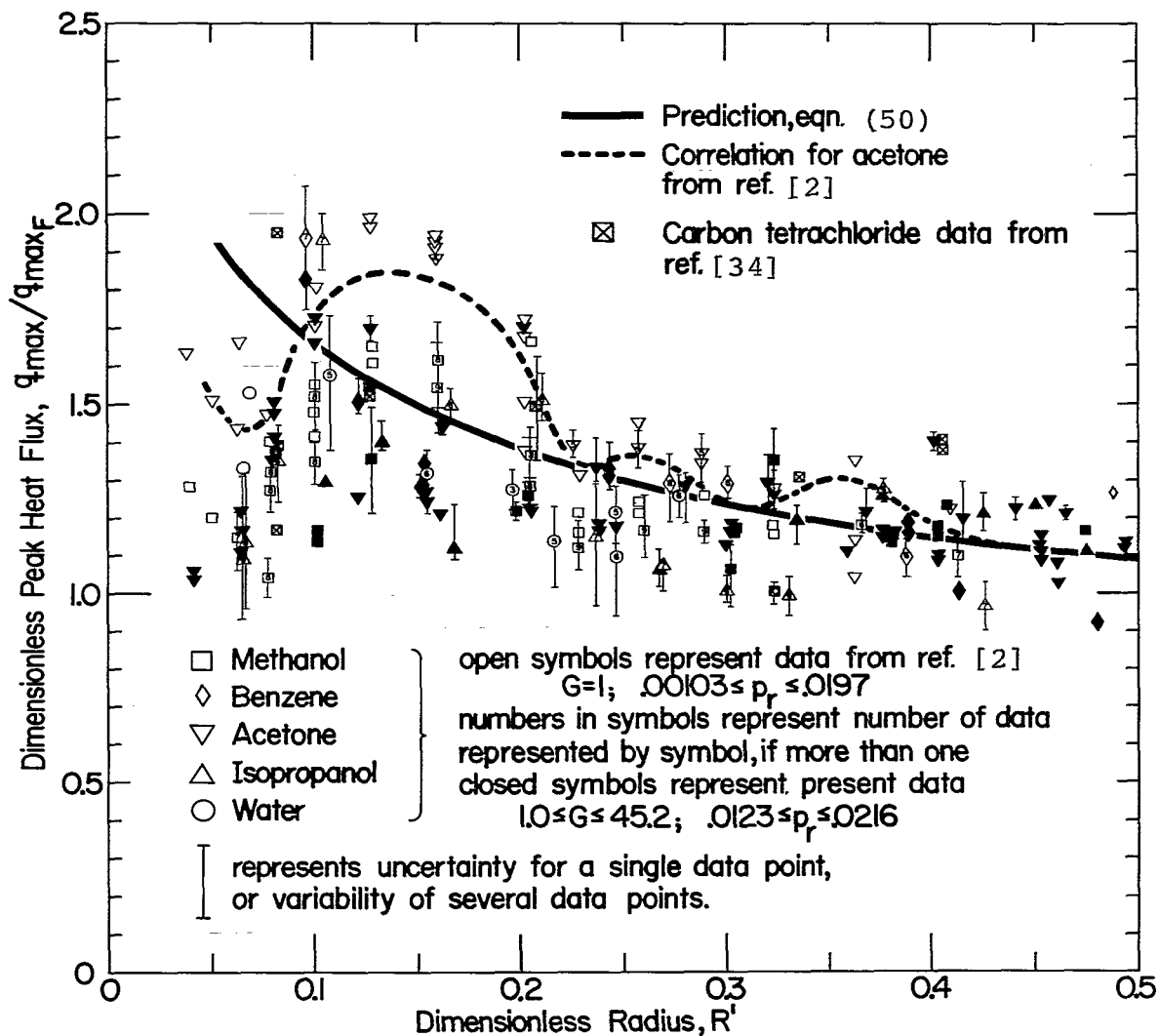Fig. 17   Zuber's q_{max_F} prediction for flat plate heaters

Fig. 18   Comparison of prediction with experimental data for R' < 0.50

in the range R'<0.5. It includes data for acetone, benzene, carbon tetrachloride, isopropanol, methanol, and water over wide ranges of pressure, gravity, and heater size. The variability of the data is on the order of ±20 percent except when R'<0.15.

The correlation curve from reference [2] has also been included as a dashed line. This curve was originally presented on different coordinates, and in placing it in Fig. 18 we have favored the original data for acetone, slightly. The small irregularities in this correlation are probably the result of minor changes in the transition mechanism, too small to be accounted in our relatively coarse analysis.

Figure 19 shows our data for a larger range of R'. Data given by Adams [35], Carne [36], Costello and Heath [37], Cumo, Farello and Pinchera [34], Frea and Costello [38], and Pramuk and Westwater [39] are also included. All these data correlate consistently in q_{max}/q_{max_F} versus R' coordinates.

Figure 20 shows our data for high R' and additional data from references [35] and [37]. The data appear to approach a constant value of q_{max}/q_{max_F} for large R' as we anticipated. This tendency was also observed by Lienhard and Keeling [15] in their study of horizontal ribbon heaters. Lyon's [18] data for boiling liquid N_2 and O_2 are also included in Fig. 20. They all fall within the scatter of ±20 percent.

Figure 21 is a general view of the results of the correlation. A variety of very low R' data obtained by Siegel and Howell [5] under reduced-gravity conditions are also included. The correlation is shown to be very successful with the existing data for all R'>0.15, but when R'<0.15, the data show a wide scatter.

The success of equation (8) in bringing together so many diverse data indicates that the three assumptions upon which it is based must be correct. In particular, it is most heartening to discover that neither surface condition nor viscosity has proved to be important--at least for R'>0.15.

In the present study, we have collected data for many smooth and very clean surfaces, in which only θ_c might have been subject to variation. Only in the very low R' range do we discover a failure of the simple correlation scheme. This might imply either technical difficulties in obtaining the experimental data or that equation (8) is incomplete in the low R' range. In particular θ_c or I might be important independent variables. The photographic studies (see, e.g., Fig. 15a) showed that bubble growth and merger mechanisms govern the vapor removal process at very small R'. In this range, both viscosity and contact angle may become very significant.
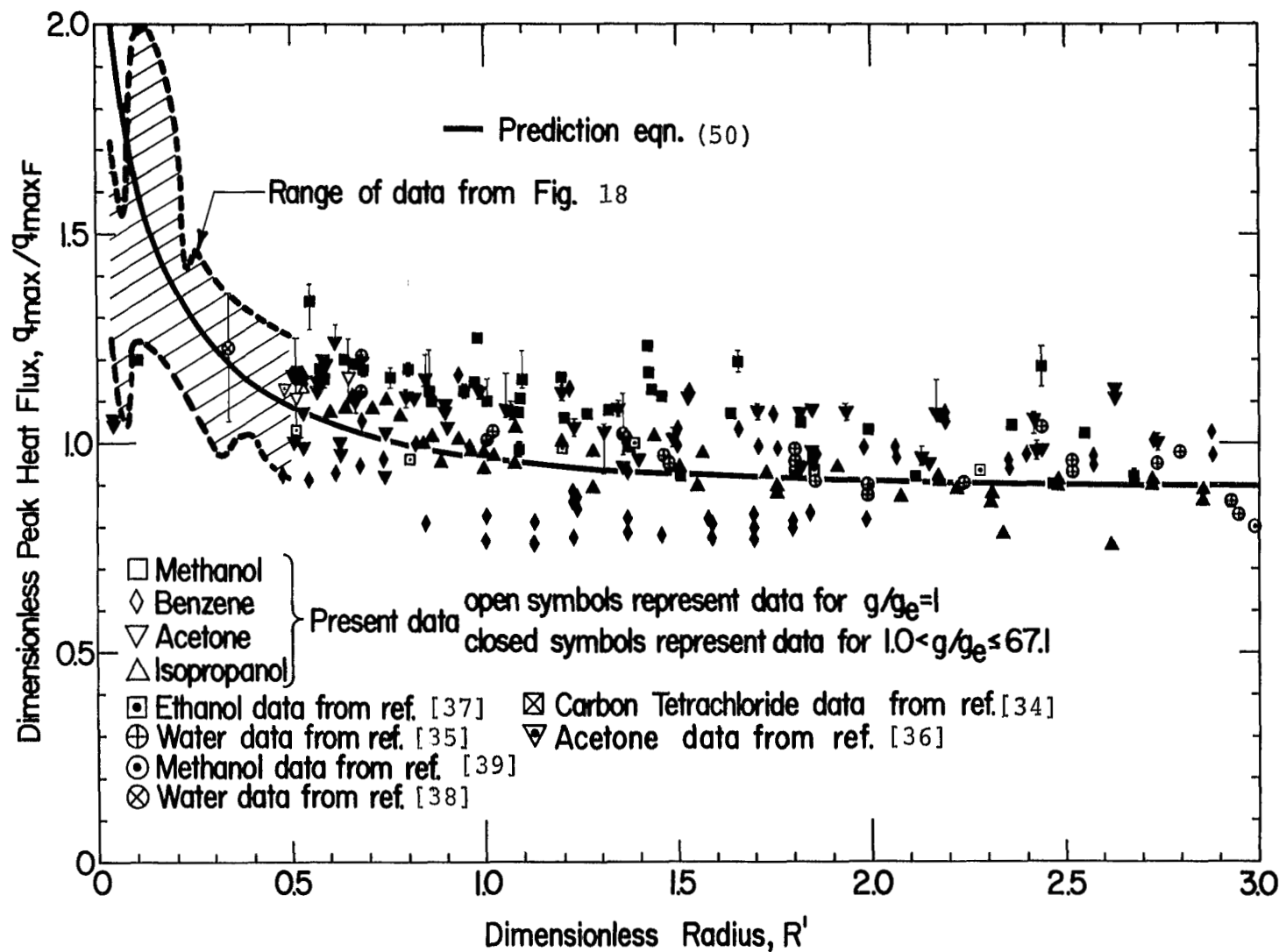
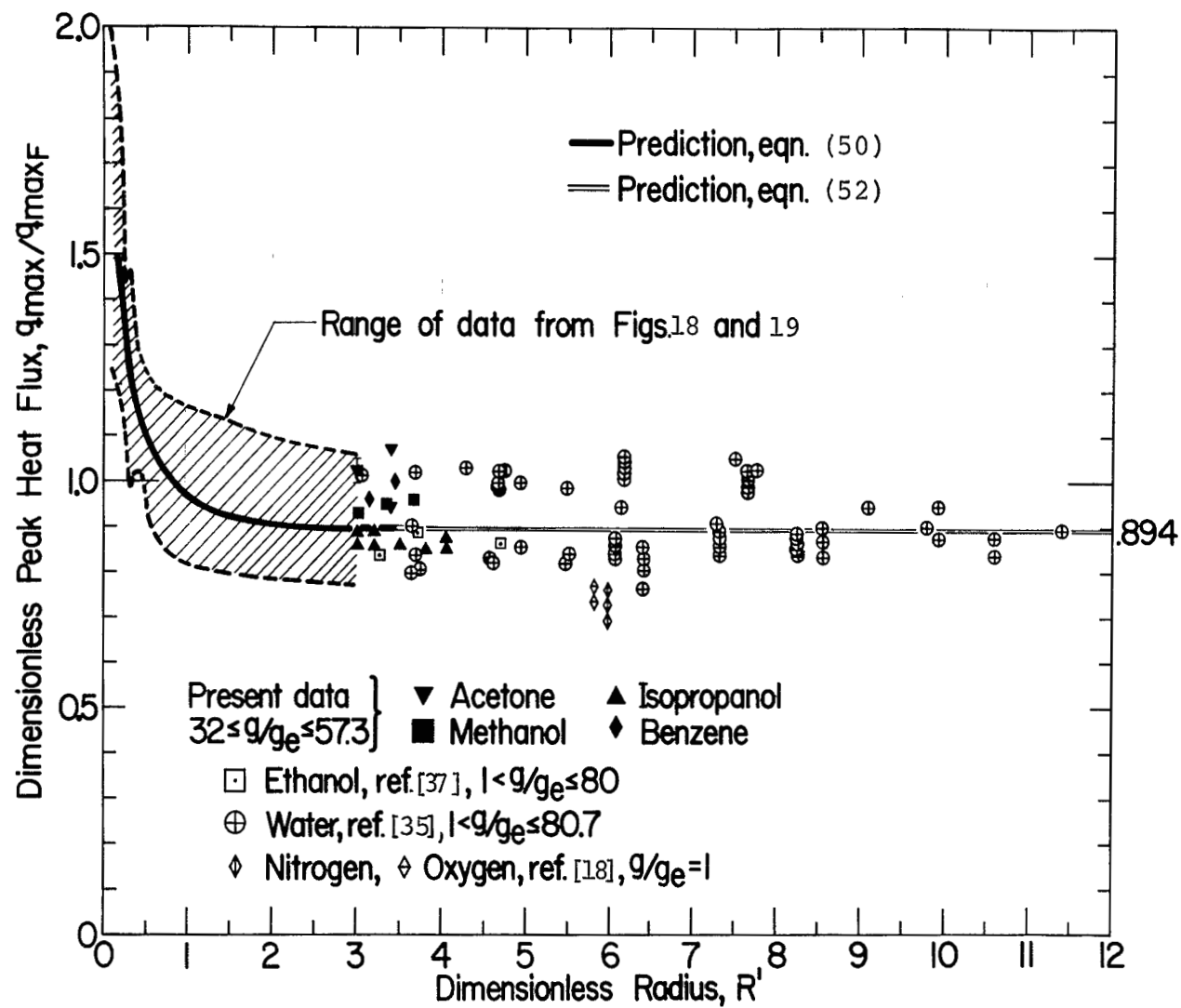Fig. 19 Comparison of prediction with experimental data for R'<3.0

Fig. 20 Comparison of prediction with experimental data for very large R'.
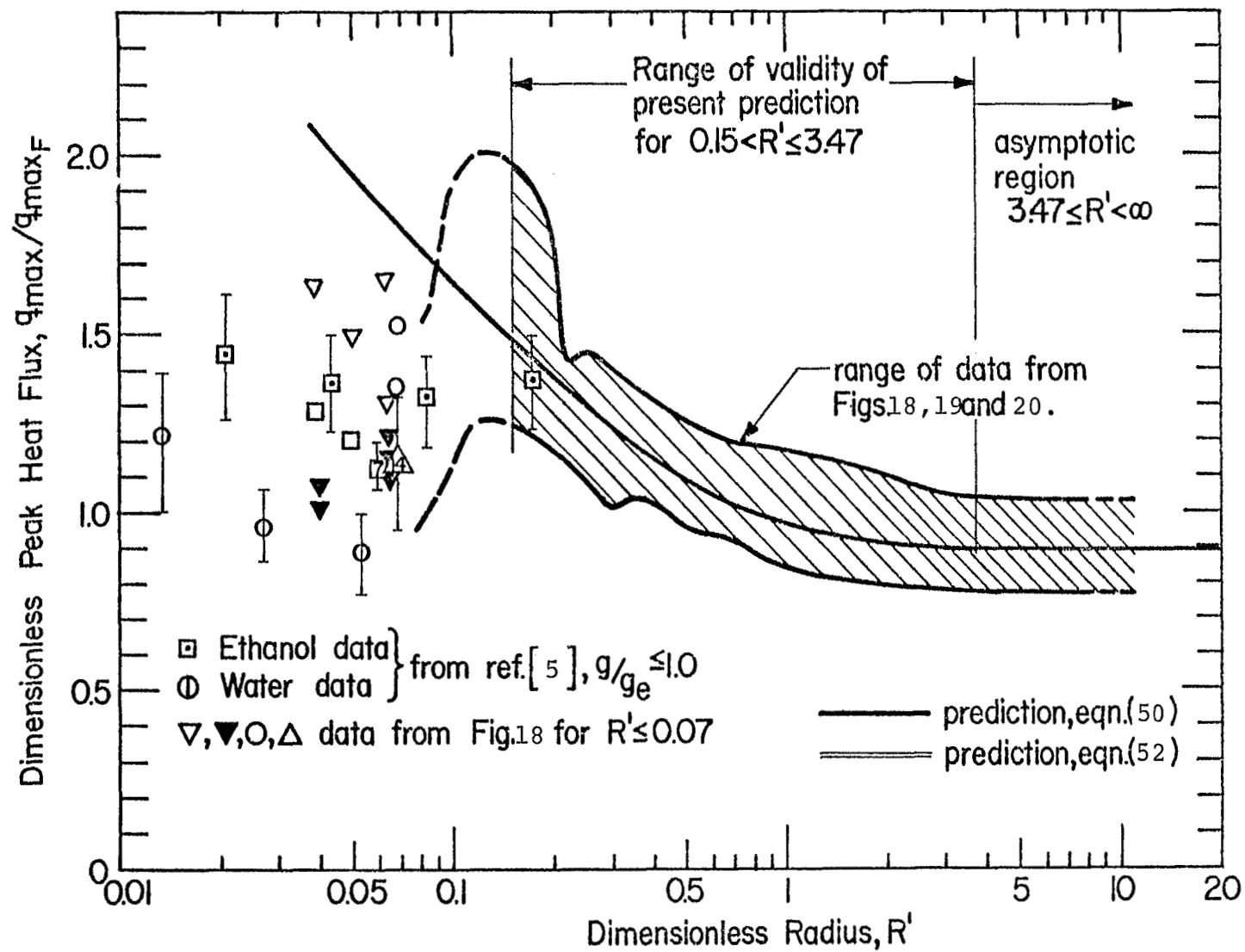
Fig. 21 General view of the results of the present correlation.

Experimental Determination of $\Delta(R')$ and
Completion of Predictions

We have now verified the functional equation for q_{max} by showing that data correlate in the dimensionless coordinates of this expression. Our prediction equations are also of this form so we can now be fairly optimistic about their success.

To complete the predictions, however, it is necessary to evaluate $\Delta = \Delta(R')$. This was done by measuring the vapor blanket thickness from the photographs. Since the blanket has to be viewed from the side, δ cannot be measured on the horizontal diametral plane. Hence, we had to approximate δ with a measurement of the blanket thickness on the bottom part of the cylinder as shown in Fig. 14b.

Figure 22 displays the measurements of δ. In an attempt to compensate the fact that the blanket might not be fully developed at the bottom, we have reported the range from the approximate mean, to the maximum size of the bubbles comprising the blanket. A data point measured from an early photograph by Westwater and Santangelo [29] is also included. The uncertainty of these measurements is on the order of ± 20 percent. No attempt was made to measure δ in the range of $R' < 0.15$.

If we had to combine the envelope of the data from Fig. 21 with equation (43), we can specify a range of Δ, consistent with the q_{max} theory, for each value of R'. The result is plotted in Fig. 22. Virtually all the measurements of δ fall within this envelope.

The "best fit" empirical equation, based on both this envelope and the data for δ, is

$$\Delta = [2.54 \ R' + 6.48 \ R' \ \exp(-3.44 \ \sqrt{R'})]^{2/3} - R' \qquad (49)$$

in the range: $0.15 < R' < 3.5$. The form of equation (49) is chosen so as to give a neat form for the q_{max}/q_{max_F} equation that we shall develop next.

The substitution of equation (49) in equation (43) yields

$$\frac{q_{max}}{q_{max_F}} = 0.89 + 2.27 \ \exp(-3.44 \ \sqrt{R'}) \qquad (50)$$

Equation (50) is plotted in Figs. 18, 19, 20, and 21 and it shows very good agreement with the existing data.

The upper limit of equation (50)--the transition point between the two models--is determined by equation (48). With the
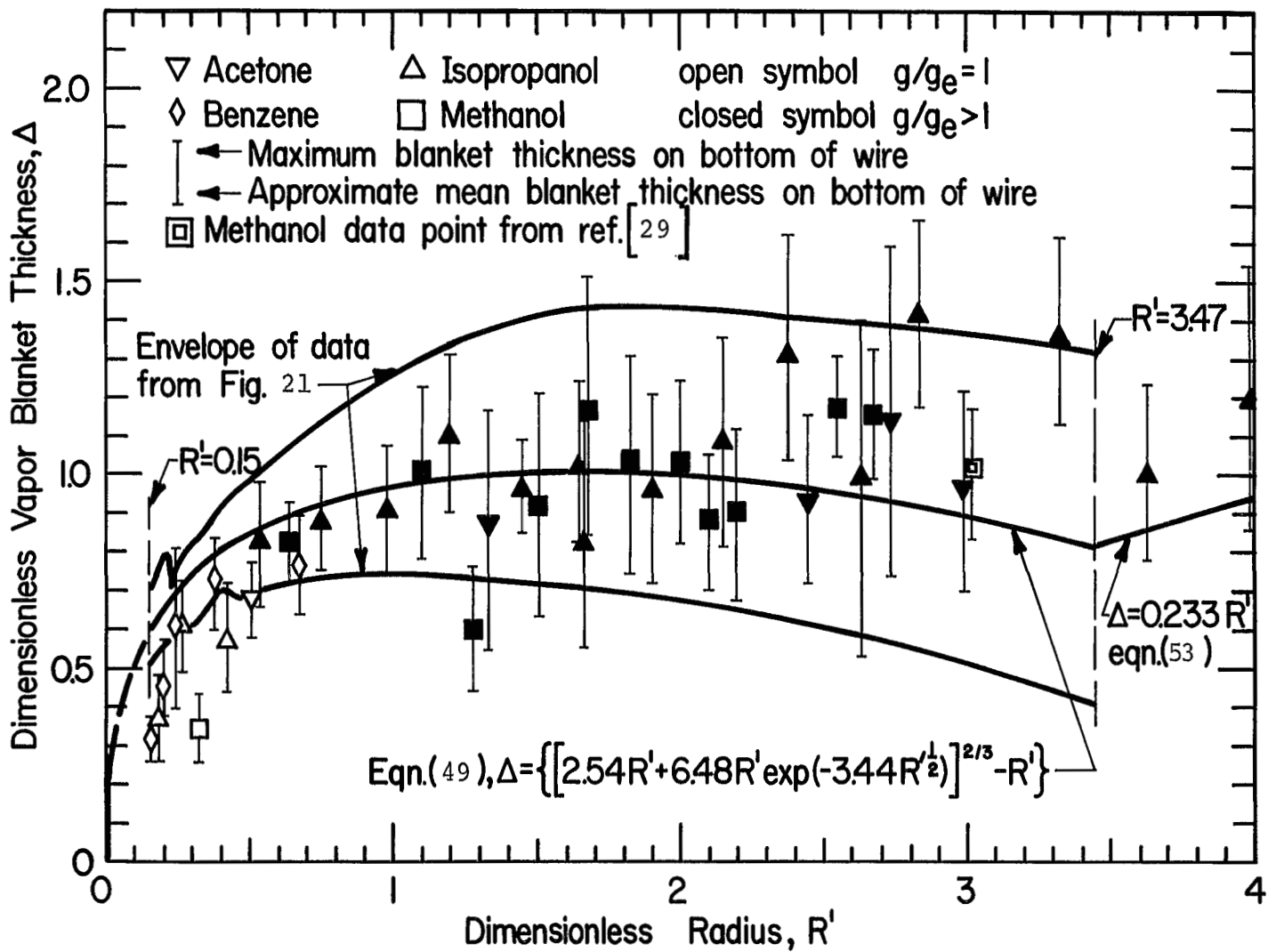
Fig. 22 Experimental determination of the dimensional vapor blanket thickness as a function of R'.

help of equation (49), we obtain

$$R' = 3.47 \quad \text{at} \quad R' + \Delta = 4.28 \tag{51}$$

The constant value for q_{max}/q_{maxF} in equation (46a) can now be fixed with the help of equations (51) and (49):

$$\frac{q_{max}}{q_{maxF}} = \frac{3^{3/4}}{\pi} \frac{4.28}{3.47} = .894; \quad R' > 3.47 \tag{52}$$

Thus the proper upper bound on equation (49) is $R'=3.47$, and the relation between Δ and R', for $R'>3.47$, can be found by combining equation (46a) with equation (52) to get

$$\Delta = 0.233 \ R' \quad\quad R' > 3.47 \tag{53}$$

Equation (53), plotted on Fig. 22, is consistent with the few measured values of the vapor blanket thickness in this range.

Figure 23 shows equation (43) for various values of Δ and the semi-theoretical equation for q_{max}/q_{maxF}. Actually equation (50) differs negligibly from equation (52) for $R'>3.47$. Therefore equation (50) can properly be used for the entire range of $R'>0.15$.

We have presented two models for the q_{max} transition. Actually, there are small aspects of the transition mechanisms which are ignored in these relatively simple descriptions. The range of R' between 1.72, at which $(R'+\Delta)=\pi\sqrt{3}/2$, and 3.47 is, for example, a transition range between two models. As R' increases in this range, the jet-spacing becomes decreasingly dependent on λ_{d_F}.

Conclusions

1. A hydrodynamic model is developed for the prediction of q_{max} on horizontal cylinders. The resulting expressions are

$$\frac{q_{max}}{q_{maxF}} = \frac{6}{\pi^2\sqrt{3}} \frac{(R'+\Delta)^{3/2}}{R'}; \quad R' + \Delta \leq 4.28$$

and

$$\frac{q_{max}}{q_{maxF}} = \frac{3^{3/4}}{\pi} \frac{R'+\Delta}{R'} = \text{constant}; \quad R' + \Delta > 4.28$$

2. The dimensionless vapor blanket thickness, Δ, is determined by an empirical equation

$$\Delta = [2.54 \ R'+6.48 \ R' \ \exp(-3.44 \ \sqrt{R'})]^{2/3} - R'; \quad R' < 3.47$$
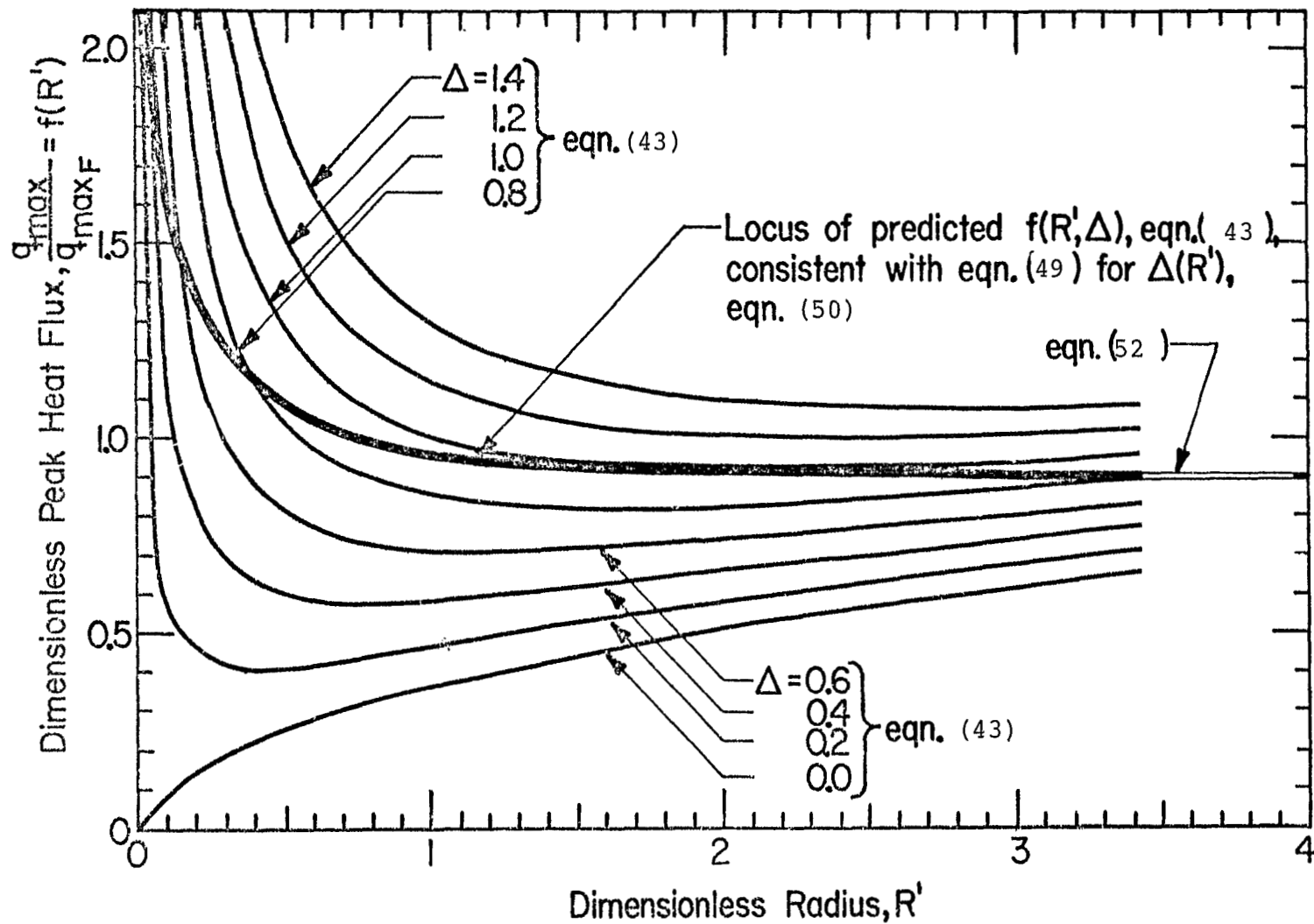
Fig. 23 Theoretical dimensionless peak heat fluxes for various values of Δ, compared with final prediction.

from which we find that R'=3.47 at R'+Δ=4.28. Therefore,

$$\Delta = 0.233 \ R'; \quad R' > 3.47$$

3. About 900 q_{max} data for cylindrical heaters of various sizes, under different pressure and gravity conditions, and in a variety of liquids were correlated successfully on q_{max}/q_{max_F} versus R' coordinates.

4. The resulting equation for q_{max} on horizontal cylinders is

$$q_{max}/q_{max_F} \simeq 0.890 + 2.27 \ \exp(-3.44 \ \sqrt{R'}); \quad 0.15 < R'$$

5. When R'<0.15, the q_{max} data start deviating from the prediction and scatter widely on the q_{max}/q_{max_F} versus R' coordinates. When R'<0.07, the hydrodynamic instability theory of transition is no longer applicable. If a transition of any kind still exists in this range, it is one in which capillary forces are dominant.

54

VI. q_{max} ON HORIZONTAL RIBBONS

The Role of N or I

Viscosity appears to exert no influence whatever on the peak heat flux on horizontal cylinders. But there is evidence that it might be very significant in certain more susceptible configurations. Borishanski [16], as we observed in Chapter III, found some combined influence of viscosity, buoyancy, and surface tension upon q_{max}.

A much stronger indication of such influence was given by Costello, Bock, and Nichols [40] in 1965. They observed the burnout of ribbons mounted in water as shown in Fig. 24. The rising bubbles induced a transverse flow which altered q_{max}. The smaller
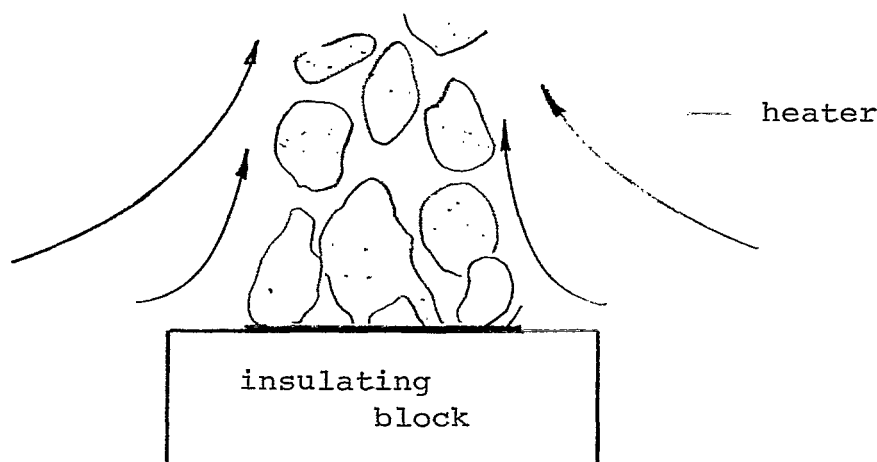
Fig. 24   Configuration studied by Costello, Bock and Nichols

ribbons burned out at higher heat fluxes than the larger ones, and the lowest heat fluxes were observed when vertical sidewalls were placed along the edges of the ribbon to block the liquid inflow.

Costello et al. also measured rates of liquid inflow, and they suggested that a superposition of forced-convection and pool-boiling effects might account for heat transfer in this case. However, they did not provide a correlative procedure and they gave data for only three situations.

We have repeated their experiment in a slightly modified configuration over a wide range of sizes, gravities, and pressures, in five fluids. We used the heater on the right hand side of Fig. 3 in the test capsule on the left. This yielded the cross-

sectional configuration shown in Fig. 25.

In this configuration we would expect the following modif-
ications in the basic correlation equation, equation (16) or (20).
The dimensionless width, W', should replace L', where W' is simp-
ly an L' based on L=W. Since we are using common nichrome rib-
bons in a range of fairly substantial W', the effect of contact
angle should be small and we shall ignore it. Our pressure range
is low so the influence of $\rho_g/(\rho_f-\rho_g)$ should also be negligible.

Finally, a secondary parameter is introduced into the prob-
lem by the limited width, W_C, of the capsule. We shall assume
that, since recirculation results from the confinement of the
capsule width, W_C should appear in a second induced convection
scale parameter, I_C. Since the capsule is a good deal larger
than the ribbon, recirculation should not exert a large influence
on q_{max}, but it cannot be ignored. Accordingly, we can expect
to correlate data with

$$\frac{q_{max}}{q_{max_F}} = f(W', I, I_C) \tag{54}$$

If we wish to use equation (20), which incorporates Bori-
shanski's induced convection buoyancy parameter, N, then it is
not possible to introduce W_C in a second N, since N is not a
scale parameter. We must instead use an aspect ratio, W/W_C, so

$$\frac{q_{max}}{q_{max_F}} = f(W', N, W/W_C) \tag{55}$$

The primary objective of the work described in this chapter
is to learn whether or not any induced convection influence act-
ually becomes significant. We do not anticipate a strong influ-
ence of I_C but its effect will also be investigated. If we are
wrong in looking for an influence of I or N then equations (54)
and (55) will reduce once again to equation (8).

Development of Correlation Surfaces from Data

Carefully cleaned nichrome ribbons were cut from 0.228,
0.051, or 0.025 mm stock and stretched out on the mounting block.
The capsule was charged with reagent grade acetone, methanol,
benzene, isopropanol, or double distilled water, and mounted on
the centrifuge. During a run, the liquid level was held in the
range 2.5 to 3.8 cm above the ribbon surface and noted to make a
hydrostatic head correction, and the temperature held to within
a degree of saturation. The angular speed of the centrifuge
was   read,   and   (with   the   preheater   turned   off)   the   cap-

56

$$\frac{q_{max}}{q_{max_F}} = f(W',I,I_c)$$
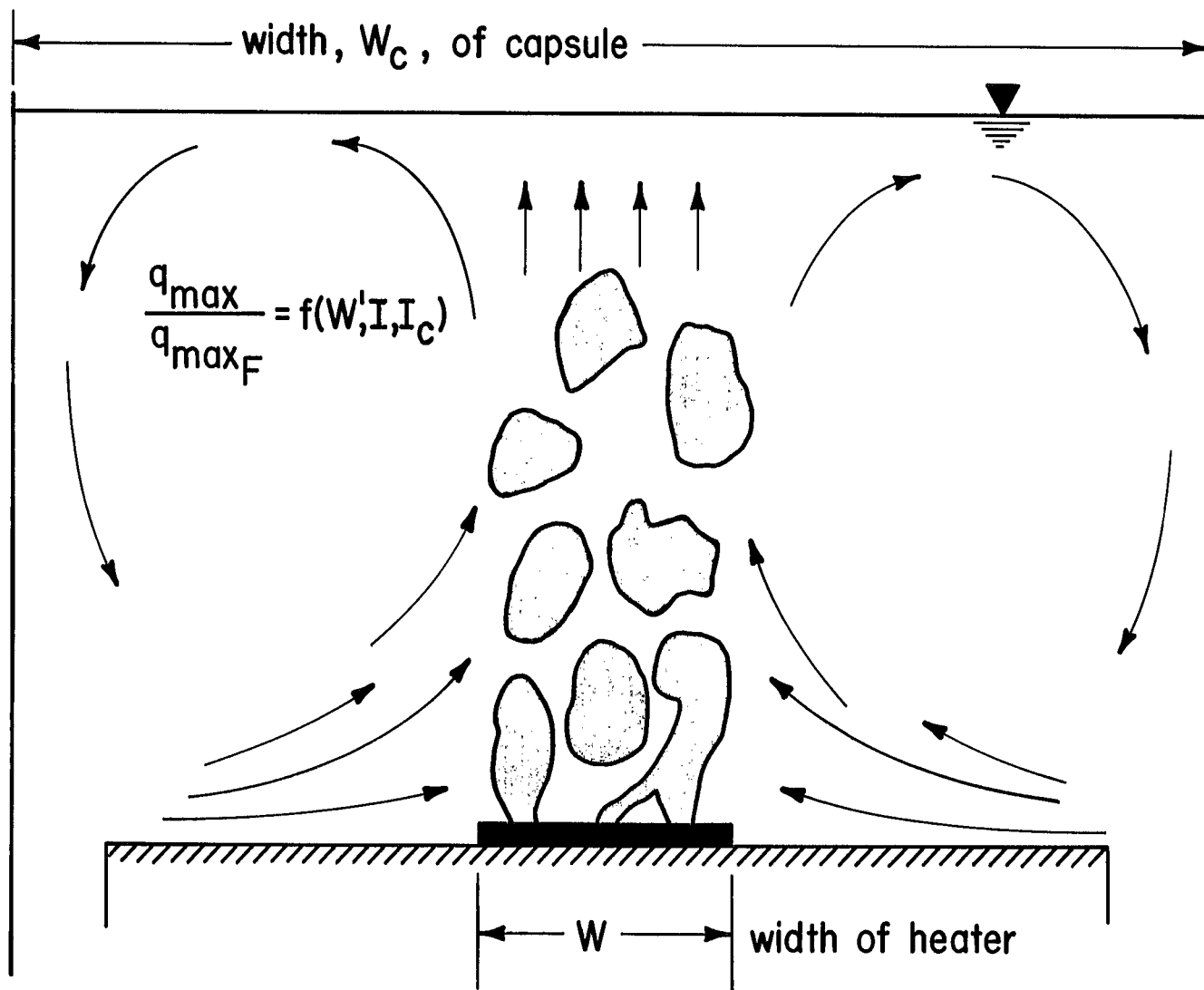
width, W_c, of capsule

W

width of heater

Fig. 25   End view of ribbon heater configuration

sule pressure was recorded. Finally, the power supplied to the ribbon was increased until the peak heat-flux transition was observed, and there it was read.

About 874 observations were made--roughly 419 in acetone, 262 in methanol, 104 in isopropanol, 81 in benzene, and 8 in water. These raw data are tabulated fully in reference [14]. The probable errors of the variables, computed in [14], are about ±6 percent for q_{max}, ±4 percent for W', and ±2 percent for I. The variability of observed q_{max} values was on the order of ±15 percent, as is typical of q_{max} data. Data were measured over a reduced pressure range from 0.0016 to 0.0246, and a range of gravity from 1 to 87 times earth normal gravity.

All of these data and Costello's three points were plotted twice: first on q_{max}/q_{maxF} versus W' coordinates for comparatively narrow ranges of I; then on q_{max}/q_{maxF} versus I coordinates for ranges of W'. Fig. 26 shows a typical example of one of these crossplots.[6]

Figure 26 reveals some things that were generally true of all the data. The great majority of the data for any substance clustered within ±15 percent of a mean surface through them, and a geometrically similar family of surfaces could be drawn through all of the substances. Methanol was most representative of the substances used. Acetone and water presented the highest q_{max}/q_{maxF} values--about 25 percent above methanol--and isopropanol the lowest--about 30 percent below the methanol. The benzene data lie between the methanol and acetone data.

This is consistent with the fact that we have failed thus far to account for the remaining weak parameter I_c. We shall return to this point briefly, but let us continue for a moment as though the influence of I_c could be neglected.

The correlating surfaces that result from the crossplots are each presented in sets of contours. The correlation function

---

[6]The method of correlation used in reference [14] was based on a Law of Corresponding States correlation instead of equation (54). This resulted in a doubling of those errors introduced by the Law of Corresponding States and an awkward scaling of q_{max}. The present correlation overcomes these difficulties but required replotting the data instead of using the curves in [14]. The effectiveness of equation (54) was, of course, made clear in Chapter V. The shape of our resulting surface differs somewhat from that plotted in reference [14].
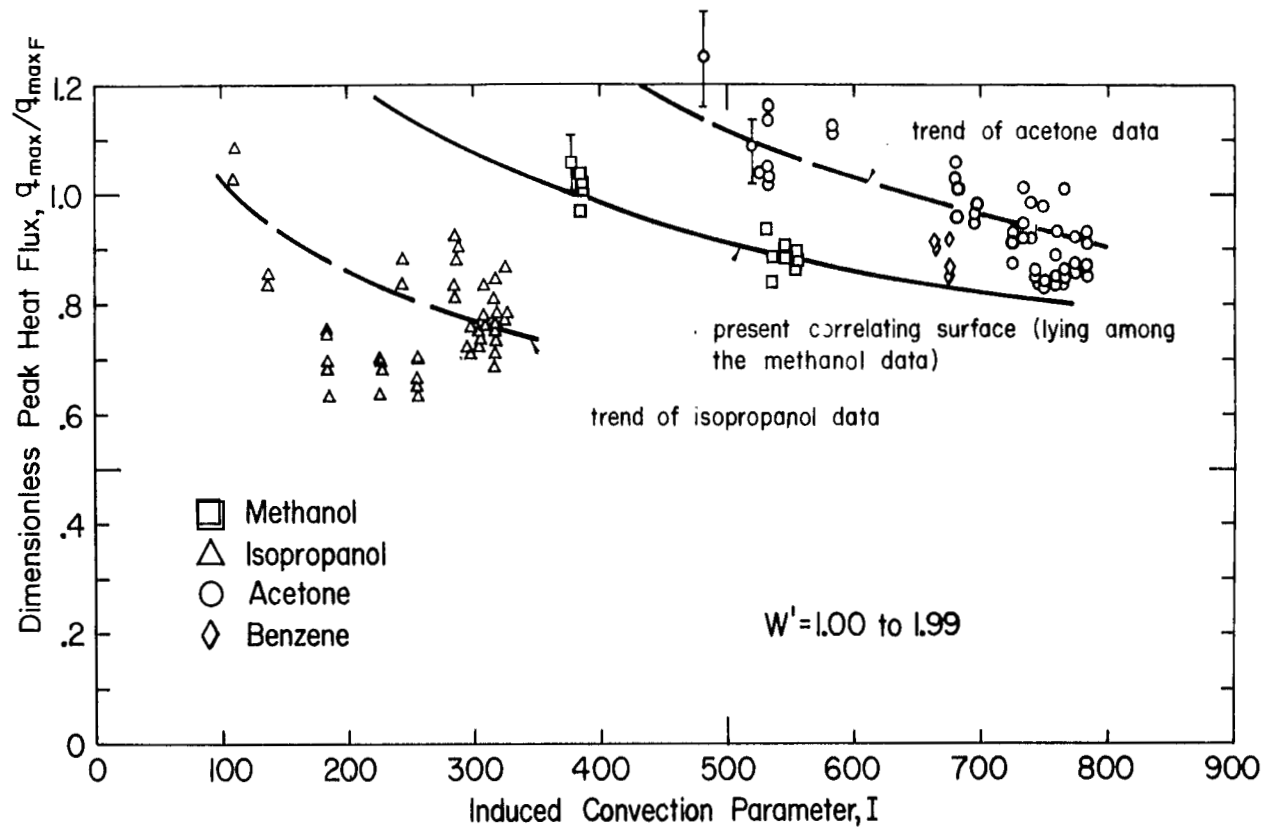
58

Fig. 26   A typical crossplot for peak heat flux data in a range of W'

$f(W',I)$ is presented in Figs. 27 and 28 which give q_{max}/q_{maxF}
versus W' and q_{max}/q_{maxF} versus I contours, respectively, as ob-
tained from the 21 crossplots. This surface generally follows
the mean of the data for methanol and is consistent with trends
that can be identified individually in each of the remaining sub-
stances.

The correlation in terms of N was obtained by transforming
the curves given in Figs. 27 and 28 with the help of equation (18),
$I=\sqrt{NW'}$. It is given in a single plot of q_{max}/q_{maxF} versus W',
with N as parameter, in Fig. 29.

Figures 27, 28, and 29 are limited in their applicability
to just methanol. More specifically they are restricted to the
present configuration in a narrow band of I_C. Table 1 gives I_C
ranges for the fluids used here.

Table 1 I_C for the Present Tests

Liquid	I_C for atmos-pheric pressure	I_C for minimum pressure	Represent-ative I_C
isopropanol	2150	948	2000
methanol	3385	2375	3200
benzene	4100	2190	3800
acetone	4650	3300	4500
water	7520	--	7520

Figure 30 shows constant W' curves for acetone and isopropanol
to show how I_C influences the surface. This figure is in the
same form as Fig. 28, and two lines in it have been borrowed
from Fig. 28 to illustrate what the relative influence of I_C is.

Discussion

The correlation surfaces reveal the strong influence of
the parameters I and N, that we anticipated, and they also show
that this influence vanishes when the scale parameters, I and W',
become large. This was to be anticipated in the context of equa-
tion (21), since buoyancy completely overbalances both capillary
and viscous forces as the scale is increased. Thus we find for
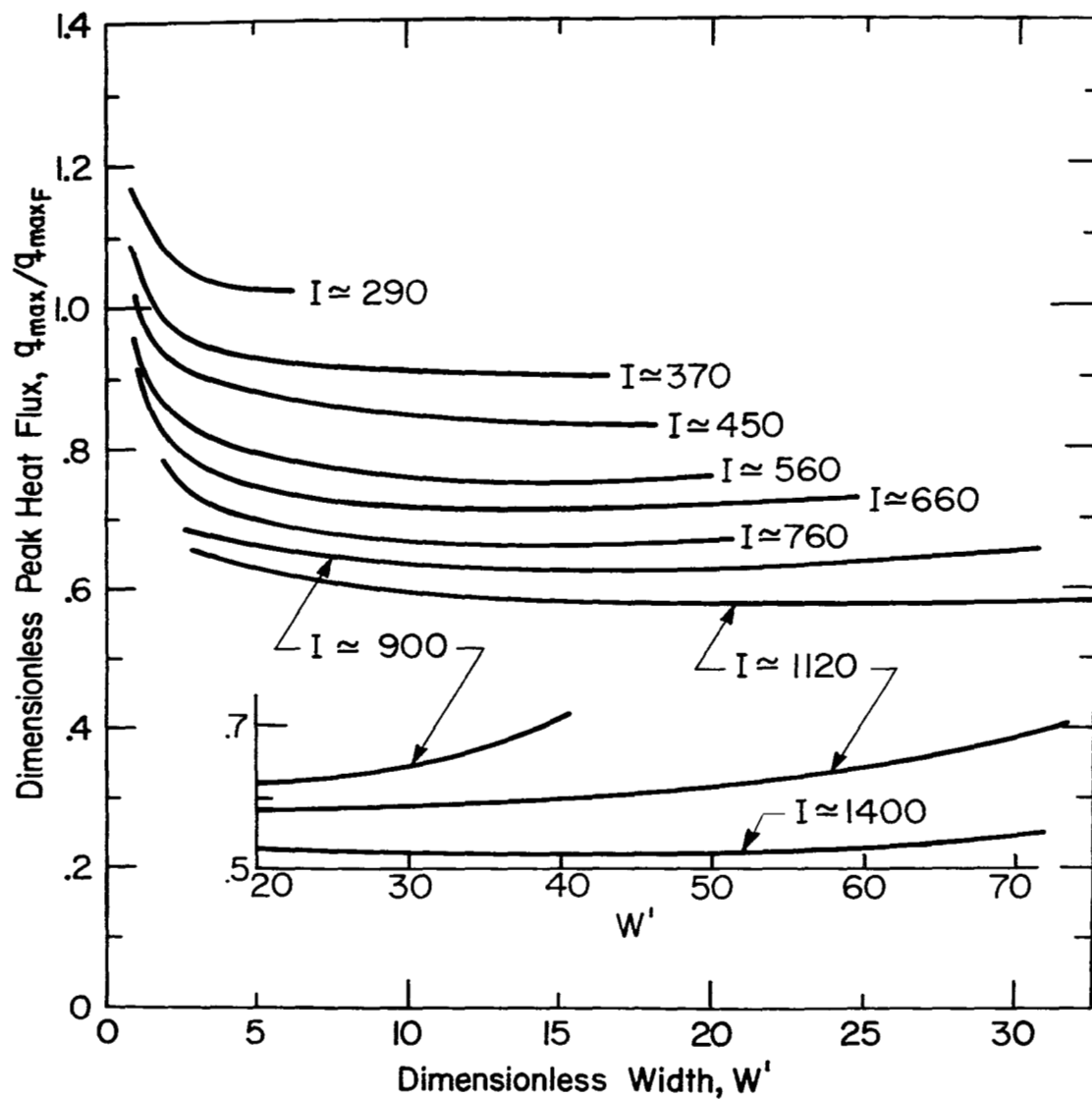the methanol data that:

60

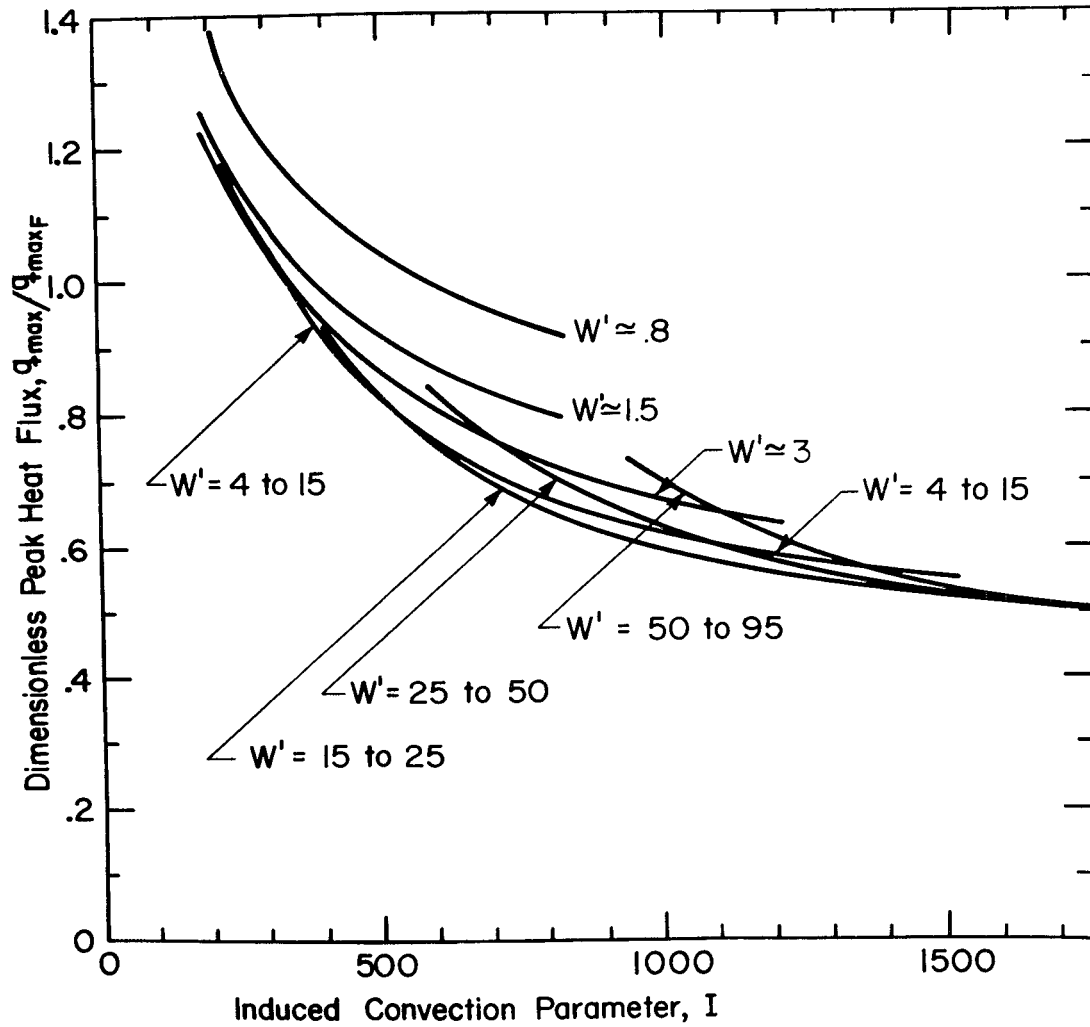Fig. 27 q_{max}/q_{max_F} vs. W' contours for 9 values of I

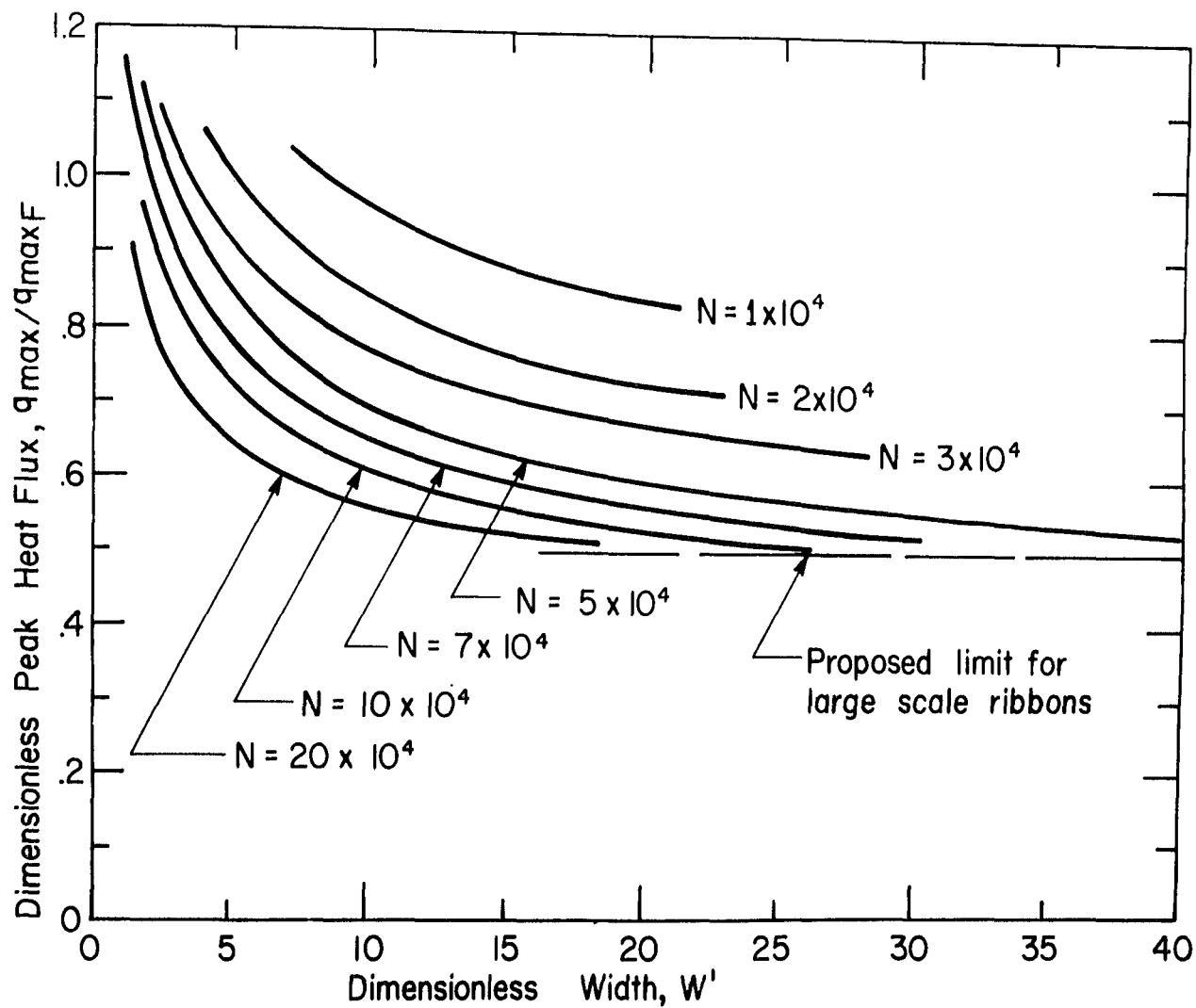Fig. 28 q_{max}/q_{max_F} vs. I contours for 8 values of W'

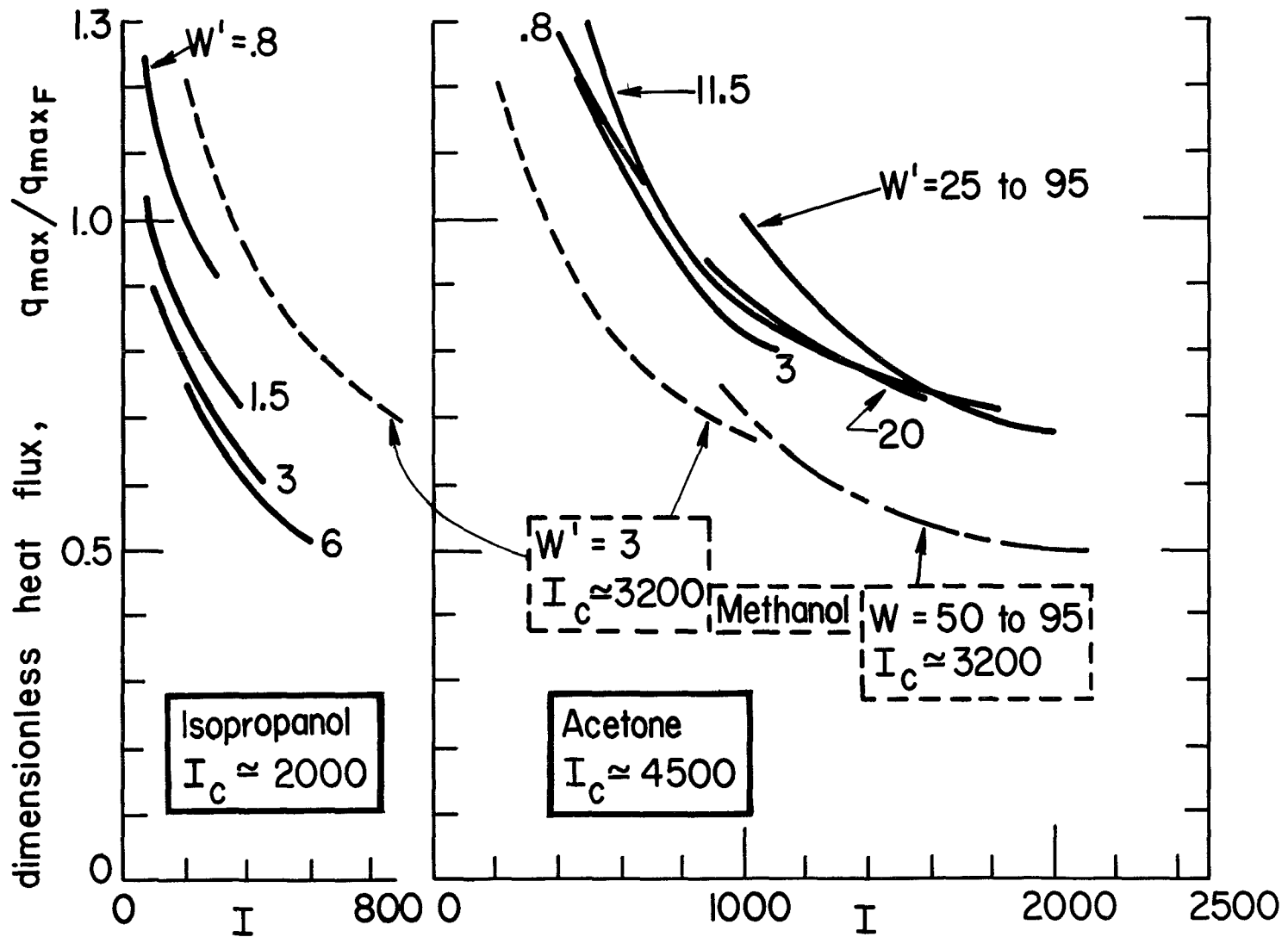Fig. 29 q_{max}/q_{max_F} vs. W' contours for 7 values of N

Fig. 30 The influence of I_c on the $(q_{max}/q_{max_F}) - W' - I$ surface

$$\text{limit } \frac{q_{max}}{q_{max_F}} \simeq 1/2, \text{ large I and W'} \qquad (56)$$

This limit appears to be valid for all I>1500, and W' on the order of 50, depending upon the value of I.   Since N is not a scale parameter we cannot propose a proper criterion in terms of it.   However, the various lines of constant N seek $q_{max}/q_{max_F}=1/2$ as an asymptote in Fig. 29.

That this limiting q_{max} is less than the flat plate value might reflect either or both of two factors: The primary factor is the finite size of the centrifuge capsule which doubtless results in a limiting high Reynolds number circulation.   This circulation in turn affects the peak heat flux.   A secondary factor might lie in the fact that Zuber's equation has not really been subjected to broad testing in a proper flat plate configuration, and some error in the constant, $\pi/24$, could conceivably contribute to a deviation of the present data from the supposed flat plate equation.

When W' falls below unity, surface tension assumes very strong control over the peak heat flux transition and q_{max} rises sharply.   We saw in Chapter V that this was also true as 2R'-- the comparable scale parameter for cylinders--fell below 0.40.

Figure 30 shows that while the induced convection effect is pronounced, it is also susceptable to the geometry of the container as reflected in I_c.   The surfaces for acetone fall 25 or 30 percent above those for methanol while those for isopropanol fall about 30 percent below.

Throughout the preceding discussion we have made no mention of the thinness of the ribbons used in the tests, however the method of correlation involved no consideration whatsoever of heat conduction or capacitance effects.   These effects can influence q_{max} as the ribbon becomes thin and they should be discussed further.

The low thermal capacity of thin ribbons led to surface temperature oscillations, owing to the alternating current power supply.   This required that we change to direct current supply when the ribbon thickness became small.   The criterion for this change was based on the heat conduction solution for this problem given by Switzer and Lienhard [41].   Overlapping ac and dc experiments verified that we did not suffer difference in results at the point of transition.

It has long been observed that very thin ribbons can actually melt out at heat fluxes less than the hydrodynamic limit,

q_{max}, if they lack the protection of enough "thermal mass."
This burnout mechanism is discussed at length in [42] and a cri-
terion is given for determining the limiting thickness. We took
care to keep our observations within this limit.

Conclusions

1. Induced convection can exert a strong influence on the peak
    pool-boiling heat flux, if the configuration is one which is
    susceptible to it.

2. The present data should not be viewed as having broad applic-
    ability. They are restricted to a particular configuration
    of heater and container, and their value lies in that they
    illustrate the induced-convection effect.

3. The expressions

$$\frac{q_{max}}{q_{max_F}} = f(W', I) \tag{54a}$$

    and

$$\frac{q_{max}}{q_{max_F}} = f(W', N) \tag{55a}$$

    are the appropriate expressions to correlate q_{max} data for
    the present heater configuration, in a larger container,
    over ranges of pressure, gravity, and size (as long as $W' \gtrsim 1$),
    and for different liquids.

4. The peak heat flux for a horizontal ribbon heater (and prob-
    ably for other geometries as well) approaches a constant min-
    imum fraction of q_{max_F} when the scale parameter, I and W',
    become large. It also approaches this limit as the induced-
    convection buoyancy parameter, N, increases.

66

VII. SUMMARY OF DESIGN RESULTS

Assessment of the Role of Gravity

Let us now return to the initial motivation for this study--namely that of determining the interacting influences of gravity and configuration on the extreme heat fluxes. The preceding three chapters have shown beyond any doubt that

$$\frac{q_{max}}{q_{max_F}} \text{ or } \frac{q_{min}}{q_{min_F}} = \phi(L', I) \tag{57}$$

is the appropriate expression[7] for correlating q_{max} and q_{min}. The use of equation (57) assumes that pressures are not close to the critical pressure; that L' is on the order of magnitude of unity or greater' and that surfaces are clean.

Equation (57) is an adaptation of equation (20). For the present discussion it will be chosen in preference to equation (16) which uses the induced buoyancy parameter, N. Thus the g-dependence of the expression is limited to q_{max_F} and L', and our subsequent manipulations will be significantly simplified. Rewriting equation (57) as

$$q_{max} \text{ or } q_{min} = (q_{max_F} \text{ or } q_{min_F})\phi(L', I) \tag{57a}$$

we can form the following derivative:

$$\frac{d(q_{max} \text{ or } q_{min})}{dg} = \frac{(q_{max_F} \text{ or } q_{min_F})\phi}{g}\left[\frac{1}{4} + \frac{1}{2}\frac{d\ell n\ \phi}{d\ell n\ L'}\right] \tag{58}$$

But $(q_{max_F} \text{ or } q_{min_F})\phi \equiv (q_{max} \text{ or } q_{min})$, so equation (58) becomes

$$\frac{d\ell n(q_{max} \text{ or } q_{min})}{d\ell n\ g} = \frac{1}{4} + \frac{1}{2}\frac{d\ell n\ \phi}{d\ell n\ L'} \tag{59}$$

Equation (59) displays the influence of g on the extreme heat fluxes in a very evocative way. It shows that the basic influence of gravity is to increase q_{max} or q_{min} as $g^{1/4}$ (i.e. the lead term on the right hand side is 1/4). However there is a second term--usually negative in sign--which can strongly detract from the $g^{1/4}$ influence. This is the $d\ell n\phi/2d\ell nL'$ term which re-

---

[7]We introduce the special symbol ϕ at this point to denote the ratio (q_{max}/q_{max_F}) or (q_{min}/q_{min_F}), instead of the general function, f.

flects the additional influence of the scale parameter, L'.

The transition between the ranges in which gravity augments the extreme heat flux, and detracts from it is also of major interest. This can be found by setting the right hand side of equation (59) equal to zero, whence

$$\frac{d\ln \phi}{d\ln L'} = -\frac{1}{2} \tag{60}$$

Accordingly we have the following criterion:

$$\frac{d\ln \phi}{d\ln L'} \begin{cases} > -1/2, & q_{max} \text{ or } q_{min} \text{ increases with } g \\ < -1/2, & q_{max} \text{ or } q_{min} \text{ decreases with } g \end{cases} \tag{60a}$$

Thus, to satisfy our interest in the influence of gravity we should prefer to see the collected design results of the present work presented on $\ln\phi$ versus $\ln L'$ coordinates. We shall assemble the results in this way after first exploring one more geometry that we have not yet mentioned.

q_{max} and q_{min} on Spheres

No sphere data have been obtained in the present study; however, a limited number of data obtained by other investigators provide the basis for further extending our set of correlation surfaces. Merte and Clark [6]; Lewis, Merte and Clark [7]; and Korayem [43] give a total of nine usable q_{min} data for nitrogen at atmospheric pressure. Reference [7] also provides about 14 q_{max} points for spheres.

The q_{min} data were assembled in reference [3] under a slightly different scheme of correlation. We have correlated the same data on ϕ versus R' coordinates in Fig. 31, and we have correlated the q_{max} data in the same way in Fig. 32.

The resulting correlation lines must be accepted hesitantly. The data are restricted to nitrogen at one atmosphere. Thus, if any systematic deviations of nigrogen data occur within the present scheme of correlation, they will be entirely reflected in these lines. Furthermore there are too few data to clearly define the behavior in the small R' regime.

In the large R' limit the data rather strongly suggest that

$$\lim_{R' \to \infty} \frac{q_{max}}{q_{max_F}} \simeq 0.84, \text{ and } \lim_{R' \to \infty} \frac{q_{min}}{q_{min_F}} \simeq 0.45 \tag{61}$$
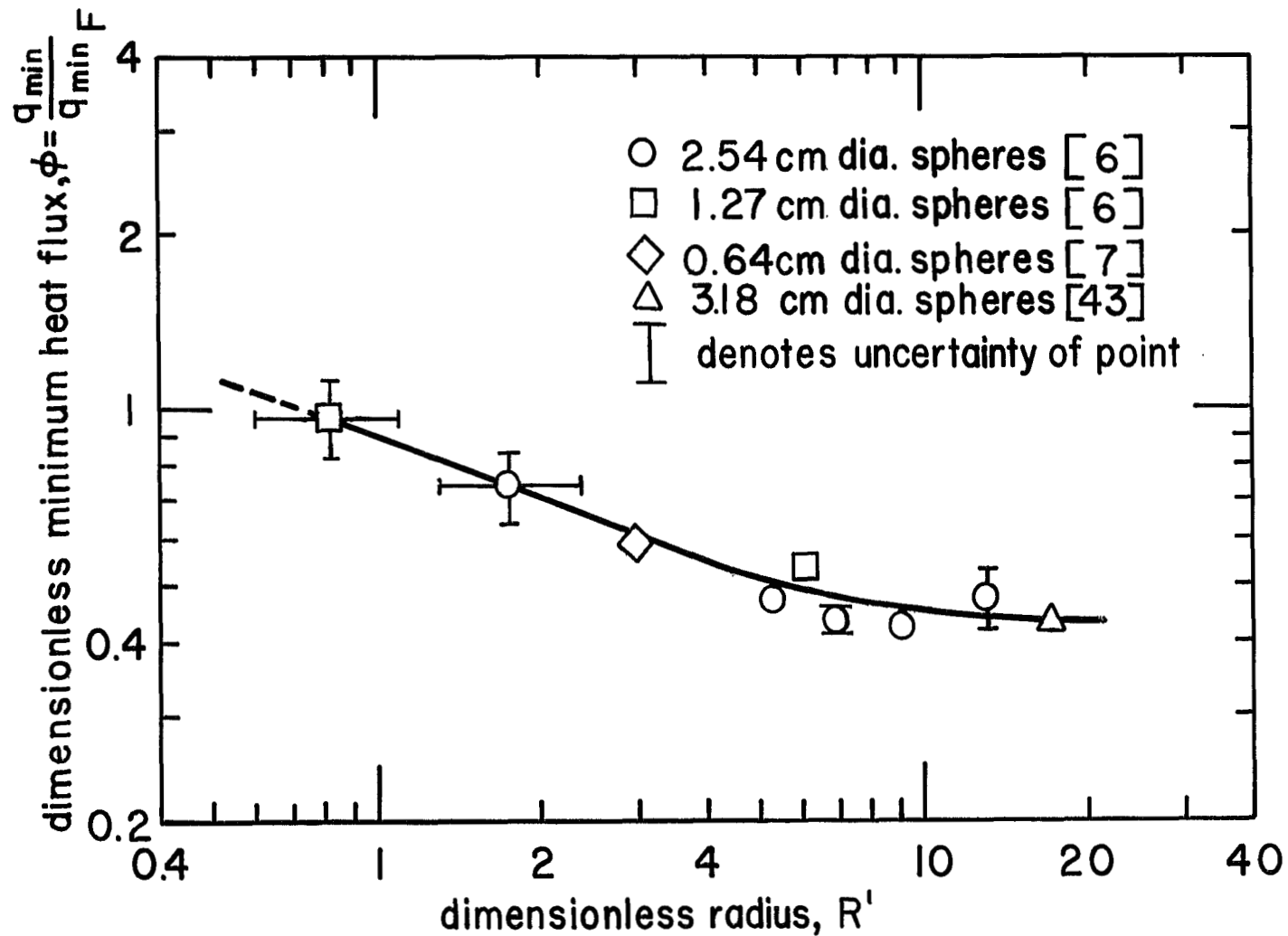
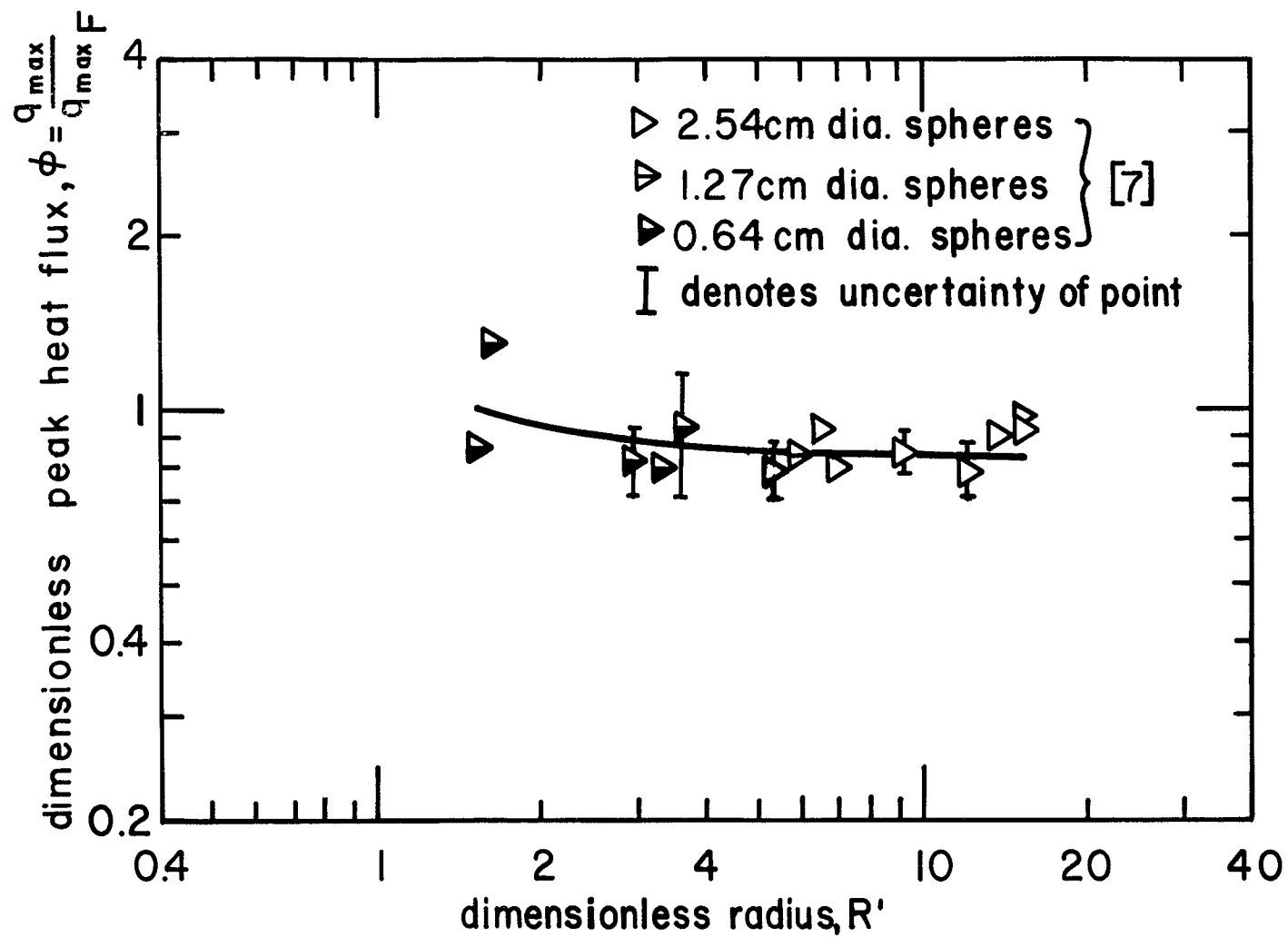Fig. 31   Minimum heat flux on spheres in nitrogen at I atm.

Fig. 32   Peak heat flux on spheres in nitrogen at 1 atm.

for spheres. The limit of hydrodynamic behavior, or the R' be-low which the present scheme of correlation no longer applies, is not specified. However, we doubt that it should be valid very much below a diameter equal to half of a wavelength, or below 2.73R'.

Collected Dimensionless Heat Flux Curves

Figure 33 presents the collected results for spheres and cylinders on ϕ versus L' coordinates. Some selected values for q_{max} on ribbons for $I_C=3200$ are included for comparison on this plot. Let us note some of the important general characteristics of these curves:

a.) All curves are monotonically decreasing in L'. This means that, to the best of our knowledge, the "quarter-power" de-pendence of the extreme heat flux on g is an upper limit. Most configurations result in a slower increase of extreme heat flux.

b.) The great success of Zuber's equation for q_{max_F} in de-scribing q_{max} for a variety of configurations is borne out in these curves. In all cases that we have considered q_{max} is with-in about 50 percent of q_{max_F}.

c.) As $L' \to \infty$, the quarter-power dependence is re-established. This fact has not been borne out with data in the case of q_{min} on cylinders, since no such data exist for sufficiently large values of R'.

d.) q_{min} exhibits much greater deviations from flat plate behavior than q_{max} does.

e.) q_{min} for cylinders actually decreases with g in the range that we have investigated.
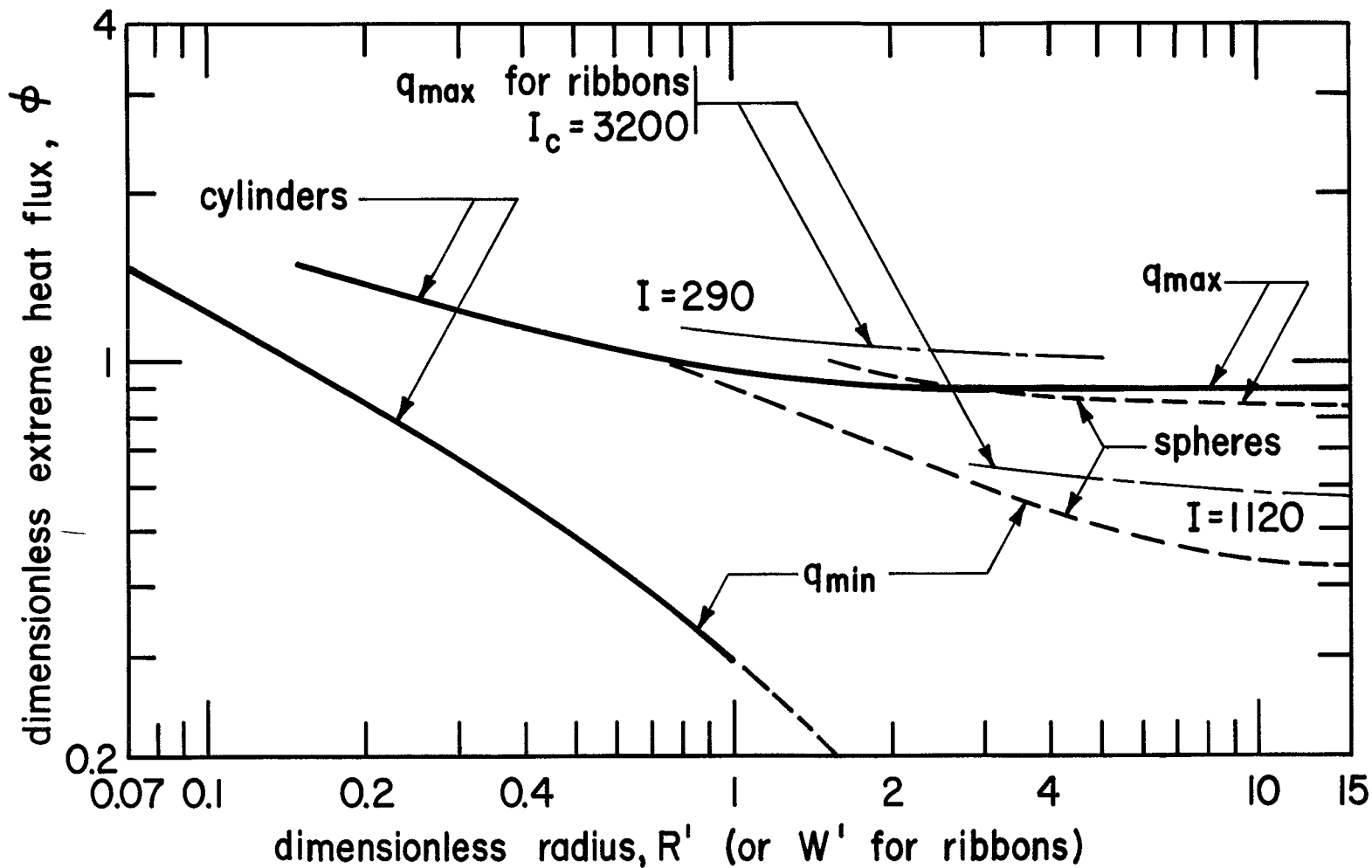
Fig. 33   Collected   dimensionless   extreme   heat   flux   results.

VIII. CONCLUSIONS

The present studies were originally motivated by the need to understand how gravity and size interact in their influence on the peak and minimum pool boiling heat fluxes. A sequence of prior studies [10, 2, 3] had verified that q_{max} and q_{min} could be correlated by

$$\frac{q_{max}}{q_{max_F}} \text{ and } \frac{q_{min}}{q_{min_F}} = f(L') \tag{8}$$

under a wide variety of conditions. The dimensionless characteristic length, L', is

$$L' = L[g(\rho_g - \rho_f)/\sigma]^{1/2} \tag{7a}$$

This idea had served to explain the limited success of Zuber's flat plate equations in variable gravity as noted by Costello, Siegel, Clark and others. Earlier investigators had attempted to compare their variable gravity data with the $\sqrt[4]{g}$ dependence in Zuber's equation, but without understanding the dependence of q_{max} upon $f(\sqrt{g})$ that enters through the scale parameter, L', the effect of gravity could not be completely accounted for.

Our first efforts under the support of NASA have therefore been directed specifically at a critical study of equation (8). A large portion of these efforts are reported in references [11, 12, 13, 14, and 15], and are reviewed in the preceding Chapters. They have briefly led to the following findings:

A. Dimensional analysis combined with consideration of the physical nature of the problem leads to a general correlation which can be written in the form:

$$\frac{q_{max}}{q_{max_F}} \text{ or } \frac{q_{min}}{q_{min_F}} = f(L', \text{ I or N}, \sqrt{1 + \rho_g/\rho_f}, \theta_c) \tag{16 or 20}$$

The roles of θ_c and of $\sqrt{1 + \rho_g/\rho_f}$ are conjectural in this expression. We believe that they can exert an influence under appropriate circumstances, but we have not provided documentation of such influences in the present studies.

B. In the studies of film boiling, there was no liquid-solid contact, the role of $\sqrt{1 + \rho_g/\rho_f}$ was presumably incorporated in q_{min_F}, and the liquid flow pattern probably did not induce disruptive convective currents. Thus equation (16 or 20) reduced to equation (8) in this work.

The wavelength λ_d, of vapor removal during film boiling was found to vary as

$$\lambda_d/\lambda_{d_F} = (1+1/2[(1+b/R)R']^2)^{-1/2} \tag{30}$$

where R' is an L' based upon the wire radius, λ_{d_F} is the most susceptible wavelength on a flat plate, and the vapor blanket thickness, b, is usually a minor factor which can be estimated by the method of Baumeister and Hamill. A variability of +60 percent and -25 percent in λ was found to be inherent by virtue of the almost neutrally-stable character of the Taylor instability. Equation (30) was compared with data for many fluids over large ranges of g and R.

The "best estimate" of q_{min} was found to be

$$q_{min} = q_{min_F}[0.0217/R'^2(2R'^2+1)] \tag{35}$$

where q_{min_F} is Berenson's minimum heat flux for a flat plate, equation (14).

Zuber's "wave-collapse" mechanism of vapor removal was found to give way to a bubble-merger mechanism that was totally dominated by capillary forces, over the range: $0.07 \leq R' \leq 0.12$. When R' exceeded unity, the "wave-collapse" mechanism deteriorated, although wavelengths equal to λ_{d_F} could still be identified up to $R' \simeq 2.5$-- the upper limit of the observations.

C. The peak heat flux on horizontal cylinders has been predicted analytically. The result is in the form of equation (8) since I, θ_c, and $(1+\rho_f/\rho_g)$ exert negligible influence:

$$\frac{q_{max}}{q_{max_F}} = \frac{6}{\pi^2\sqrt{3}} \frac{(R'+\Delta)^{3/2}}{R'} \quad , \quad 0.15 \leq R' \leq 3.47 \tag{43}$$

and

$$\frac{q_{max}}{q_{max_F}} = 0.894, \quad R' \geq 3.47$$

where Δ is an L' based upon the vapor blanket thickness. The following empirical expression for the dimensionless blanket thickness was written to represent data over the range $0.15 \leq R' \leq 3.47$:

$$\Delta = [2.54R' + 6.48R' \exp(-3.44\sqrt{R'})]^{2/3} - R' \tag{49}$$

Combining equations (43) and (49) gave the following expression which converges almost to 0.894, and is valid for all $R' > 0.15$:

$$\frac{q_{max}}{q_{max_F}} = 0.89 + 2.27 \exp(-3.44\sqrt{R'}) \tag{50}$$

These results conform with the simple version of our correlation strategy--equation (8).

74

More than 400 original data points, and a comparable number of data from a variety of other sources verified equation (50) within ± 20 percent.

D. Application of equation (16 or 20) in the correlation of about 900 original data for horizontal ribbons on an insulating base revealed a strong influence of I or N, especially for large N's or small I's. This influence was illustrated graphically in Figs. 27, 28, and 29. These Figures reinforced another finding of the present studies--namely that as the scale parameters, L' and I, become large, q_{max}/q_{max_F} approach constant values.

E. One of the chief overall conclusions to be drawn from the preceding studies is that an extraordinarily successful general scheme of correlation has been developed. However, Figure 21 shows that it will not serve to predict the extreme heat fluxes when R' becomes small. For cylinders the method fails when R'<0.15. Our horizontal ribbon data only reached down to W'/2≃.35, but at that point q_{max} was also beginning to rise sharply and scatter broadly. Thus we are tempted to conclude that in any geometry the present correlation will fail when L'^2 (the ratio of gravity to capillary forces, or "Bond number") falls below the order of 1/10.

Thus it remains for us to identify the correct limiting behavior for q_{max} under very low gravity. The correlations and predictions that have been developed are useful in specifying q_{max} and q_{min} for systems that are not too small, under low gravity. But the basic change of behavior that occurs at small L' prevents extrapolation of results in that direction.

F. As long as R' is not so small as to invalidate our method of correlation, the influence of gravity on q_{max} and q_{min} can be characterized by

$$\frac{d\ell n(q_{max} \text{ or } q_{min})}{dg} = \frac{1}{4} + \frac{1}{2}\frac{d}{dL'}\left[\ell n \frac{q_{max}}{q_{max_F}} \text{ or } \frac{q_{min}}{q_{min_F}}\right] \qquad (59)$$

The combined results of the present study, shown in Fig. 33, indicate that this derivative can become negative for only one of the cases that we have studied, namely q_{min} on horizontal cylinders.

75

APPENDIX A   NOMENCLATURE

A_g — cross-sectional area of a vapor jet during strong nucleate boiling on a horizontal cylinder

A_H — area of heater surface within the "unit cell" subtended by a vapor jet

a — amplitude of an interfacial wave (see Fig. 6)

b — thickness of the vapor blanket in film boiling

c_v — specific heat at constant volume

$f(x)$ — any arbitrary function of x

g — acceleration of gravity

g_e — acceleration of gravity under earth normal conditions

G — g/g_e

h_{fg} — latent heat of vaporization

$h_{fg}^{\dagger}$ — corrected h_{fg}, equation (33)

I — induced convection scale parameter, $[\rho_f L \sigma]^{1/2}/\mu$

I_c — I based on W_c

k — wave number, $2\pi/\lambda$

L — any characteristic length

L' — $L[g(\rho_f-\rho_g)/\sigma]^{1/2}$, dimensionless characteristic length

N — induced convection buoyancy parameter, I^2/L'

p_r — reduced pressure, pressure of system divided by critical pressure

q — heat flux

q_{max} — peak nucleate pool boiling heat flux

q_{max_F} — q_{max} on an infinite flat plate (after pg. 1, q_{max_F} is taken to be the value defined by equation (3), whenever it is used)

q_{min} — minimum film pool boiling heat flux

76

q_{min_F}	q_{min} on an infinite flat plate (after pg. 12, q_{min_F} is taken to be the value defined by equation (14) whenever it is used)
R	radius of a horizontal cylindrical heater
R'	$R[g(\rho_f-\rho_g)/\sigma]^{1/2}$, dimensionless radius
U_f	velocity of liquid approaching a heater
U_g	velocity of vapor leaving a heater
U_{gc}	critical U_g for which liquid-vapor interface becomes Helmholtz unstable
W	width horizontal ribbon heater
W_c	width of test capsule
W'	$W[g(\rho_f-\rho_g)/\sigma]^{1/2}$, dimensionless width
γ	dimensionless peak heat flux for $R'<<1$, $(q_{max}$ or $q_{min})/\rho_g h_{fg}(\sigma/\mu)$
δ	effective vapor blanket thickness during strong nucleate boiling on a horizontal cylinder (see Fig. 14b)
Δ	$\delta[g(\rho_f-\rho_g)/\sigma]^{1/2}$, dimensionless vapor blanket thickness
ΔT	heater surface temperature minus saturated liquid temperature
θ_c	contact angle among liquid, vapor, and the heater surface
λ	wavelength
λ_d	most susceptible (or "most dangerous") Taylor unstable wavelength during film boiling
λ_{d_F}	λ_d for a plane horizontal interface
Λ	λ_d/λ_{d_F}
Λ_{BH}	Baumeister-Hamill Λ. based on equation (31)
Λ_{LW}	Lienhard-Wong Λ, based on equation (23) or (30)
Λ_{SK}	Siegel-Keshock Λ, based on equation (29)
μ	liquid viscosity

ρ_f, ρ_g saturated liquid and vapor densities, respectively

σ surface tension between a liquid and its vapor

ϕ (q_{max}/q_{max_F}) or (q_{min}/q_{min_F})

ω frequency of a wave in the complex plane

Ω dimensionless frequency defined by equation (26)

Ω_{max} Ω for the maximum value of $(i\omega)$

REFERENCES

[1] Costello, C.P. and Adams, J.M., "The Interrelation of Geometry, Orientation and Acceleration in Peak Heat Flux Problem," Mech. Engr. Dept. Report, Univ. of Wash., Seattle, (c. 1963).

[2] Lienhard, J.H. and Watanabe, K., "On Correlating the Peak and Minimum Boiling Heat Fluxes with Pressure and Heater Configuration," Jour. Heat Transfer, vol. 88, no. 1, 1966.

[3] Lienhard, J.H., "Interacting Effects of Geometry and Gravity upon the Extreme Boiling Heat Fluxes," Jour. Heat Transfer, vol. 90, no. 1, 1968, p. 180.

[4] Costello, C.P. and Adams, J.M., "Burnout Heat Fluxes in Pool Boiling at High Accelerations," International Developments in Heat Transfer, ASME, New York, 1963, pp. 255-261.

[5] Siegel, R. and Howell, J.R., "Critical Heat Flux for Saturated Pool Boiling from Horizontal and Vertical Wires in Reduced Gravity," NASA Tech. Note TND-3123, December 1965.

[6] Merte, H. Jr. and Clark, J.A., "Boiling Heat Transfer with Cryogenic Fluids at Standard, Fractional and Near-Zero Gravity," ASME Paper No. 63-HT-3, 6th Natl. Heat Trans. Conf. ASME-AIChE, 1963.

[7] Lewis, E.W., Merte, H. Jr., and Clark, J.A., "Heat Transfer at 'Zero Gravity'," 55th Natl. Meeting, AIChE, Houston, February 1965.

[8] Zuber, N., "Hydrodynamic Aspects of Boiling Heat Transfer," AEC Report No. AECU-4439, Physics and Mathematics, 1959.

[9] Zuber, N., Tribus, M., and Westwater, J.W., "The Hydrodynamic Crisis in Pool Boiling Saturated and Subcooled Liquids," # 27, International Developments in Heat Transfer, ASME, New York, 1963, pp. 230-236.

[10] Lienhard, J.H. and Wong, P.T.Y., "The Dominant Unstable Wavelength and Minimum Heat Flux during Film Boiling on a Horizontal Cylinder," Jour. Heat Transfer, vol. 86, no. 2 1965, p. 220.

[11] Lienhard, J.H. and Carter, W.M., "Gravity Boiling Studies," Tech. Report 1-68-ME-1, University of Kentucky, 1968.

[12] Lienhard, J.H. and Sun, K.H., "Effects of Gravity and Size upon Film Boiling from Horizontal Cylinders," ASME paper 69-WA/HT-12, Winter Annual ASME Meeting, Los Angeles, December 1969. (To appear in Jour. Heat Transfer.)

[13] Sun, K.H., "The Peak Pool Boiling Heat Flux on Horizontal Cylinders," M.S. Thesis, University of Kentucky, 1969. (Also presented as Bulletin 88, College of Engineering, University of Kentucky.)

[14] Keeling, K.B., "Effect of Gravity Induced Convection on the Peak Boiling Heat Flux on Horizontal Strip Heaters," M.S. Thesis, University of Kentucky, 1969. (Also presented as College of Engineering Tech. Report 11-69-ME-4, University of Kentucky.)

[15] Lienhard, J.H. and Keeling, K.B., "An Induced Convection Effect upon the Peak Boiling Heat Flux," Paper no. 69-H-68, ASME-AIChE Heat Transfer Conf., Minneapolis, August 1969. (To appear in Jour. Heat Transfer.)

[16] Borishanski, V.M., "An Equation Generalizing Experimental Data on the Cessation of Bubble Boiling in a Large Volume of Liquids," Zhurnal Teknicheski Fiziki, vol. 25, 1956, p. 252.

[17] Berenson, P.J., "Transition Boiling Heat Transfer from a Horizontal Surface," M.I.T. Heat Transfer Laboratory Tech. Report No. 17, 1960.

[18] Lyon, D.N., "Peak Nucleate Boiling Heat Transfer Coefficients for Liquid N_2, Liquid O_2, and Their Mixtures in Pool Boiling at Atmospheric Pressure," Int. Jour. Heat Mass Transfer, vol. 7, 1964, pp. 1097-1116.

[19] Costello, C.P. and Frea, W.J., "A Salient Non-Hydrodynamic Effect on Pool Boiling Burnout of Small Semi-Cylindrical Heaters," AIChE preprint no. 15, 6th Nat'l. Heat Transfer Conf., Boston, August 1963.

[20] Cichelli, M.T. and Bonilla, C.F., "Heat Transfer to Liquids Boiling under Pressure," Trans. AIChE, vol. 41, 1945, p.755.

[21] Bellman, R. and Pennington, R.H., "Effects of Surface Tension and Viscosity on Taylor Instability," Quar. App. Math., vol. 12, 1954, p. 151.

[22] Siegel, R. and Keshock, E.G., "Nucleate and Film Boiling in Reduced Gravity from Horizontal and Vertical Wires," NASA TR R-216, February 1965.

[23] Baumeister, K.J. and Hamill, T.D., "Film Boiling from a Thin Wire as an Optimal Boundary-Value Process," ASME Paper 67-HT-62, ASME-AIChE Heat Transfer Conference, Seattle, 1967.

[24] Nishikawa, K., Shimomura, R., Hatano, M., and Nagatamo, H., "Investigation of Surface Film Boiling under Free Convection," Bulletin JSME, vol. 10, no. 37, 1967, pp. 123-131.

[25] Kovalev, S.A., "An Investigation of Minimum Heat Fluxes in Pool Boiling of Water," Int. Jour. Heat and Mass Transfer, vol. 9, 1966, p. 1219.

[26] Grigull, U. and Abadzic, E, "Heat Transfer from a Wire in the Critical Region," Proc. Instn. Mech. Engrs., vol. 182, Pt3I, 1967-68, pp. 52-57.

[27] Corty, C. and Faust, A., "Surface Variables in Nucleate Boiling," Chem. Engr. Prog. Symp. Ser., no. 17, 1955, p.1-12.

[28] Pomerantz, M.L., "Film Boiling on a Horizontal Tube in Increased Gravity Fields," Jour. Heat Transfer, vol. 86, no. 2, 1964, p. 213.

[29] Westwater, J.W. and Santangelo, J.G., "Photographic Study of Boiling," Ind. and Engr. Chem., vol. 47, 1955, p. 1605.

[30] Jordan, D.P., "Film and Transition Boiling," Advances in Heat Transfer, vol. 5, T.F. Irvine, Jr. and J.P. Hartnett, eds., Academic Press Inc., New York, 1968, pp. 55-127.

[31] Siegel, R., "Effects of Reduced Gravity on Heat Transfer," Advances in Heat Transfer, vol. 4, T.F. Irvine, Jr. and J.P. Hartnett, eds., Academic Press, New York, 1967, pp. 143-227.

[32] Lamb, Sir H., Hydrodynamics, 6th ed., Dover Publications, New York, 1945.

[33] Vliet, G.C. and Leppert, G., "Critical Heat Transfer for Nearly Saturated Water Flowing Normal to a Cylinder," Jour. Heat Transfer, vol. 86, no. 1, 1964, pp. 59-67.

[34] Cumo, M., Farello, G.E. and Pinchera, G.C., "Some Aspects of Free Convection Boiling Heat Transfer," Congresso A.T.I., Genova, September 1965.

[35] Adams, J.M., "A Study of the Critical Heat Flux in an Accelerating Pool Boiling System," Tech. Rept., Heat Transfer Lab., University of Washington, September 1962, (see also ref. [4]).

[36] Carne, M., "Studies of the Critical Heat Flux for Some Binary Mixtures and Their Components," Canadian Jour. Chem. Engr., December 1963, pp. 235-241.

[37] Costello, C.P. and Heath, C.A., "The Interaction of Surface Effects and Acceleration in the Burnout Heat Flux Problem," AIChE Jour., vol. 10, 1964, pp. 351-359.

[38] Frea, W.J. and Costello, C.P., "Mechanisms for Increasing the Peak Heat Flux in Boiling Saturated Water at Atmospheric Pressure," Report, Heat Trans. Lab., Mech. Engr. Dept., University of Washington, June 1963.

[39] Pramuk, F.S. and Westwater, J.W., "Effect of Agitation on the Critical Temperature Difference for a Boiling Liquid," Chem. Engr. Progress Symposium Series, no. 18, vol. 52, 1956, pp. 79-83.

[40] Costello, C.P., Bock, C.O., and Nichols, C.C., "A Study of Induced Convection Effects on Pool Boiling Burnout," C.E.P. Symposium Series, vol. 61, 1965, pp. 271-280.

[41] Switzer, K.A. and Lienhard, J.H., "Surface Temperature Variations on Electrical Resistance Elements Supplied with Alternating Current," Wash. State Univ. Inst. of Tech., Bulletin No. 280, 1964, Pullman, Washington.

[42] Houchin, W.R. and Lienhard, J.H., "Boiling Burnout in Low Thermal Capacity Heaters," Paper No. 66-WA/HT-40, Winter Annual ASME Meeting, New York, November 1966.

[43] Korayem, A.Y., "Quenching Heat Transfer," unpublished report for Boiling Heat Transfer Seminar, Univ. of Calif., Berkeley, Spring 1961.

"The aeronautical and space activities of the United States shall be conducted so as to contribute . . . to the expansion of human knowledge of phenomena in the atmosphere and space. The Administration shall provide for the widest practicable and appropriate dissemination of information concerning its activities and the results thereof."

—NATIONAL AERONAUTICS AND SPACE ACT OF 1958

NASA SCIENTIFIC AND TECHNICAL PUBLICATIONS

TECHNICAL REPORTS: Scientific and technical information considered important, complete, and a lasting contribution to existing knowledge.

TECHNICAL NOTES: Information less broad in scope but nevertheless of importance as a contribution to existing knowledge.

TECHNICAL MEMORANDUMS: Information receiving limited distribution because of preliminary data, security classification, or other reasons.

CONTRACTOR REPORTS: Scientific and technical information generated under a NASA contract or grant and considered an important contribution to existing knowledge.

TECHNICAL TRANSLATIONS: Information published in a foreign language considered to merit NASA distribution in English.

SPECIAL PUBLICATIONS: Information derived from or of value to NASA activities. Publications include conference proceedings, monographs, data compilations, handbooks, sourcebooks, and special bibliographies.

TECHNOLOGY UTILIZATION PUBLICATIONS: Information on technology used by NASA that may be of particular interest in commercial and other non-aerospace applications. Publications include Tech Briefs, Technology Utilization Reports and Notes, and Technology Surveys.

Details on the availability of these publications may be obtained from:

SCIENTIFIC AND TECHNICAL INFORMATION DIVISION

NATIONAL AERONAUTICS AND SPACE ADMINISTRATION
Washington, D.C. 20546